



**Enhanced detectability of human serum  
albumin by aggregation-induced emission  
bioprobes with fiber optics**

by

Qi Hu, M. Eng. (Biomedical)

Supervisor: Professor Youhong Tang

Submitted to the College of Science and Engineering in partial fulfilment of the requirements for the  
degree of Master of Engineering (Biomedical) at Flinders - University Adelaide Australia

Sep 2020

## **Declaration**

I certify that this work does not incorporate without acknowledgment any material previously submitted for a degree or diploma in any university; and that to the best of my knowledge and belief it does not contain any material previously published or written by another person except where due reference is made in the text.

Qi Hu

Sep 2020

## **Abstract**

Human serum albumin (HSA) is a very important biomarker in human body fluids, and its content is of great significance in clinical diagnosis and detection of various diseases. Critical illness alters the distribution of albumin level in body fluids such as chronic kidney disease (CKD) that causes albumin to leak into the urine. There is a new aggregation-induced emission (AIE) bioprobe TC-380, which is used to evaluate the feasibility of albumin detection. In this work, a comprehensive and effective detection method for measuring HSA levels in deionized water, artificial urine and human urine has been established. However, autofluorescence in environment of urine testing interferes with albumin detection by ordinary spectrometers. Due to lower light loss, higher light stability and strong ability of anti-electromagnetic interference, the introduction of fiber optics system enhances the detection signal of albumin and obtains promising achievements in urine detection. Finally, it is proved that the optical fiber system has higher sensitivity than ordinary spectrometers in albumin detection.

# Table of Contents

<b>1</b>	<b>Literature review .....</b>	<b>11</b>
1.1	<b>Chronic kidney disease (CKD).....</b>	<b>11</b>
1.1.1	Common health problem worldwide.....	11
1.1.2	Mortality and risk.....	11
1.1.3	Definition and classification .....	12
1.1.4	Early detection of CKD.....	12
1.2	<b>Fiber optics.....</b>	<b>13</b>
1.2.1	Description.....	13
1.2.2	Chemical and biomedical sensors based on fiber optics.....	13
1.2.3	Advantages and disadvantages of fiber optic sensors.....	14
1.2.4	Applications of fiber optic sensors.....	14
<b>2</b>	<b>Introduction.....</b>	<b>17</b>
2.1	<b>Background.....</b>	<b>17</b>
2.1.1	Human serum albumin detection .....	17
2.1.2	Routine clinical methods to detect albumin .....	18
2.2	<b>Fluorescent technology.....</b>	<b>18</b>
2.2.1	Aggregation-induced emission (AIE).....	18
2.2.2	Application of AIE bioprobe to test HSA.....	18
2.2.3	New AIE fluorophores .....	19
2.3	<b>Fiber optics system .....</b>	<b>21</b>
2.4	<b>Purpose .....</b>	<b>22</b>
<b>3</b>	<b>Experimental .....</b>	<b>23</b>
3.1	<b>Material .....</b>	<b>23</b>
3.1.1	AIE bioprobes .....	23
3.1.2	Sample preparation.....	23
3.2	<b>Device.....</b>	<b>23</b>
3.2.1	Traditional spectrometer .....	23
3.2.2	Fiber optics system.....	24
3.3	<b>Method.....</b>	<b>24</b>
3.3.1	Evaluation of the range of albumin concentration .....	25
3.3.2	Evaluation in different environments.....	26

3.3.3	Evaluation of biosensors' optimal working conditions.....	26
3.3.3.1	Dilution of urine ratio.....	26
3.3.3.2	Reaction time .....	27
3.3.3.3	Bioprobe to HSA solution ratio.....	27
3.3.4	Evaluation of SOP validation.....	27
3.3.4.1	Correlation between different HSA concentrations and their fluorescence intensity .....	27
3.3.4.2	Master curve.....	28
3.3.4.3	Detection of random spiked samples .....	28
3.3.5	Evaluation of the practical aspects of the operating conditions.....	29
3.3.5.1	Creatinine influence .....	29
3.3.5.2	Detection limit.....	29
<b>4</b>	<b>Results .....</b>	<b>31</b>
<b>4.1</b>	<b>Traditional spectrometer .....</b>	<b>31</b>
4.1.1	Measurement of seven bioprobes.....	31
4.1.2	Optimal working conditions of TC-380 in deionized water .....	35
4.1.2.1	Reaction time .....	35
4.1.2.2	TC-380 to HSA solution ratio.....	35
4.1.2.3	Correlation between different HSA concentrations and their fluorescence intensity .....	38
4.1.2.4	Master curve.....	38
4.1.2.5	Validation.....	40
4.1.3	Optimal working conditions of TC-380 in artificial urine .....	41
4.1.3.1	Reaction time .....	41
4.1.3.2	TC-380 to HSA solution ratio.....	42
4.1.3.3	Correlation between different HSA concentrations and their fluorescence intensity .....	44
4.1.3.4	Master curve.....	45
4.1.3.5	Validation.....	46
4.1.3.6	Creatinine influence .....	47
4.1.4	Optimal working conditions of TC-380 in human urine.....	48
4.1.4.1	Dilution of urine ratio.....	48
4.1.4.2	Obstacles to urine testing in traditional spectrometer and potential improvement.....	49
4.1.5	Comparison between DI water and artificial urine using traditional spectrometer.....	50
4.1.5.1	Master curve comparison between DI water and artificial urine .....	50
4.1.5.2	Detection limit in spectrometer.....	51
4.1.6	Result of SOP using spectrometer.....	52
<b>4.2</b>	<b>Optical fiber system.....</b>	<b>53</b>
4.2.1	Measurement of seven bioprobes.....	53
4.2.2	Optimal working conditions of TC-380 in deionized water .....	54
4.2.2.1	Reaction time and TC-380 to HSA solution ratio.....	54

4.2.2.2	Correlation between different HSA concentrations and their fluorescence intensity .....	54
4.2.2.3	Master curve.....	55
4.2.2.4	Validation.....	56
4.2.3	Optimal working conditions of TC-380 in artificial urine .....	58
4.2.3.1	Reaction time and TC-380 to HSA solution ratio.....	58
4.2.3.2	Correlation between different HSA concentrations and their fluorescence intensity .....	58
4.2.3.3	Master curve.....	59
4.2.3.4	Validation.....	60
4.2.3.5	Creatinine influence .....	61
4.2.4	Optimal working conditions of TC-380 in human urine.....	62
4.2.4.1	Dilution of urine ratio.....	62
4.2.4.2	Reaction time .....	65
4.2.4.3	TC-380 to HSA solution ratio.....	65
4.2.4.4	Correlation between different HSA concentrations and their fluorescence intensity .....	68
4.2.4.5	Master curve.....	68
4.2.4.6	Validation.....	69
4.2.4.7	Creatinine influence .....	71
4.2.5	Comparison among DI water, artificial and human urine using fiber optics system.....	71
4.2.5.1	Master curve comparison among DI water, artificial urine and human urine .....	71
4.2.5.2	Detection limit in fiber optics system .....	73
4.2.6	Result of SOP using fiber optics .....	74
<b>5</b>	<b>Discussion.....</b>	<b>76</b>
<b>5.1</b>	<b>The difference of reaction peak between ordinary spectrometer and optical fiber ....</b>	<b>76</b>
<b>5.2</b>	<b>Master curves comparison between two systems in DI water and artificial urine.....</b>	<b>76</b>
<b>6</b>	<b>Conclusion .....</b>	<b>79</b>
<b>7</b>	<b>Acknowledgment.....</b>	<b>80</b>
<b>8</b>	<b>Reference .....</b>	<b>81</b>

## List of figures

Figure 1. Chemical Structure of IDATPE and BSPOTPE.....	19
Figure 2. (A) Chemical Structure of TPE-4TA and (B) Schematic of interaction mechanism for TPE-4TA with albumin .....	19
Figure 3. Chemical structures of ASC and ASCP including its derivatives: ASCP-HE, ASCP-CA, ASCP-ES and ASCP-SO .....	20
Figure 4. (A) Chemical structure of TC-426 and (B) Absorbance and PL spectra of TC-426 in DMSO solvent .....	21
Figure 5. Chemical structure of TC-380 .....	21
Figure 6. Experimental setup for the detection of bioprobe towards albumin using optical fibres. LP filter: long pass filter. ....	24
Figure 7. Method of evaluation in three different environments .....	25
Figure 8. Seven bioprobes excitation wavelengths. (A) TC-374 excitation wavelength; (B) TC-379 excitation wavelength; (C) TC-380 excitation wavelength; (D) TC-381 excitation wavelength; (E) TC-449 excitation wavelength; (F) TC-559 excitation wavelength; (G) TC-426 excitation wavelength. ....	31
Figure 9. AIE attributes in emission wavelengths of 7 bioprobes .....	32
Figure 10. Reaction time at (A) 200 mg/L and (B) 800 mg/L HSA concentration in DI water .....	35
Figure 11. TC-380 to albumin ratio at 200 mg/L HSA concentration in DI water.....	36
Figure 12. TC-380 to albumin ratio at 800 mg/L HSA concentration in DI water.....	36
Figure 13. Different ratios of TC-380 to HSA solution at 200 and 800 mg/L HSA concentration in DI water.....	37
Figure 14. Trends of different ratios of TC-380 to HSA at 200 and 800 mg/L HSA concentration in DI water.....	37
Figure 15. Correlation between different HSA concentration and their fluorescence intensity in DI water.....	38
Figure 16. Master curve in DI water from 25- 200 mg/L HSA concentration using traditional spectrometer .....	39
Figure 17. Master curve in DI water from 25- 800 mg/L HSA concentration using traditional spectrometer .....	40
Figure 18. Validation of Master curve in DI water using five sets of samples with three different HSA concentrations: 50, 100, 200 mg/L.....	41
Figure 19. Reaction time at (A) 200 mg/L and (B) 800 mg/L HSA concentration in artificial urine ..	42
Figure 20. TC-380 to albumin ratio at 200 mg/L HSA concentration in artificial urine .....	42
Figure 21. TC-380 to albumin ratio at 800 mg/L HSA concentration in artificial urine .....	43

Figure 22. Different ratios of TC-380 to HSA solution at 200 and 800 mg/L HSA concentration in artificial urine.....	43
Figure 23. Trends of different ratios of TC-380 to HSA at 200 and 800 mg/L HSA concentration in artificial urine.....	44
Figure 24. Correlation between different HSA concentration and their fluorescence intensity in artificial urine.....	45
Figure 25. Master curve in artificial urine from 25- 200 mg/L HSA concentration using traditional spectrometer.....	46
Figure 26. Master curve in artificial urine from 25- 800 mg/L HSA concentration using traditional spectrometer.....	46
Figure 27. Validation of Master curve in artificial urine using five sets of samples with three different HSA concentrations: 50, 100, 200 mg/L.....	47
Figure 28. Creatinine influence in artificial urine.....	48
Figure 29. Dilution of urine ratio at 200 mg/L HSA concentration in human urine.....	49
Figure 30. Dilution of urine ratio at 800 mg/L HSA concentration in human urine.....	49
Figure 31. Master curve comparison between DI water and artificial urine using traditional spectrometer.....	51
Figure 32. Detection limit in DI water using traditional spectrometer.....	52
Figure 33. Detection limit in artificial urine using traditional spectrometer.....	52
Figure 34. AIE attributes in emission wavelength of 7 bioprobes using fiber optics.....	53
Figure 35. Correlation between different HSA concentration and their fluorescence intensity in DI water using optical fiber.....	55
Figure 36. Master curve in DI water from 25- 200 mg/L HSA concentration using fiber optics.....	56
Figure 37. Master curve in DI water from 0 - 800 mg/L HSA concentration using fiber optics.....	56
Figure 38. Validation of Master curve in DI water using five sets of samples with three different HSA concentrations: 50, 100, 200 mg/L under fiber optics system.....	57
Figure 39. Correlation between different HSA concentration and their fluorescence intensity in artificial urine using optical fiber.....	58
Figure 40. Master curve in artificial urine from 25- 200 mg/L HSA concentration using fiber optics.....	59
Figure 41. Master curve in artificial urine from 0- 800 mg/L HSA concentration using fiber optics.....	60
Figure 42. Validation of Master curve in artificial urine using five sets of samples with three different HSA concentrations: 50, 100, 200 mg/L under fiber optics system.....	60
Figure 43. Creatinine influence in artificial urine using fiber optics.....	62
Figure 44. Dilution of urine ratio at 200 mg/L in human urine.....	63
Figure 45. Dilution of urine ratio at 800 mg/L in human urine.....	63
Figure 46. Normalized dilution of urine ratio at 200 mg/L in human urine.....	64
Figure 47. Normalized dilution of urine ratio at 800 mg/L in human urine.....	65



Figure 48. TC-380 to albumin ratio at 200 mg/L HSA concentration in human urine.....	66
Figure 49. TC-380 to albumin ratio at 800 mg/L HSA concentration in human urine.....	66
Figure 50. Different ratios of TC-380 to HSA solution at 200 and 800 mg/L HSA concentration in human urine.....	67
Figure 51. Correlation between different HSA concentration and their fluorescence intensity in human urine using optical fiber .....	68
Figure 52. Master curve in human urine from 25- 200 mg/L HSA concentration using fiber optics...	69
Figure 53. Master curve in human urine from 0- 800 mg/L HSA concentration using fiber optics.....	69
Figure 54. Validation of Master curve in human urine using five sets of samples with three different HSA concentrations: 50, 100, 200 mg/L under fiber optics system .....	70
Figure 55. Creatinine influence in human urine using optical fiber .....	71
Figure 56. Master curve comparison among DI water, artificial urine and human urine using fiber optics system .....	72
Figure 57. Detection limit in DI water using fiber optics .....	73
Figure 58. Detection limit in artificial urine using fiber optics .....	74
Figure 59. Detection limit in human urine using fiber optics .....	74
Figure 60. Normalized master curves in DI water between two systems .....	77
Figure 61. Normalized master curves in artificial urine between two systems .....	78

## List of tables

Table 1. Stages of CKD .....	12
Table 2. Thresholds of albuminuria .....	13
Table 3. Codename of 7 bioprobes .....	23
Table 4. Excitation and emission wavelengths of 7 bioprobes (— represents no peak found). .....	32
Table 5. Six bioprobes emission wavelengths in DI water containing HSA at 200 and 800 mg/L.....	34
Table 6. Concentration of HSA detected by the SOP for TC-380 in DI water.....	41
Table 7. Concentration of HSA detected by the SOP for TC-380 in artificial urine .....	47
Table 8. Result of Standard operating procedure of TC-380 (‘—’ represents no results or no measurements) .....	53
Table 9. Excitation and emission wavelength of 7 bioprobes.....	54
Table 10. Concentration of HSA detected by the SOP for TC-380 in DI water using fiber optics.....	57
Table 11. Concentration of HSA detected by the SOP for TC-380 in artificial urine using fiber optics .....	61
Table 12. Concentration of HSA detected by the SOP for TC-380 in human urine using fiber optics	70
Table 13. Result of SOP for TC-380 in optical fiber system (‘—’ represents no results or no measurements) .....	75

# **1 Literature review**

## **1.1 Chronic kidney disease (CKD)**

### **1.1.1 Common health problem worldwide**

Chronic kidney disease is a kind of kidney function loss. With the aging of the population and the global increase in the prevalence of diabetes and other chronic non-communicable diseases, the prevalence of chronic kidney disease and renal failure have increased globally (James et al., 2010). According to statistics, 11.6% of adult residents in the United States suffer from chronic kidney disease, which is about 26 million and the prevalence is still on the rise (William G Couser et al., 2011). According to the current international standards for clinical evaluation of renal function, the prevalence of CKD (all stages) in the general adult population in the United States is 13.1%, and that in Australia is 13.4%. Furthermore, more than two thousand patients in Australia with chronic kidney disease are diagnosed with dialysis or even kidney transplantation every year (White et al., 2010). These facts all show that chronic kidney disease is a public health issue that requires close attention all over the world.

### **1.1.2 Mortality and risk**

The mortality rate of chronic kidney disease is very high. Because it is difficult to detect in the early stage of the disease, most patients are already in the middle or end-stage renal disease (ESRD) when they are diagnosed. In addition, chronic kidney disease is usually a complication caused by non-communicable diseases such as cardiovascular disease, cancer, diabetes and chronic respiratory disease. This has greatly increased the mortality of patients.

In the late stage of chronic kidney disease, there are very limited treatment options, and expensive renal replacement therapy is generally required in the form of dialysis or transplantation. At this stage, more than 2 million people worldwide need renal replacement therapy to maintain their lives, but this may only account for less than 10% of those who need it (William G Couser et al., 2011). Especially in middle-income and low-income countries, the cost of long-term dialysis is unaffordable. In fact, most patients cannot afford renal replacement therapy, which brings serious financial difficulties to those who have access to alternative therapy. Every year, more than 1 million people die from untreated kidney failure (Meguid El Nahas, 2005). This is due to the high mortality rate of kidney failure, limited treatment methods and high cost, hence people expect to monitor early kidney disease to slow down or prevent the progression of end-stage renal disease.

### 1.1.3 Definition and classification

Chronic kidney disease is defined as a continuous decrease in the glomerular filtration rate or abnormalities in the structure or function of the kidney found in urinalysis, biopsy, or imaging (James et al., 2010). According to the US National Kidney Foundation's Kidney Disease Outcomes Quality Initiative, this disease has established a five-stage classification system, which is shown as Table 1 below.

Stage	Description	Glomerular filtration rate (GFR, mL per min per 1.73 m <sup>2</sup> )
—	At risk	≥ 60
1	Kidney damage with normal or increased GFR	≥ 90
2	Kidney damage with mildly diminished GFR	60-89
3	Moderately reduced GFR	30-59
4	Severely decreased GFR	15-29
5	End-stage renal disease (kidney failure)	< 15

Table 1. Stages of CKD

It can be seen from the table that the severity of chronic kidney disease mainly depends on the glomerular filtration rate. The decrease in GFR indicates the degree of renal damage in the patient, and the direct result is proteinuria. By classifying them, it can be used directly for diagnosis and prognostic examination and gives corresponding treatment methods.

### 1.1.4 Early detection of CKD

Early detection of CKD is crucial because it can effectively control and prevent progress. They also pointed out that most people have no symptoms before CKD progresses to the advanced stage. In this case, it will be difficult to treat the damage to the kidney, and the kidney function cannot be restored through conventional treatment (Narva, A.S., 2008). It is reported that a person can lose up to 90% of their total kidney function before any symptoms appear (White et al., 2010). Therefore, early diagnosis can reduce the progression of renal failure and its complications by up to 50% (Chen et al., 2017).

Early detection of CKD depends on the urine protein content and blood serum creatinine test results. Data from the general population in the United States indicate that albuminuria is the

most typical sign of chronic kidney disease (James et al., 2010). It can effectively identify people at high risk of developing renal failure. In addition, albuminuria screening is attractive because it is easy to perform, and it is more predictive of a decrease in glomerular filtration rate than a reduction in estimated glomerular filtration rate.

	24-Hour Urine: Urinary Albumin Excretion, mg/24 hours	Urinary Albumin Concentration, mg/L	First Morning Void		
			Albumin:Creatinine Ratio		
			Sex	mg/mmol	mg/g
Normoalbuminuria	<30	<20	Male	<2.5	<20
			Female	<3.5	<30
Microalbuminuria	30–300	20–200	Male	2.5–25	20–200
			Female	3.5–35	30–300
Macroalbuminuria	>300	>200	Male	>25	>200
			Female	>35	>300

Table 2. Thresholds of albuminuria

Because of this, clinical practice guidelines in the United States, Australia, and Europe recommend the use of the urine albumin to creatinine ratio (UACR) for the early detection of CKD. It also can be used in conjunction with the estimated glomerular filtration rate (eGFR) of the test to screen for CKD and its related classifications (Narva, A.S., 2008). Generally, there is no albumin in human urine when the glomerular filtration is normal. However, in the case of kidney damage, a small amount of albumin can leak into the urine. When the albumin concentration in urine is between 20 mg/L and 200 mg/L, this condition is defined as microalbuminuria. Obviously, microalbuminuria testing in urine becomes the initial screening technique for chronic kidney disease.

## 1.2 Fiber optics

### 1.2.1 Description

Optical fiber is a communication medium made of glass or plastic fiber, which is used to transmit and send optical signals between the two ends of the fiber. An optical fiber consists of a core surrounded by a cladding. Through total internal reflection of light, the fiber can be transmitted along the core and the cladding traps the light in the core. The outermost buffer can protect the fiber from moisture and physical damage (Senior, J. & Kazovsky, 1987).

### 1.2.2 Chemical and biomedical sensors based on fiber optics

Chemical or biomedical fiber optic sensors basically use the same components: light source (laser or LED), optical sensing element (optical fiber), photodetector, and recording equipment. These components belong to the optical hardware of the sensor. By adjusting the selectivity, sensitivity and time response of the sensor. The existing optical response (from chemical or

physical changes) can be easily captured. After that, optical information and signals can be obtained through intensity changes, wavelength changes, phase changes, polarization changes and time domain changes (Kasik, I. et al., 2006).

Fluorescence is particularly suitable for optical sensing. Therefore, optical fiber is mainly used for remote sensing of chemical substances through their inherent absorption or fluorescence in chemical or biomedical fields. The constructed chemical or biological sensor can allow fluorescence to be easily detected. Generally, fiber optic sensors measure fluorescence at a single wavelength. Due to the difference in wavelengths, the detected radiation can be distinguished from the probe radiation. Furthermore, fluorescence is an inherently sensitive technique, which enable to measure low analyte concentrations. At low fluorophore levels, if the fluorescence intensity varies with the concentration of the analyte, the response to the analyte is linear, which can prove that the analyte can work at the reagent level (Seitz, W.R.R., 1984).

### **1.2.3 Advantages and disadvantages of fiber optic sensors**

First of all, the optical fiber system is absolutely safe, which is not electrically connected to the human body. It is very small and flexible, being included in the catheter for multiple inductions. Certainly, Fiber optic sensors have obvious cost advantages over traditional electrical sensors (Peterson, J. I., & Vurek, G. G., 1984). Moreover, remote sensing function, high sensitivity in a wide dynamic range, online performance, anti-electromagnetic interference, the possibility of internal reference and the potential of fully distributed sensing along the length of the fiber, and the possibility of point or multipoint detection are undoubtedly the advantages of fiber optic sensors (Kasik, I. et al., 2006).

For the limitation of fiber optic sensors, ambient light will directly interfere with the optical fiber sensor, thereby it must be used in a dark environment. Specifically, it is necessary to make a reference of the background light so that the required optical information can be distinguished from the environmental background. On the other hand, long-term stability may be an issue for reagent systems. Because the reagent and analyte are in different phases, a mass transfer step must be performed before a constant response is achieved. In turn, this limits the response time of the optical sensor (Seitz, W.R.R., 1984).

### **1.2.4 Applications of fiber optic sensors**

The geometry and material properties of optical fibers also make them an indispensable sensing tool in medicine because they can be applied to various parts of the human body. In addition, optical fibers are also used to detect explosives or flammable substances (such as hydrogen, gasoline, etc.) as fiber probes, eliminating the risk of overheating or fire (Kasik, I. et al., 2006).

There are many researches on the applications of optical fiber sensors in different fields. Ruan, Shuai et al. reported a polytriazole-coated fiber optic tip sensor with AIE activity to detect picric acid (PA). It has high permeability, good mechanical properties, excellent chemical stability and excellent optical clarity. By fixing the P3a molecule, a group of new tetraphenylethene (TPE)-containing polytriazoles, on the tip of a multimode (MM) optical fiber through a silica gel sol-gel, its porous structure allows PA molecules to penetrate into P3a from the surroundings, causing the fluorescence of P3a to be quenched. The detection limit is as low as 100 ppb (mass concentration), which indicates that P3a molecule has the excellent performance. Furthermore, the strong aggregation of p3a molecules makes the excitation laser power only need 250 mW, and cheap LEDs in practical applications also can meet this requirement. It is proved that a simple and reliable optical tip sensor can be used for remote detection/monitoring of explosives, which is very useful for applications in hazardous environments.

In terms of heavy metal ion detection, a fiber optic turn-on fluorescence sensor for detecting mercury ions has been developed. Specifically, Silica sol-gel is used to attach Rhod-5N molecules to fibers to detect mercury ions. When only immersing the optical fiber in a mixed solution of fluorophores and mercury ions to send excitation laser and collect signals, it was found that the detection limit in its aqueous solution was as low as 0.3 ppb. When the silica sol-gel/Rhod-5N mixture is fixed on the fiber endface, the optically excited state of the embedded Rhod-5N molecule can be combined with the surrounding mercury ions, resulting in an increase in the detected fluorescence signal. The detection limit is 25 ppb (Ruan, S. et al., 2018). In this way, a simple and practical  $\text{Hg}^{2+}$  sensitive optical fiber sensor can be realized with high sensitivity and no damage to the sample. This fiber optic probe has the potential to be used for online remote monitoring of mercury ions in water.

As for healthcare monitoring, there are designed optical fiber sensors embedded into medical textiles for the monitoring of respiratory movements in a magnetic resonance imaging environment. Based on the measurement of the elongation of the abdominal circumference during breathing movement, three different designs have proved that they can successfully sense textile elongation between 0% and 3%, while maintaining the tensile properties of the textile substrate to make the patient feel comfortable. In addition to being compatible with MRI, the system has the potential to simultaneously sense movements from different positions of the patient (such as the abdomen and chest) through a single monitoring unit and can better distinguish weak breathing movements. Ultimately, medical textiles are a potential new niche market for fiber optic sensors (Grillet, A. et al., 2008).

Optical fiber is also used in monitoring pH value. There is a new optical pH sensor, which is based on an intensity ratiometric fluorescence readout. Optical fiber is used to process pH-responsive fluorescent materials and record the response on a fiber optic spectrometer. By adding two highly light-stable fluorescent dyes to the sensor material, and by directly covalently attaching the dye to the porous ORMOSIL-based sensor matrix material, ratiometric readings can be achieved, thereby achieving low drift and response within one-minute time. Two different modifications with pKa values of 5.30 and 6.11 were confirmed. The accuracy of the pH sensor in its effective range is 0.02 or higher, therefore it can be compared with conventional pH electrodes. Consequently, it is an ideal choice for the biotechnology industry (Rosenberg, M. et al., 2018).

In the way of protein monitoring, optical fiber can still play an important role. The detection of quantum dot-labeled proteins has been demonstrated in lead silicate soft glass microstructured optical fibers using near-infrared light. The guided light in the optical fiber is used for both excitation light and fluorescence photon collection. More ideally, the detection limit of 1 nM can be achieved by using only the 3% guiding mode of the fiber without optimizing the fiber geometry. The article also mentions that by reducing the core size, background fluorescence can be reduced. In addition, this change also increases the power fraction in the well, which increases the contrast between fluorescence and background signals, and ultimately improves detection sensitivity. Therefore, this new method has the potential to significantly improve sensitivity. The advantages of optical fiber monitoring include real-time monitoring, in-situ measurement and lower cost, allowing low protein concentration detection to be achieved (Ruan, Y. et al., 2007).



## 2 Introduction

### 2.1 Background

#### 2.1.1 Human serum albumin detection

As is known to all, Human Serum Albumin (HSA) is the most abundant proteins in blood plasma, accounting for 55–60% of the measured serum protein. HSA whose concentration is 35-50 g/L as the major soluble proteins component of the circulatory system in human body, it has many physiological and pharmacological functions (Prakash, S., 2017).

Functionally, albumin provides 80% of normal plasma colloidal osmotic activity, and due to the existence of Gibbs-Donnan effect, albumin provides an attractive force for the retention of positively charged solute particles in blood vessels (Nicholson, J.P. et al., 2000). Additionally, the binding function of albumin prompts to incorporate many different substances such as bilirubin, vitamin D and thyroxin, reducing the free concentration of compounds, thus limiting their biologic activity, distribution, and rate of clearance (Levitt, D. et al., 2016). Besides, albumin under physiological environment has obvious antioxidant activity, providing more than 50% of the total antioxidant of normal plasma. The reason is that abundant reduced sulfhydryl groups exist in albumin that is shown to scavenge a variety of oxygen-free radicals (Levitt, D. et al., 2016).

Structurally, the overall structure of human serum albumin is composed of alpha helices similar to the shape of a heart, which is formed by the assembly of three homologous domains: I, II and III, and each homologous domain has two subdomains, A and B. Furthermore, subdomains with separate helical structures mediate human serum albumin binding with various endogenous and exogenous ligands, but each domain has a different ligand binding affinity and function nevertheless (Lee P, Wu X., 2015). To be specific, Sudlow sites I and II that are located in subdomain IIA and IIIA respectively are two important binding sites on human serum albumin. Sudlow site I is more liable to combine with bulky heterocyclic compounds. Sudlow site II is prone to bind preferentially to aromatic compounds (Lee P., Wu X., 2015).

On the strength of the importance of HSA in structure and function, detecting abnormal albumin levels in biological fluids becomes a sign of disease diagnosis. Concretely, albumin is extremely important in blood physiology indicators. Critical illness always alters the distribution of albumin between the intravascular and extravascular compartments (Nicholson, J.P. et al., 2000). Many studies have used it as a clinical indicator for cancer, diabetes, liver disease, inflammation, rheumatic diseases and cardiovascular diseases so far.

### **2.1.2 Routine clinical methods to detect albumin**

At presents, the routine methods used to detect albumin clinically are immunoassay and colorimetry. As for immunoassay, it has not only the limitation of detection at 2-10 mg/L, but also tends to underestimate the amount of albumin due to the chemical structure of albumin. To be specific, the urine environment is complex, which makes it difficult for the antibodies to detect the forms of albumin that has more than five antigenic sites. Hence, the immunoassays are considered as an inaccurate method for testing microalbumin (Martin, H., 2011). As regards colorimetric method, it includes Lowry assays, Biurets reagents test and the Bradford test. However, these methods have low detection accuracy and do not selectively detect HSA. For example urine dipsticks are colorimetric method of detection which has low detection sensitivity because of its high detection limit of 150 mg/L of HSA, known as the trace designation (Gaitonde, Cook & Rivera 2017).

## **2.2 Fluorescent technology**

### **2.2.1 Aggregation-induced emission (AIE)**

The phenomenon of aggregation-induced emission refers to the formation of aggregates of luminogenic molecules. The structural basis formed by the conventional luminophores is  $\pi$  conjugated molecules with planar conformations, which can promote effective emission. Specifically, in the aggregate state, the luminogenic molecules cannot be stacked through the  $\pi - \pi$  stacking process, and the intramolecular rotation of the aryl rotor is greatly restricted due to physical constraints. This limitation of intramolecular rotation (RIR) prevents non-radiative pathways and opens up radiation pathways. Finally, molecules emit fluorescence in an aggregated state (Hong, Y. et al., 2011). Because of the AIE characteristics above, it has become a reliable, effective and direct detection strategy, which can be designed as a fluorescent probe and has a very wide range of uses (Tu, Y. et al., 2019).

### **2.2.2 Application of AIE bioprobe to test HSA**

In recent years, there have been more and more examples of biosensors based on fluorescent materials used for the measurements of proteins and other organic molecules, all due to their sensitivity, selectivity and rapidity. After being complexed or bound to the protein, the luminophore shows emission changes and/or spectral shifts, so that the biopolymer can be detected and quantified. Thereinto, fluorescent probes with AIE characteristics can be used to detect albumin.

IDATPE and BSPOTPE were used to explore their utility as biological probes for HSA detection, quantification and creatinine influence (Chen, Tong et al., 2017). This article also evaluated the potential mutual interference of creatinine and HSA in artificial urine during the

detection and quantification process for the urine albumin to creatinine ratio (UACR) application. The results show that IDATPE is used to detect and quantify creatinine in water and artificial urine. Within a certain range, there is an excellent correlation between FL light intensity and creatinine concentration. Besides, creatinine in the range of 5–70 mM has no significant effect on the HSA detection of BSPOTPE in the range of 0–16 mM. The clear linear relationship between FL light intensity and HSA concentration is still valid (Chen, T. et al., 2017).

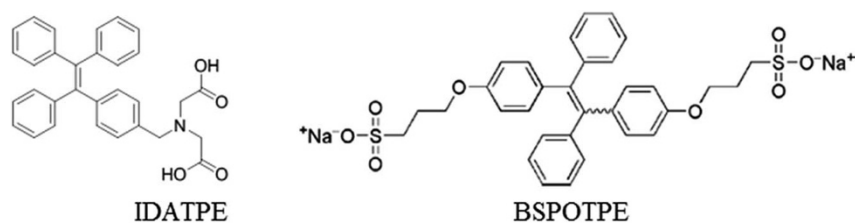


Figure 1. Chemical Structure of IDATPE and BSPOTPE

There is a reported AIE-active anionic fluorescent albumin bioprobe, TPE-4TA, which belongs to tetrazolate-tagged tetraphenylethylene derivatives. This probe can specifically bind to the sites of albumin and selectively light them up. The results showed that the lowest detection limit was 0.21 nM, and the tetrazolate functional group gave the probe excellent water solubility ( $> 0.01$  M) and high binding affinity towards albumin ( $K_D = 0.25$   $\mu$ M). Finally, TPE-4TA has been proven to be a sensitive and selective luminescent probe, making the current fluorogenic albumin sensing an attractive alternative strategy (Tu, Y. et al., 2019).

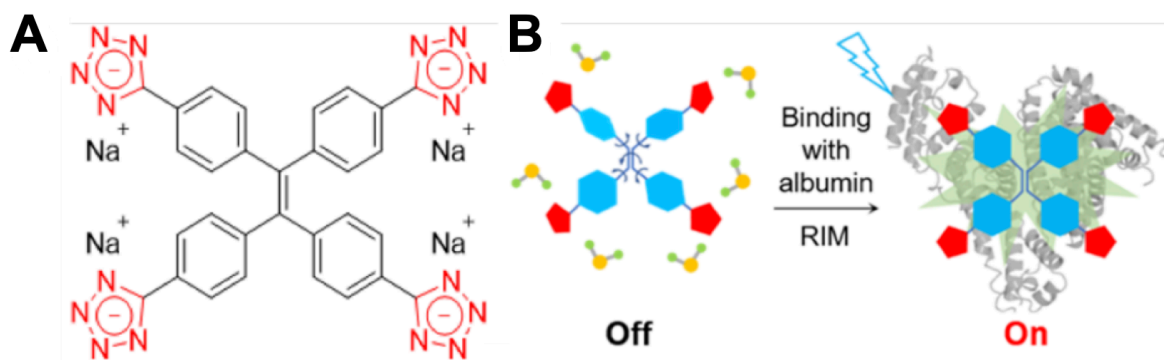


Figure 2. (A) Chemical Structure of TPE-4TA and (B) Schematic of interaction mechanism for TPE-4TA with albumin

### 2.2.3 New AIE fluorophores

ASC is a cationic  $\alpha$ -cyanostilbene and ASCP belongs to a new AIE-active  $\alpha$ -cyanostilbene derivative that is used to mark mitochondria and nucleolus in living cells, with unique fluorescence, high specificity and excellent photostability (Yu, C.Y.Y. et al., 2016).

Additionally, ASCP also contains the ability to modulate the dimethylamino moiety emitted to the red region and the pyridinium unit targeting the mitochondria (Zhou, Y. et al., 2019). By adding different substituent groups, a series of derivatives based on the chemical structure of ASCP are designed and synthesized. There are molecules at this stage: ASC, ASCP and 4 derivatives with different substituents (ASCP-HE, ASCP-CA, ASCP-ES and ASCP-SO). Their chemical structure is shown as Figure 3 below.

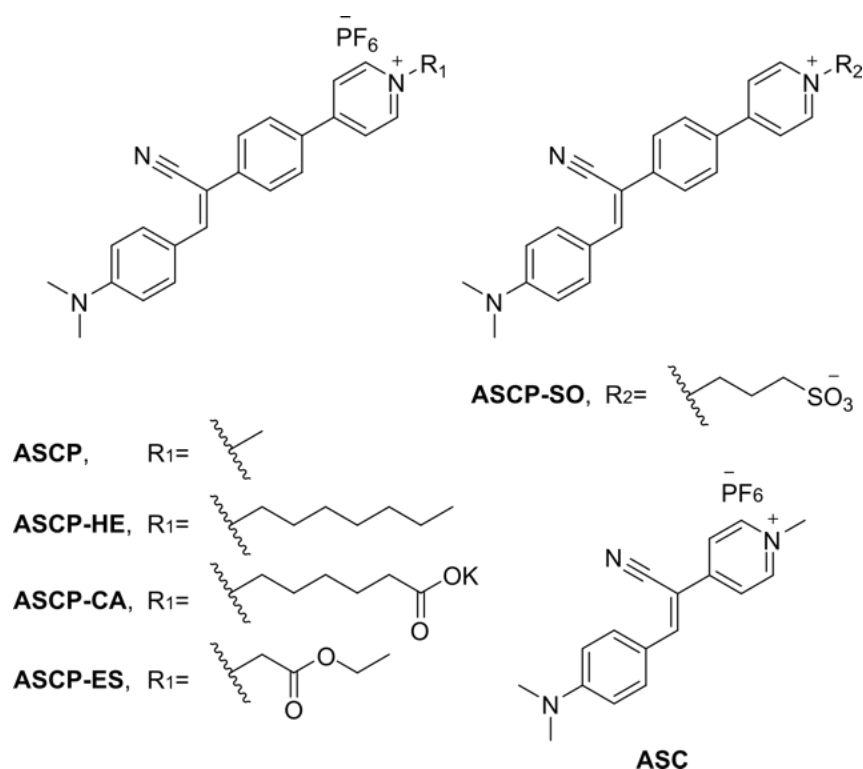


Figure 3. Chemical structures of ASC and ASCP including its derivatives: ASCP-HE, ASCP-CA, ASCP-ES and ASCP-SO

In addition, a novel AIE-based biosensor TC-426 has been also detected. Through the performance of probe toward albumin in previous work, the potential mechanism of the interaction between albumin and TC-426 is of the significance in the hydrophobic phenyl rings of TC-426, which encourages the luminogenic molecules to enter into the hydrophobic cavities of albumin and aggregate together (Wang, C., 2020). The structure of TC-426 and its absorbance and PL spectra are shown as Figure 4.

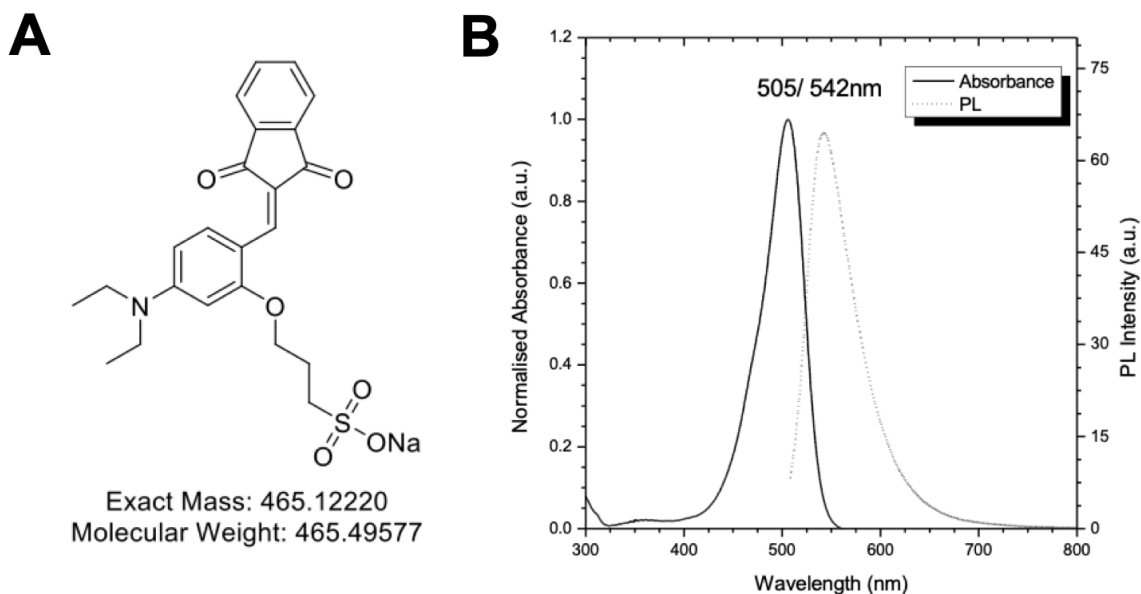


Figure 4. (A) Chemical structure of TC-426 and (B) Absorbance and PL spectra of TC-426 in DMSO solvent

In this work, there is a new AIE-based bioprobe called TC-380 (ASCP-HE). The dimethylamino group is an electron donor while the CN group is an electron acceptor. This push-pull electron structure makes the emission wavelength red shift. In addition, the group of pyridine salt increases water solubility and N-octyl is a flexible, hydrophobic alkyl chain, which helps increase the solubility of molecules in organic solvents. The chemical structure of TC-380 is shown as below.

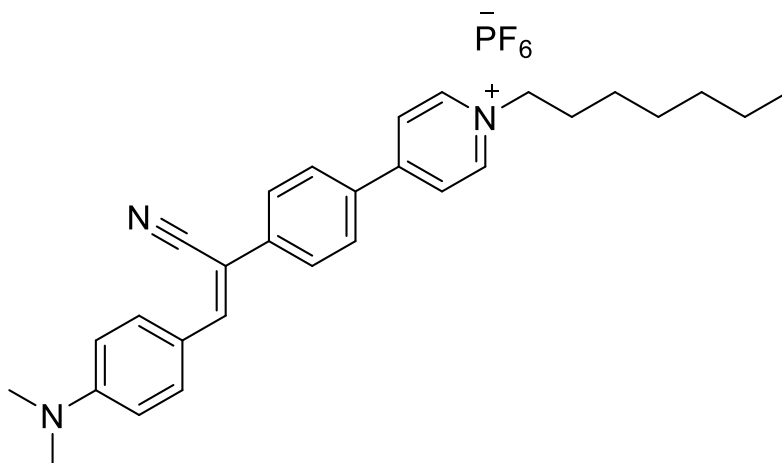


Figure 5. Chemical structure of TC-380

### 2.3 Fiber optics system

There is an example proves that optical fiber sensor can improve the light stability and detection limit of AIE materials (Ruan, S. et al., 2016). Based on the advantages of optical fiber systems such as low-cost, good flexibility, low light-intensity loss, high sensitivity in a wide dynamic

range and strong ability of anti-electromagnetic interference (Kasik, I. et al., 2006). The fiber optic system is a potential means for enhancing detection performance. At this stage, There is only one study on the use of fiber optic systems to build a portable urine analyzer (Liu, G. & Ma, Z., 2018). The author proposes a new portable urine analyzer with a new optical structure. The optical structure composed of fiber bundles can effectively reduce the impact of ambient light and provide measurable high-level resolution, which is expected to reduce the cost of urine reagent strips. The analyzer has good test stability, accuracy, reliability, repeatability and measurement accuracy of more than 97%, and has good practical value and wide application prospects. However, there are currently no examples of using fiber optic systems to detect albumin in human urine environment. Therefore, this is a good opportunity to explore the feasibility of human urine testing using optical fiber.

#### **2.4 Purpose**

In this work, new AIE fluorophores were screened to find biological probes with good capability to detect albumin. Additionally, the probe is used in the human urine measurement while the results and problems in the actual process are further optimized and improved.

At first, in order to ensure that the probe can perform optimally in a reasonable range, a comprehensive and effective detection method for measuring HSA levels is built up, which is the standard operating procedure of TC-380. Next, after ensuring that the probe detection in the simulated environments work well, the feasibility of human urine testing can be explored and evaluated. At last, the complex environment of human urine is bound to interfere with albumin detection. the optical fiber system is introduced to evaluate its albumin detection capabilities of optimization and enhancement instead of ordinary spectrometer.

## 3 Experimental

### 3.1 Material

#### 3.1.1 AIE bioprobes

In this study, seven different AIE probes were provided by La Trobe University, Australia. The remaining chemicals are purchased from Sigma-Aldrich, Australia.

In order to facilitate statistics and distinguish data between different biological probes, specific codes corresponding to different probes are used and all the probes mentioned in the following thesis are represented by their codename. the codename is displayed as Table 3.

Abbreviated name	Code name
ASCP	TC-374
ASCP-CA	TC-379
ASCP-HE	TC-380
ASCP-ES	TC-381
—	TC-426
ASCP-SO	TC-449
ASC	TC-559

Table 3. Codename of 7 bioprobes

#### 3.1.2 Sample preparation

Seven different AIE probes were dissolved in DMSO solvent, and finally were formulated these probe solutions with working concentration of  $10\mu M$ , and store it at  $4\text{ }^{\circ}\text{C}$  in a dark environment. Moreover, the artificial urine is prepared according to the published paper from Chen, Tong et al (Chen, T. et al, 2017). The collection and utilization of human urine have been approved by Flinders University. Furthermore, in accordance with the collection procedure, the fresh urine excreted for the first time in the morning is used for each experimental measurement (Martin, H., 2011). All incubation and measurement processes are performed at room temperature.

### 3.2 Device

#### 3.2.1 Traditional spectrometer

In order to record fluorescence results from different samples, a Cary Eclipse fluorescence spectrophotometer was employed in this work, which can scan and record the excitation and emission wavelengths of the sample in the spectrum of 200-900 nanometers and display its corresponding fluorescence intensity related to arbitrary units.

### 3.2.2 Fiber optics system

In this experiment, the setup of the fiber optics system is shown in the Figure 6 below. Continuous wave (CW) light from a 480 nm semiconductor laser diode was reflected off a long pass filter and went directly into the sample using a 40x microscope objective. The excited fluorescence signal at the cuvette endface was collected in backscattering mode, then passed through the long pass filter and recorded using a fiber coupled cooled-CCD spectrometer. Throughout this experiment, the output power is 1 mW. Additionally, the front entrance of slits is 1 mm and exposure time is 1 s.

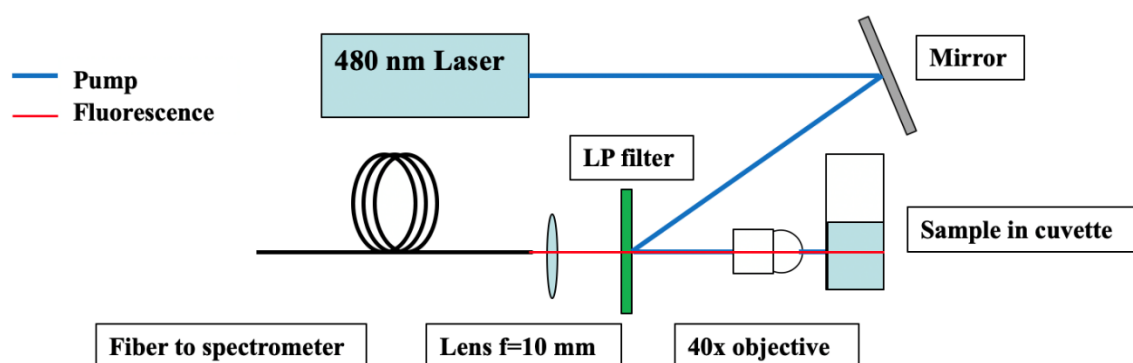


Figure 6. Experimental setup for the detection of bioprobe towards albumin using optical fibres. LP filter: long pass filter.

### 3.3 Method

For evaluation and development of a standard operating procedure (SOP) for HSA detection in three different environments (Deionized water, artificial urine and human urine) by bioprobes, investigation of operating conditions, validation and evaluation of practical aspects are required to measure. The Figure 7 shows the designed evaluation process of bioprobes.

In step 1, operating conditions includes dilution of urine ratio, reaction time and bioprobe to albumin solution ratio. In step 2, evaluating the correlation between FL intensity and HSA concentration, master curve and random spiked samples detection consists of validation of SOP. In step 3, creatinine influence and detection limit are fully considered then the SOP under these conditions are designed entirely. Finally, the above steps are repeated in deionized water, artificial urine and human urine.



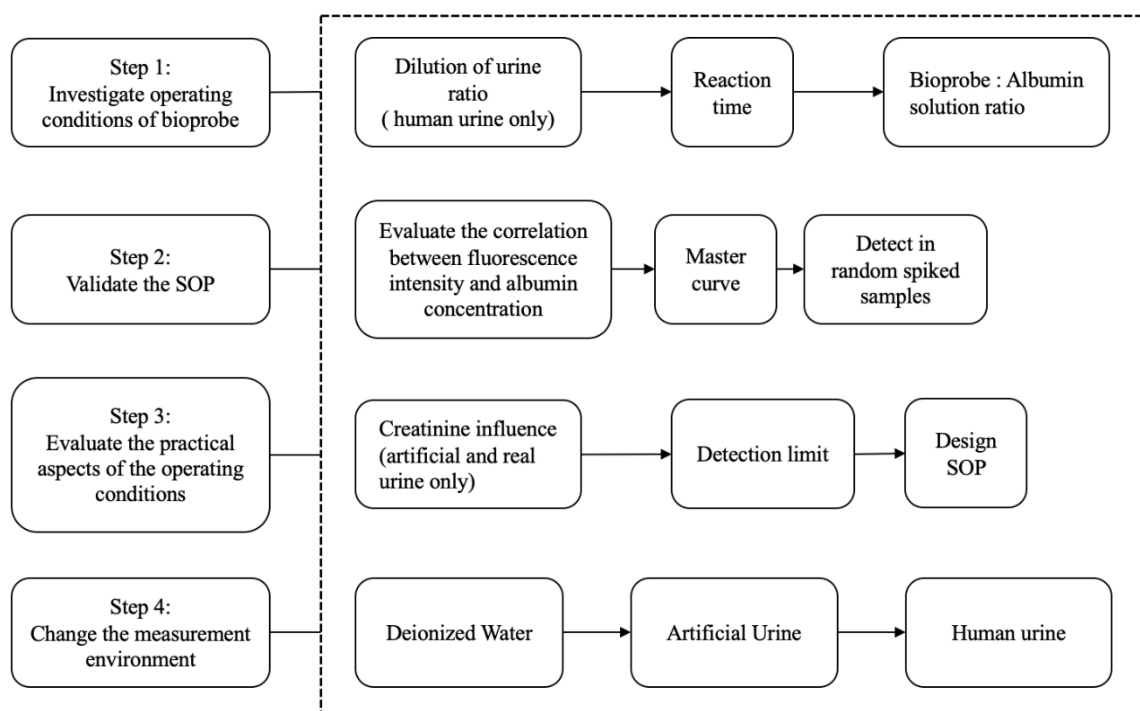


Figure 7. Method of evaluation in three different environments

### 3.3.1 Evaluation of the range of albumin concentration

For the detection of microalbuminuria, it is important to measure albumin within a meaningful range. At the same time, a relatively wide concentration gradient and detection limit are also important considerations. These factors are able to evaluate the correlation between albumin concentration and fluorescence intensity of bioprobe and determine the sensitivity of the probe in different environments.

It is known that the concentration range of microalbuminuria is 20-200 mg/L (Levey, A. S. et al., 2005). In order to maximize the detection of the fluorescence intensity change of the probe in the microalbumin range, 12 sets of concentration points are designed in this experiment, from low to high respectively : 25, 50, 75, 100, 125, 150, 175, 200, 300, 400, 600, 800 mg/L, of which 8 points are located in the microalbumin range and 4 points are outside the range. This setting can not only more accurately evaluate the correlation of the microalbumin range, but also observe and verify the fluorescence intensity changes in a wider range.

Furthermore, for the sake of comparing the difference in detection limit between the optical fiber system and the traditional spectrometer, four additional sets of points (0.1, 0.5, 1, 5 mg/L) will be set to determine the lowest concentration limit of albumin measured by these two detection systems.

### **3.3.2 Evaluation in different environments**

Deionized water is a type of water which removed all of its ions such as cations like sodium, calcium, iron, and copper, and anions such as chloride and sulfate, and it has no charge. It is the most common good solvent in many fields such as engineering, medicine, chemistry and biology. Moreover, artificial urine (AU) contains most of the components of normal human urine (except for various proteins) to simulate the normal physiological environment of the kidney and urinary tract (Chutipongtanate, S. & Thongboonkerd, V., 2010).

Obviously, the interference in the solvent is DI water < Artificial urine < Human urine. To evaluate the feasibility of the probe in real urine, these three environments can in-depth show the specific detection performance of the probe in solutions with different interference levels. More importantly, the alternation of the three environments is able to visually display the changes in probe FL intensity, and objectively evaluate and even eliminate errors caused by environmental factors.

### **3.3.3 Evaluation of biosensors' optimal working conditions**

The exploration of the optimal working conditions of the biological probe is to obtain its best detection performance, which is to have the best fluorescence intensity, correlation, peak shape, etc. under the same conditions. Specifically, there should be certain differences between different groups of specimens, which can help the experimenter identify or distinguish the characteristics of the substance and draw the most reasonable conclusions. According to Zhang, Z. et al.'s published paper (2019) about a systematic procedure for the design of biosensor, finding the best working conditions is actually a process of establishing standard operating procedures (SOP) for biosensors. In this work, the performance of the probe will be evaluated from the following aspects in different environments: dilution of urine ratio, reaction time, probe to HSA solution ratio, correlation between different HSA concentrations and their fluorescence intensity. Afterwards, under the above factors, the master curve of the bioprobe towards different HSA concentrations can be determined and verified.

#### *3.3.3.1 Dilution of urine ratio*

Human urine is a very complex body fluid and autofluorescence in urine is a common phenomenon. Due to the diversity of individuals, the composition of urine will also vary greatly from person to person (Birková, A. et al., 2020). The components in urine include many kinds of ions (such as chloride, sodium potassium and so on), proteins and enzymes, blood cells as well as inorganic and organic compounds (Baig, A., 2011), which means these components are bound to affect the detection of albumin by the probe in a certain extent. Under this

background, the dilution of urine was used to reduce the autofluorescence and interference when detecting in undiluted urine.

Two sets of solutions of 200 and 800 mg/L were prepared by adding HSA to the undiluted urine sample. The scheme of designing dilution ratio is 1:1, 1:3, 1:5, 1:7 and 1:9 (adding 1:11 in fiber optics system). According to different dilution ratios, corresponding equal proportions of deionized water will be added for dilution. Besides, blank sample represents human urine only (no bioprobe adding).

#### *3.3.3.2 Reaction time*

In order to make the results more reliable, reaction time is a very significant consideration. The probe solution should be mixed with the two sets of albumin solutions, 200 and 800 mg/L, at a ratio of 1:1. The purpose of this is to ensure that the probe can fully bind to the albumin solution. In this process, a vortex mixer is used to mix for ten seconds in the meantime three sets of parallel measurements are performed. The kinetic model of the spectrophotometer can continuously record the emitted fluorescence intensity. The scan time is set to 30 minutes.

#### *3.3.3.3 Bioprobe to HSA solution ratio*

The ratio of probe to albumin solution is one of the important factors affecting its performance. It is a fact that the best ratio can maximize the detection efficiency. Therefore, in order to evaluate the best biosensor to albumin ratio, two sets of albumin solutions with different concentrations, 200 and 800 mg/L, are used to evaluate and compare the performance of the detection results under different ratios. The five groups of bioprobe to albumin solution ratios are: 1:1, 1:3, 1:5, 1:7, 1:9 (1:11 is considered in fiber optics), taking the average of three parallel measurements. The best choice among the current five groups of ratios can be found by comparing the magnitude and change of the fluorescence intensity reflected by the corresponding ratio.

### **3.3.4 Evaluation of SOP validation**

#### *3.3.4.1 Correlation between different HSA concentrations and their fluorescence intensity*

After measuring the excitation wavelength, emission wavelength, exact reaction time and the ratio of probe to albumin, they will be used as default parameters to measure the correlation between different concentrations of albumin solution under the same conditions and corresponding fluorescence intensity. Through the previously designed multiple sets of albumin samples with different concentrations, the correlation curves are able to initially describe the relationship and trend between the probe FL intensity and the albumin concentrations from low to high. By means of this trend, the performance of detection of the

probe for HSA can be clearly emerged. Especially in the microalbumin range, this trend change is more worthy of attention.

#### 3.3.4.2 *Master curve*

According to the correlation between different HSA concentrations and their fluorescence intensity obtained in the previous step, by picking up and processing the peaks at the emission wavelength of each concentration, the master curve of bioprobe can be drawn, which are able to reflect and predict the detection performance of the probe in a certain range with the concentration change. Performance is described in FL intensity, its sensitivity and detection limit. In detail, the abscissa axis of the master curve, namely the range of concentration variation, can roughly predict the detection limit of the probe. The slope of the curve visually reflects the sensitivity of detection for the probe to target albumin in this concentration range. In general, the linear relationship is expected because if the linear relationship is established, it means that the probe is stable in its ability to detect the target protein within this concentration range.

#### 3.3.4.3 *Detection of random spiked samples*

The master curve of the probe under different albumin concentrations and its corresponding fluorescence intensity has been established. In order to ensure the accuracy of the curve in microalbumin range (20-200 mg/L), it is necessary to validate the obtained curve. In this experiment, three different albumin concentrations of 50, 100, and 200 mg/L were selected, and also 5 samples were measured and recorded in parallel at each concentration. To be specific, five groups of 200 mg/L albumin stock solutions were prepared in advance, and each group was diluted to 100 and the next 50 mg/L respectively. In the end, 15 samples can be obtained for testing the validation of master curve (Five groups of samples at each concentration of 50, 100, 200 mg/L).

Since the concentration of the prepared solution is known (50, 100, 200 mg/L), the specific fluorescence intensity of each of the 15 samples can be measured individually. When each measured fluorescence intensity is brought into the completed master curve, the corresponding concentration of the sample under this fluorescence intensity can be calculated backward. After that, the five groups of calculated concentrations at each concentration are averaged to obtain the actual average FL intensity value. Finally, the rate of change between the actual value and the theoretical concentration will be clear.

### 3.3.5 Evaluation of the practical aspects of the operating conditions

#### 3.3.5.1 Creatinine influence

The interference of creatinine with the assay in human urine sample should be considered. Creatinine is the final product of creatine metabolism, and its concentration in urine is used as an important indicator for the diagnosis of kidney disease and muscle disease (Júlia et al. 2002). The content of creatinine in urine is one of the routine indexes of clinical urine test. Therefore, it is necessary to determine and evaluate whether the presence of creatinine will affect the detection of albumin in the complex environment of human urine. According to Chen, Tong et al., 2017, urinary albumin-to-creatinine ratio (UACR) was introduced to measure and establish the standard threshold of creatinine under different albumin concentrations so that an effective scenario of creatinine in urine can be built up and utilized. The normal range of UACR is below 10 mg/g and when it is in the range of 30 mg/g to 300 mg/g, the patients are at high risk of kidney disease. Undoubtedly, when UACR is over 300 mg/g, it can be regarded as macroalbuminuria or clinical proteinuria and the kidney has been damaged into an advanced stage.

In this case, when the albumin concentration ranges from 20 mg/L to 200 mg/L, and the urinary albumin to creatinine ratio (UACR) ranges from 30 mg/g to 300 mg/g, it can be considered as microalbuminuria (Table 2). Consequently, the lowest concentration of albumin solution should add the amount of creatinine that makes UACR greater than the minimum threshold value in the meanwhile the highest concentration of albumin solution should add the amount of creatinine that makes UACR less than the maximum threshold value. It can be calculated that the creatinine added to artificial or human urine samples containing different HSA concentrations is 0.007 g in this experiment.

#### 3.3.5.2 Detection limit

The detection limit is one of the standards that directly reflects the detection capability of the equipment. In this case, in order to evaluate the limit of the probe's ability to detect albumin in different environments, albumin concentrations of 1, 5, and 25 mg/L under spectrometer in the meanwhile 0.1, 0.5, 1, 5 and 25 mg/L under fiber optics system were set individually. using all the optimal conditions measured in the experiment as parameters (dilution of urine ratio, reaction time, bioprobe to albumin solution ratio), the fluorescence intensity at each concentration can be collected. Additionally, the blanks are solutions of probe in DI water, artificial urine or human urine with [HSA] = 0 mg/L under optimal measured conditions. If the measurement result is satisfied with the model of master curve and the difference value

between them is within 20%, the result is considered meaningful and it can be regarded as the detection threshold at this concentration.

## 4 Results

### 4.1 Traditional spectrometer

#### 4.1.1 Measurement of seven bioprobes

In order to explore the performance of probes in more details and make use of them, firstly, finding and determining the excitation and emission wavelengths of the seven probes is the top priority. By using the full wavelength pre-scanning function of the spectrometer, the excitation and emission peaks of the corresponding probes can be scanned under normal circumstances. However, the detection limit of this spectrometer itself is not high enough so that the excitation peak is found but no peak found in emission wavelength for most of bioprobes. The results of seven bioprobes' excitation wavelengths are shown in the Figure 8 below.

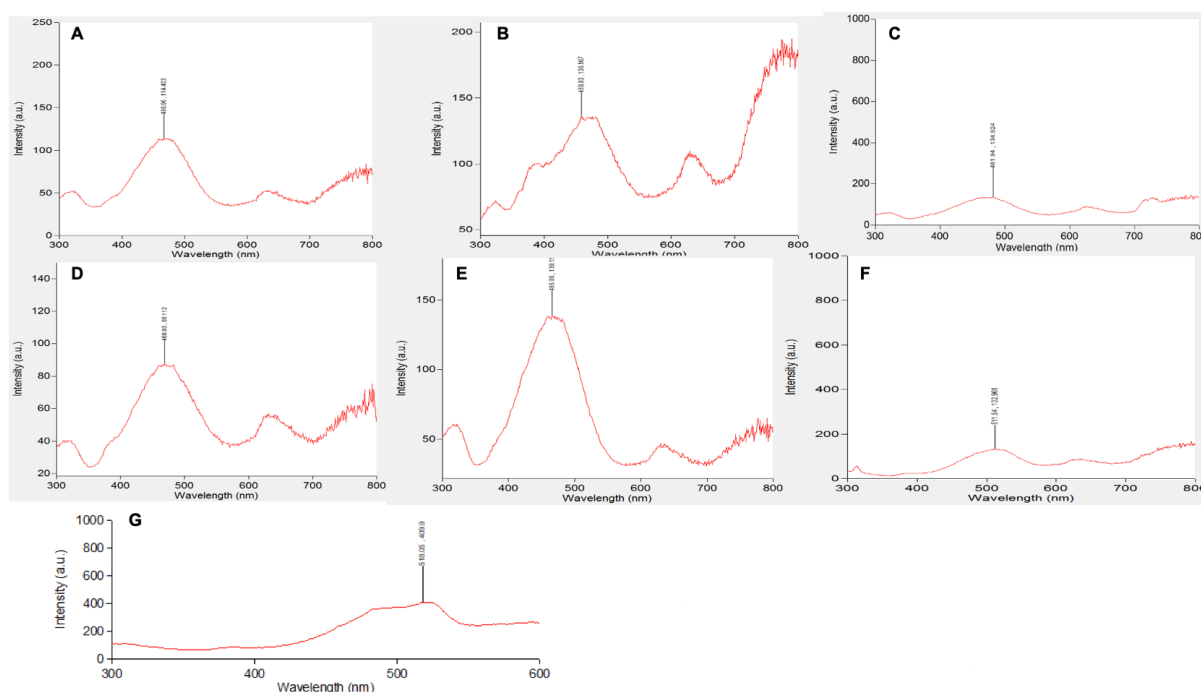


Figure 8. Seven bioprobes excitation wavelengths. (A) TC-374 excitation wavelength; (B) TC-379 excitation wavelength; (C) TC-380 excitation wavelength; (D) TC-381 excitation wavelength; (E) TC-449 excitation wavelength; (F) TC-559 excitation wavelength; (G) TC-426 excitation wavelength.

Next, according to the excitation wavelengths of the seven probes that have pro-scanned, the emission wavelength spectrum of the seven probes is summarized as shown in the Figure 9 below.

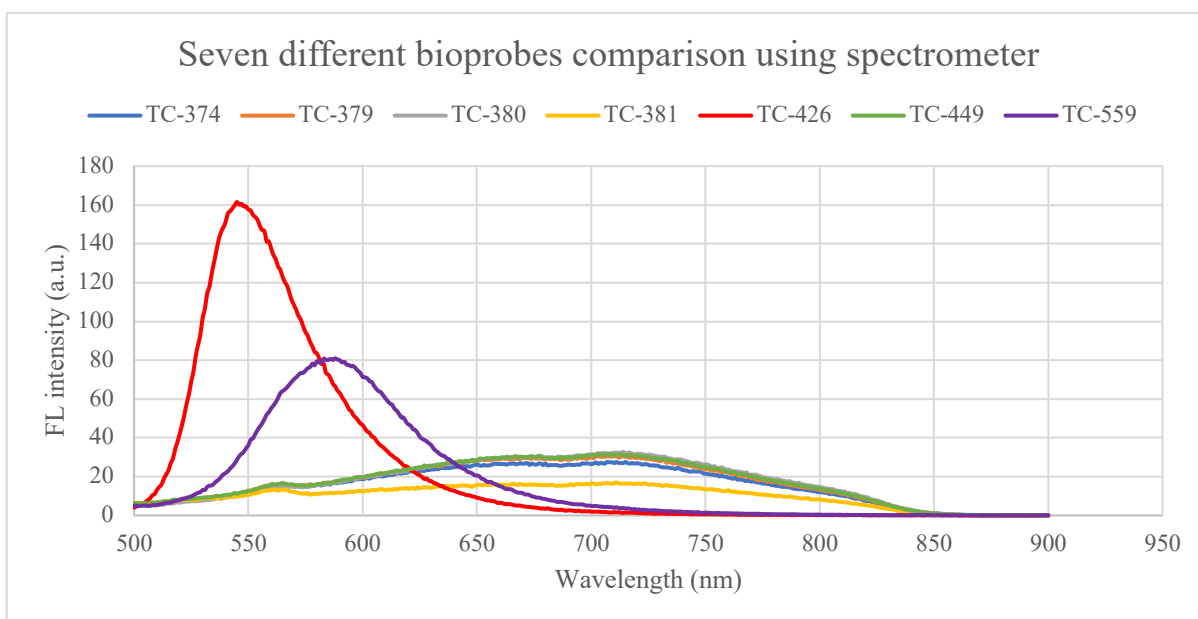


Figure 9. AIE attributes in emission wavelengths of 7 bioprobes

From the scanning results above, the excitation and emission wavelengths of the seven probes measured by the traditional spectrometer are listed as shown in the following table.

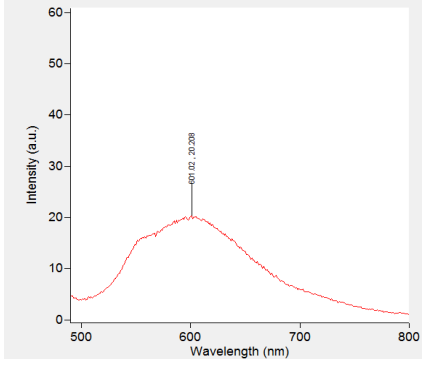
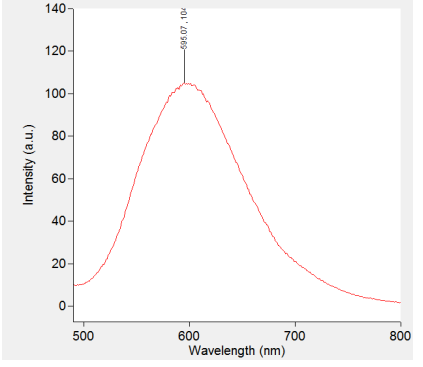
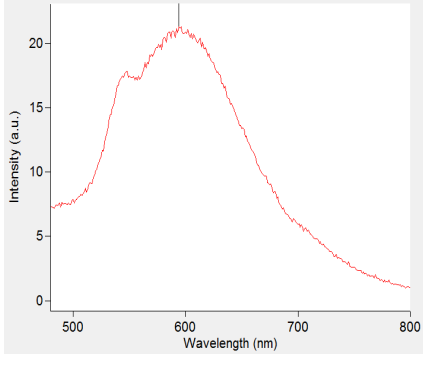
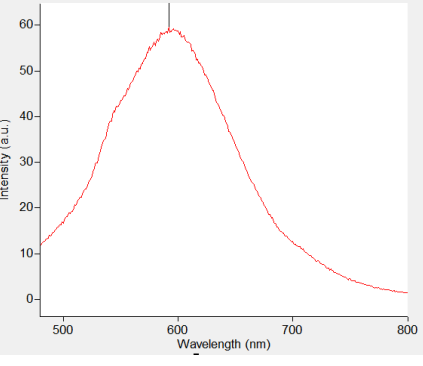
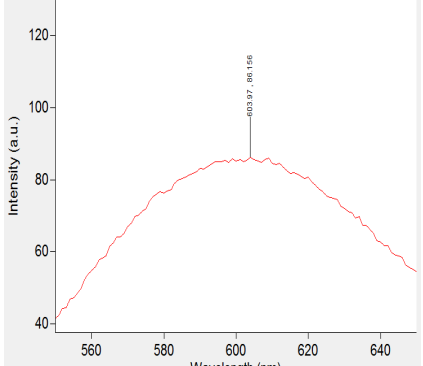
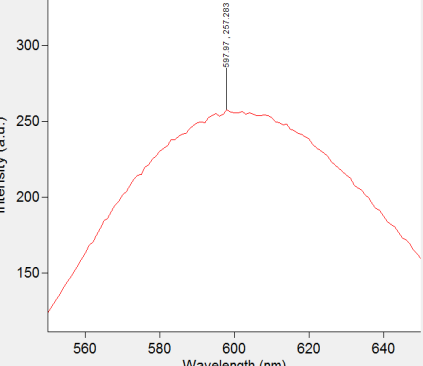
Name	Excitation wavelength (nm)	Emission wavelength (nm)
TC-374	466	—
TC-379	458	—
TC-380	481	—
TC-381	468	—
TC-426	518	545
TC-449	466	—
TC-559	511	587

Table 4. Excitation and emission wavelengths of 7 bioprobes (— represents no peak found).

At this stage, the DMSO solution of the probe cannot find its own emission wavelength except TC-426 and TC-559. A feasible strategy is to transfer it to an aqueous environment for detection and set up two sets of albumin solutions with different concentrations, and initially determine and verify whether the rest of probes will bind to albumin. By determining other variables such as probe to albumin solution ratio and operating sequence etc., the interaction between albumin and probe can only be analysed while eliminating possible interference. Therefore, the biosensor was added to two sets of albumin solutions with concentrations of 200 and 800 mg/L in a probe to albumin solution ratio of 1:5. After that, these samples were mixed on a vortex mixer for 10 seconds to accelerate the incubation process, and finally were



transferred to cuvettes for measurement. Each set of samples was measured in parallel three times and averaged (Wang, C., 2020). Using the excitation wavelength measured before, the emission wavelength of each probe in the aqueous solution containing albumin is shown in the Table 5.

Name	HSA Concentration		Emission wavelength
	200 mg/L	800 mg/L	
TC-374			595 nm
TC-379			592 nm
TC-380			602 nm

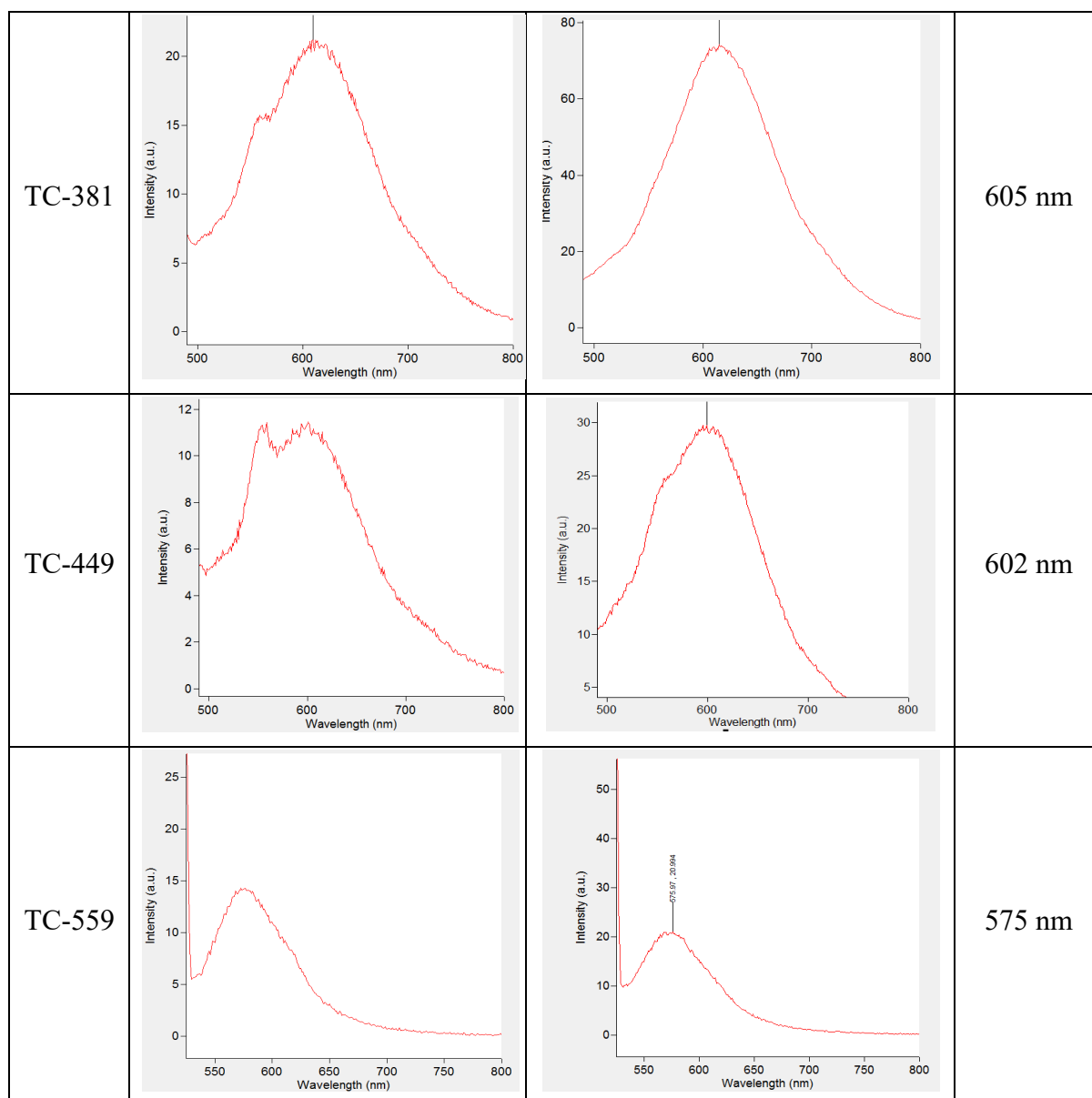


Table 5. Six bioprobes emission wavelengths in DI water containing HSA at 200 and 800 mg/L

The albumin detection of TC-426 has been evaluated (Changyu Wang, 2020). By comparing the rest of six different types of AIE probes, TC-380 exhibits the highest fluorescence intensity at these two concentrations 200 and 800 mg/L, which means that it is the probe with the strongest response to HSA among the six probes. In addition, it always has only one characteristic peak, whose shape is obvious in the entire wavelength range 500-800nm. At the same time, the other probes show a low level of response or even no response to albumin combination. Therefore, TC-380 is selected as the specific research object for follow-up detailed exploration and evaluation.

## 4.1.2 Optimal working conditions of TC-380 in deionized water

### 4.1.2.1 Reaction time

The reason for mixing with a vortex mixer is that if the probe is mixed with an aqueous solution containing albumin, the mixture will be slightly stratified without external force (the stratification here refers to the color layering) after a period of standing. The transparent water layer is on the top, and the yellow probe solution is on the bottom. This shows that the two are not sufficiently mixed, which will inevitably affect the experimental results. In order to avoid this, a vortex mixer can be equipped every time to make sure that both of them can be mixed thoroughly.

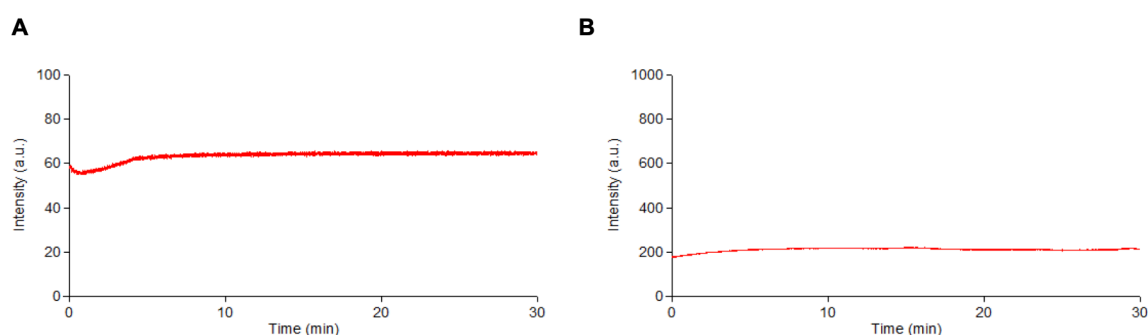


Figure 10. Reaction time at (A) 200 mg/L and (B) 800 mg/L HSA concentration in DI water

The result is shown as Figure 10, it can be seen from the figure that after 10s of full mixing, the fluorescence intensity increased slightly from 0 to 10 minutes, and after 10 minutes it was basically stable and maintained a fixed value. Throughout the experiment, the reaction time is set to 20 minutes to ensure that the reaction is complete.

### 4.1.2.2 TC-380 to HSA solution ratio

In this case, the previously measured parameters are fixed, which means that the excitation wavelength of TC-380 is 481nm and the reaction time is 20 mins. The results of different ratios at 200 and 800 mg/L HSA concentrations are shown below.

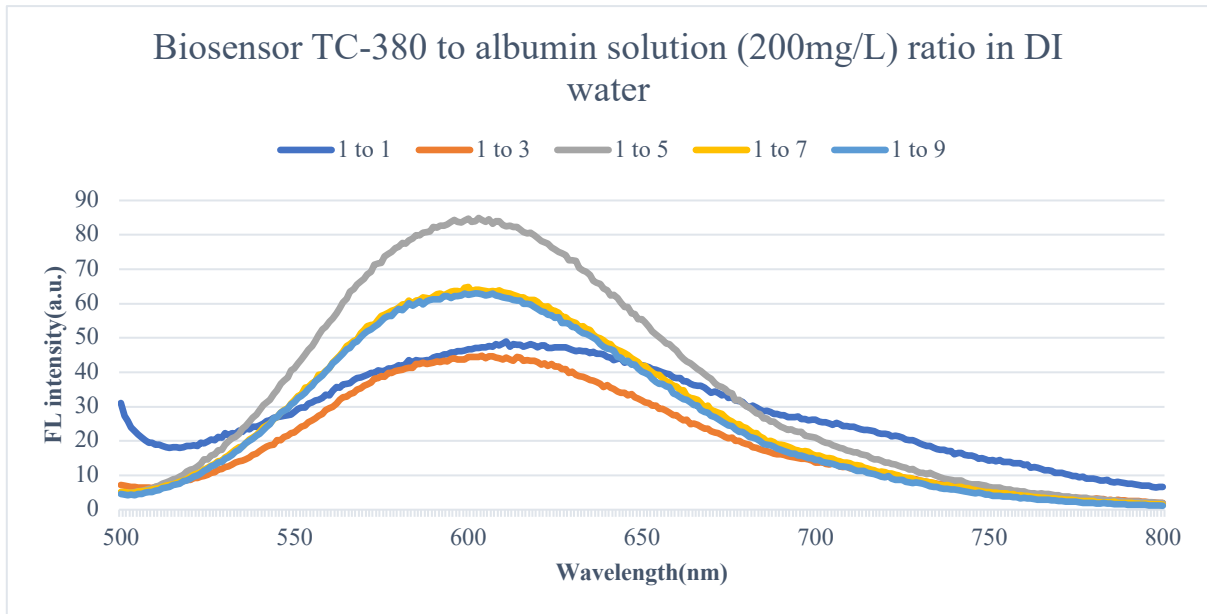


Figure 11. TC-380 to albumin ratio at 200 mg/L HSA concentration in DI water

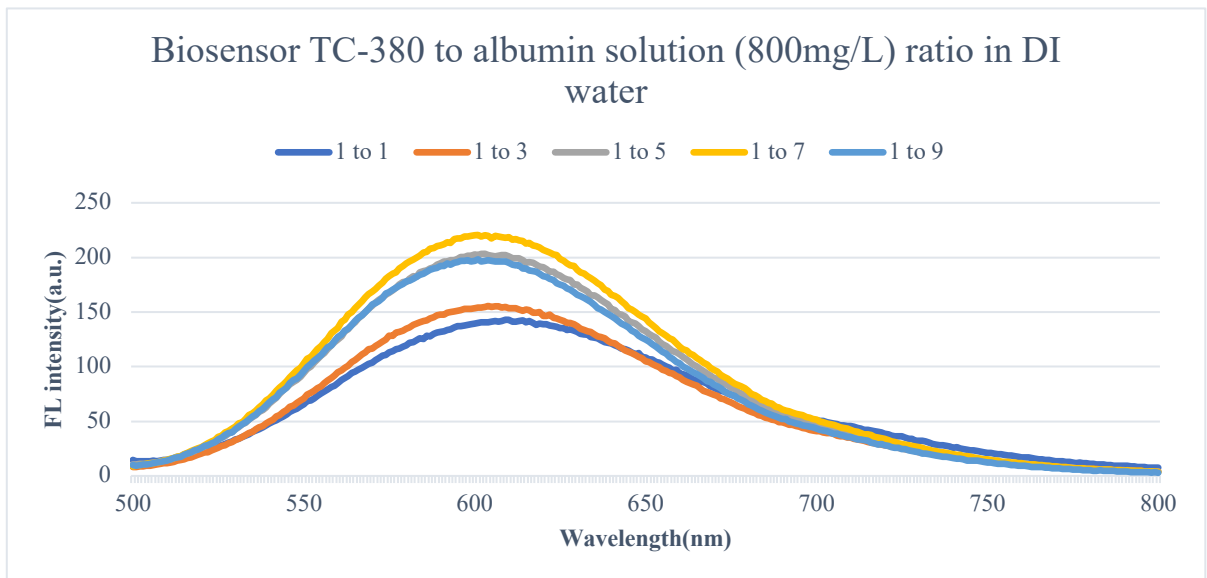


Figure 12. TC-380 to albumin ratio at 800 mg/L HSA concentration in DI water

From these two figures, it is clear that 1:5 is the best ratio in 200 mg/L HSA solution in the meantime 1:7 is the best ratio in 800 mg/L HSA solution. At a concentration of 200 mg/L, the 1:5 curve is significantly better than the other four. However, the fluorescence intensity of 1:5, 1:7 and 1:9 are relatively close at the 800 mg/L concentration, and 1:7 is only slightly higher than the other two.

By selecting the points on each emission peak at different ratios, the ratio versus fluorescence intensity changing curve and histogram are shown in the Figure 13 and 14 below.

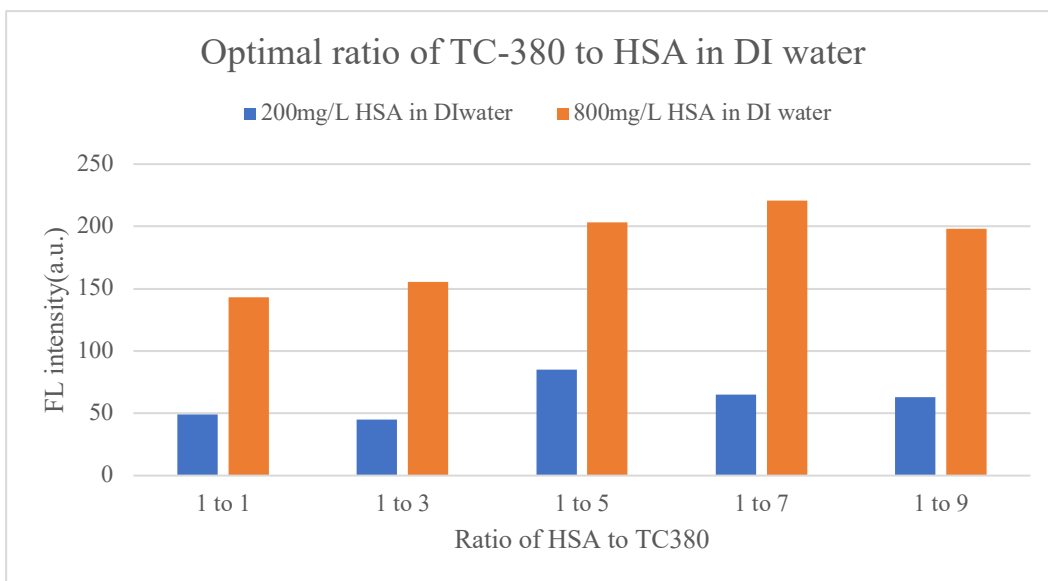


Figure 13. Different ratios of TC-380 to HSA solution at 200 and 800 mg/L HSA concentration in DI water

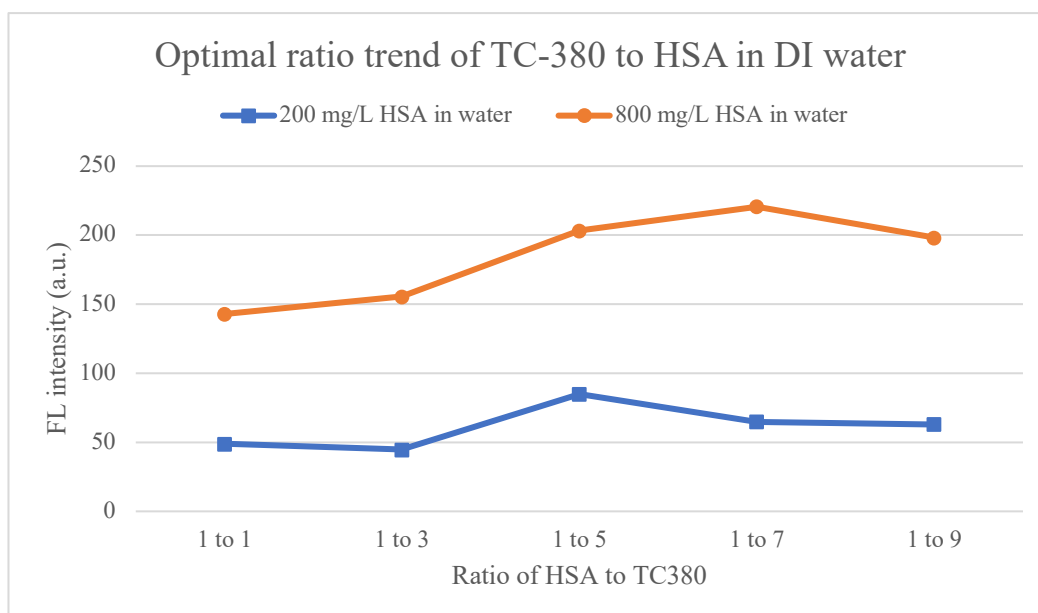


Figure 14. Trends of different ratios of TC-380 to HSA at 200 and 800 mg/L HSA concentration in DI water

From the results, there is a significant difference between the high and low concentration albumin solutions, which shows that TC-380 is directly related to the level of the albumin concentration. The difference is greatest when the ratio of probe to albumin solution is 1:7. Nevertheless, the albumin detection in this experiment was designed based on a microalbumin environment (20-200 mg/L). The stronger fluorescence intensity in the microalbumin range is more meaningful and can better reflect the sensitivity of the probe. The greater the FL intensity at the concentration of 200 mg/L, the better the performance of TC-380 in the micro range can be evaluated. Hence, 1:5 is the best bioprobe to albumin solution ratio for TC-380 in an aqueous circumstance.

#### 4.1.2.3 Correlation between different HSA concentrations and their fluorescence intensity

The previous two measurements have determined that the reaction time is 20 minutes and the ratio is 1:5. Under this condition, the correlation between different HSA concentration and their fluorescence intensity obtained by TC-380 excitation at 481nm is shown below.

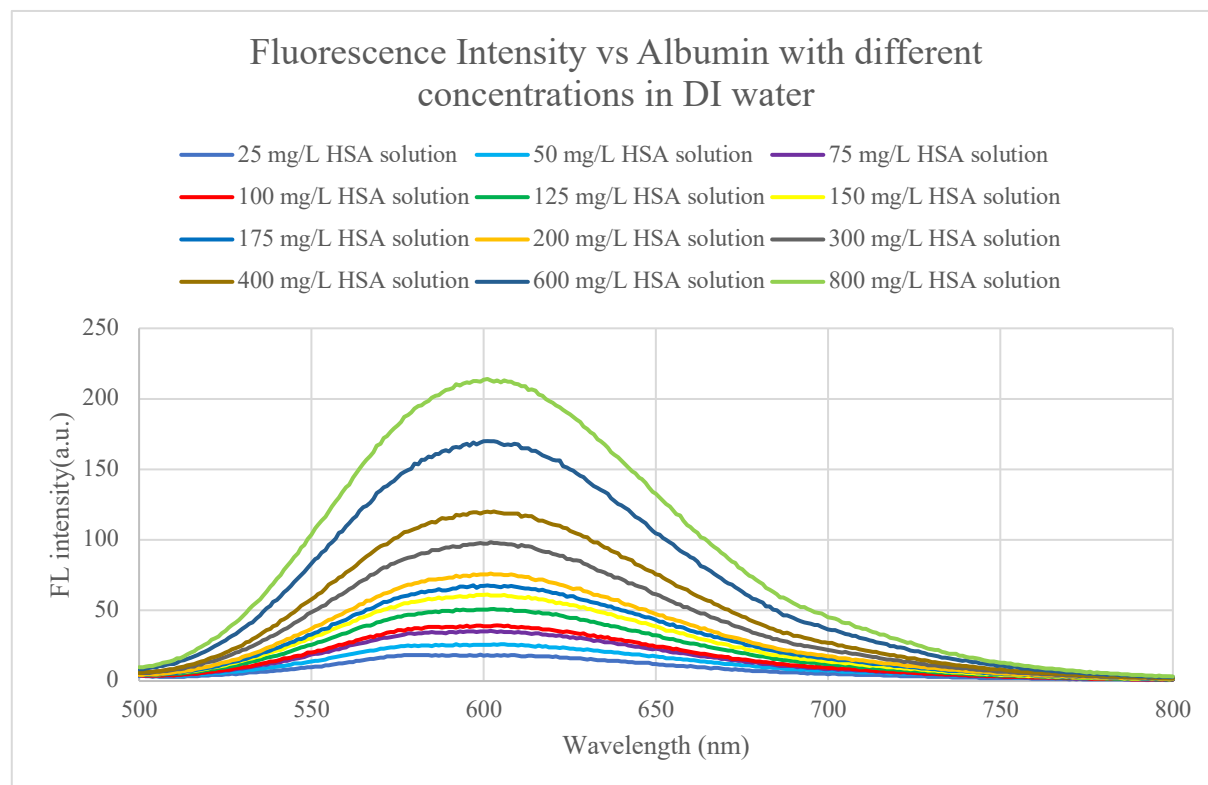


Figure 15. Correlation between different HSA concentration and their fluorescence intensity in DI water

It can be seen from the above figure that the emission peaks of all samples are around 602 nm, and as the HSA concentration increases from low to high, the fluorescence intensity also goes up and the increment in fluorescence intensity seems to be traceable. There is no doubt that the response of the probe towards the albumin solution is positive going. This indicates within a certain concentration range, the fluorescence intensity of TC-380 has a positive correlation with the albumin concentration, that is, the degree of response of TC-380 to albumin is HSA concentration dependent.

#### 4.1.2.4 Master curve

The main curve is shown in the Figure 16 below. It can be seen from the figure that the fluorescence intensity increases with the concentration gradient of HSA showing a clear positive linear relationship, and  $R^2 = 0.9943$  proves that the curve fits very well. Since there are almost no excessive external interference factors in the deionized aqueous solution, the fluorescence intensity in the aqueous solution can intuitively show the degree of response for the probe towards albumin at low concentrations. It is clear that the probe can stably detect

albumin in the microalbumin concentration range 25-200 mg/L, but the FL intensity at low concentration is not strong enough.

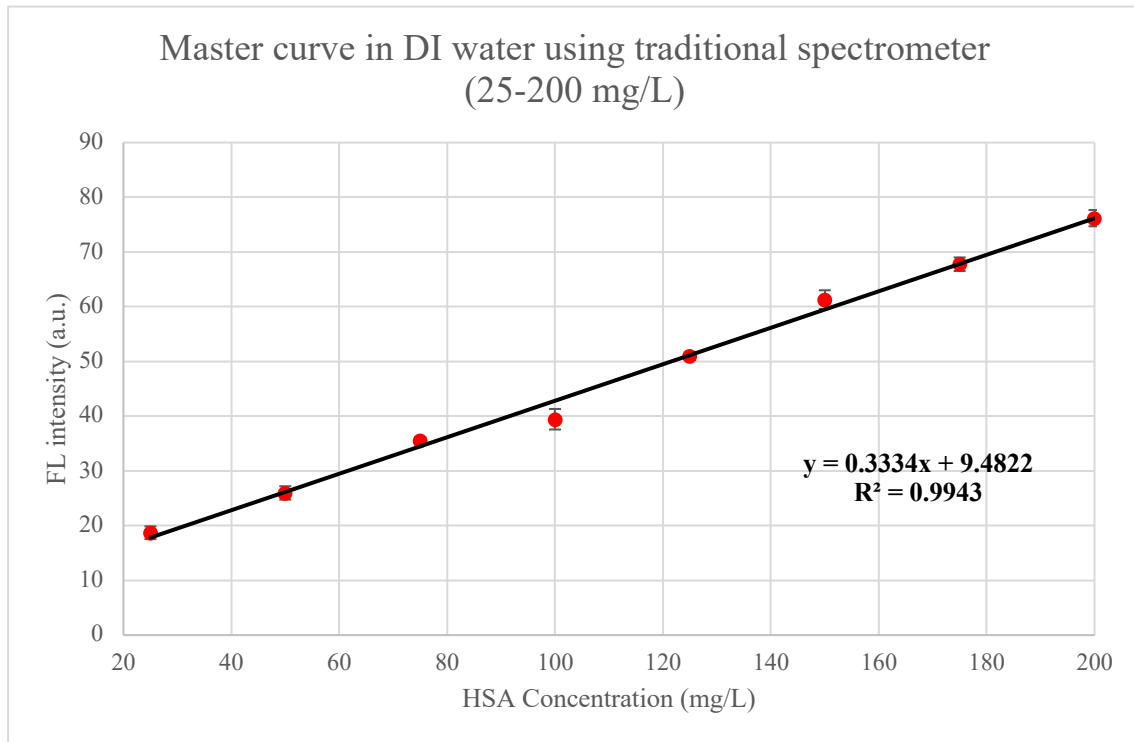


Figure 16. Master curve in DI water from 25- 200 mg/L HSA concentration using traditional spectrometer

When the master curve is in the range of 25 mg/L to 800 mg/L, the linear relationship is still very significant. This also proves that TC-380 can sensitively detect albumin in a wide range in the environment of deionized water.

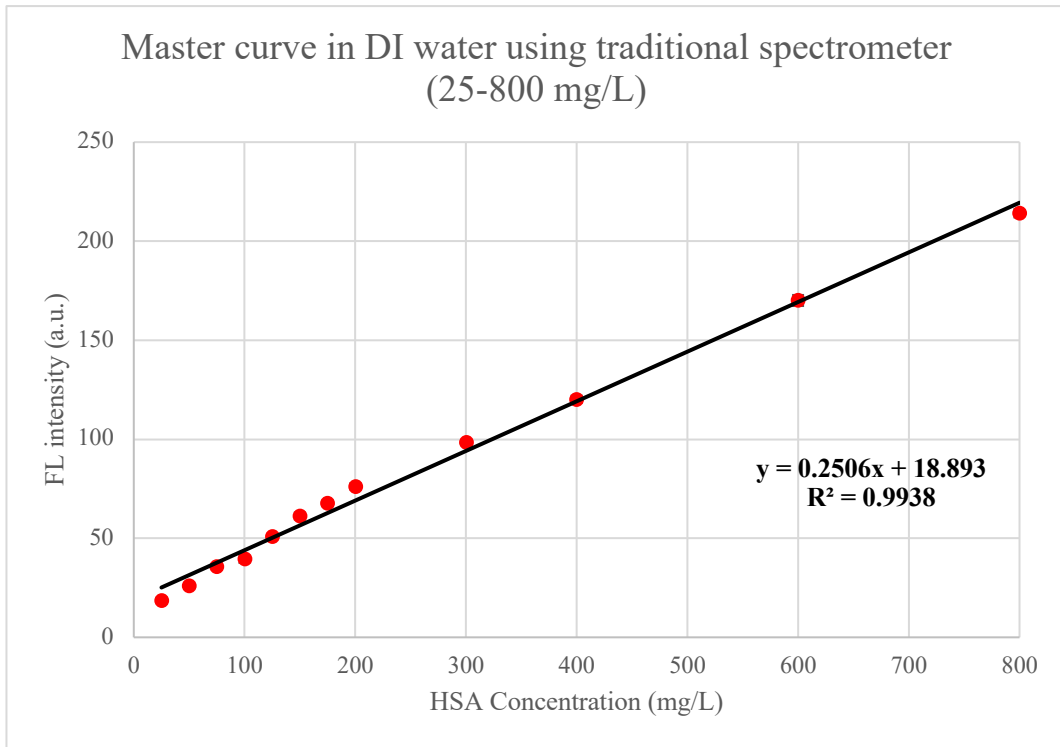


Figure 17. Master curve in DI water from 25- 800 mg/L HSA concentration using traditional spectrometer

#### 4.1.2.5 Validation

The result is shown as Figure 18 below. As the concentration increases, the fluorescence intensity increases successively. There is a little change in the three concentrations of five samples. It indicates that their fluorescence intensity values at corresponding concentration are stable, and the average value is 25, 40 and 75 arbitrary units respectively. In addition, the result also proves that the experiment itself is highly repeatable.

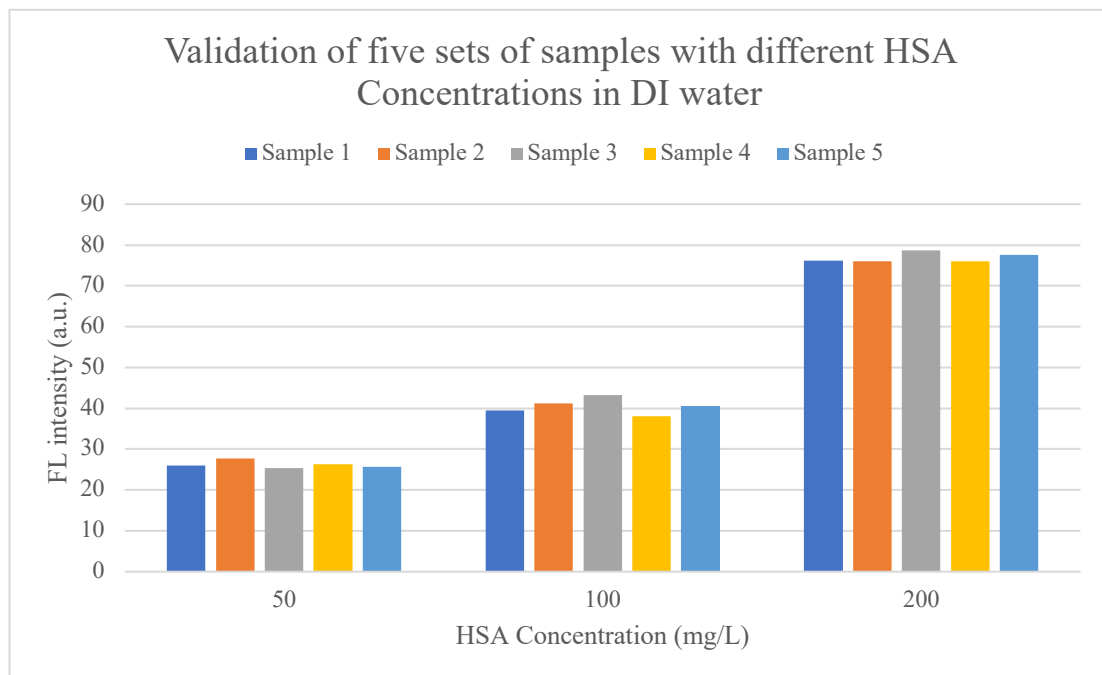




Figure 18. Validation of Master curve in DI water using five sets of samples with three different HSA concentrations: 50, 100, 200 mg/L

Through the previously designed verification method, the average value and standard deviation of each concentration are calculated as  $54.84 \pm 2.78$ ,  $101.13 \pm 5.72$  and  $207.53 \pm 3.63$  respectively. Change rates at 50, 100, 200 mg/L HSA concentration are 9.68%, 1.13% and 3.77%. Above all, the concentrations of HSA detected by TC-380 were all within 10% of the artificially added concentrations.

[HSA] (mg/L)		Change (%)
Added artificially	Detected mean $\pm$ SD	
50.00	$54.84 \pm 2.78$	9.68 %
100.00	$101.13 \pm 5.72$	1.13 %
200.00	$207.53 \pm 3.63$	3.77 %

Table 6. Concentration of HSA detected by the SOP for TC-380 in DI water

The validation result proves accuracy of the master curve in the meantime FL intensity, the sensitivity and linear range of the curve are meaningful. Furthermore, in addition to excluding the interference of artificial factors and other uncontrollable factors, the smaller rate of change and close values between actual average concentrations and spiked concentrations all represent the higher repeatability of the curve. Therefore, it can be concluded that the detection performance of the probe in DI water is excellent.

### 4.1.3 Optimal working conditions of TC-380 in artificial urine

#### 4.1.3.1 Reaction time

The measurement conditions of the reaction time in artificial urine are consistent with the previous measurement in DI water. The results are shown in the Figure 19, and it is clear that both results in water and that in artificial urine are similar. Before 10 minutes, the intensity increased slightly as the reaction progressed. After 10 minutes, the fluorescence intensity stabilized. In order to ensure that the probe and HSA can fully react, the reaction time is also set to 20 minutes.

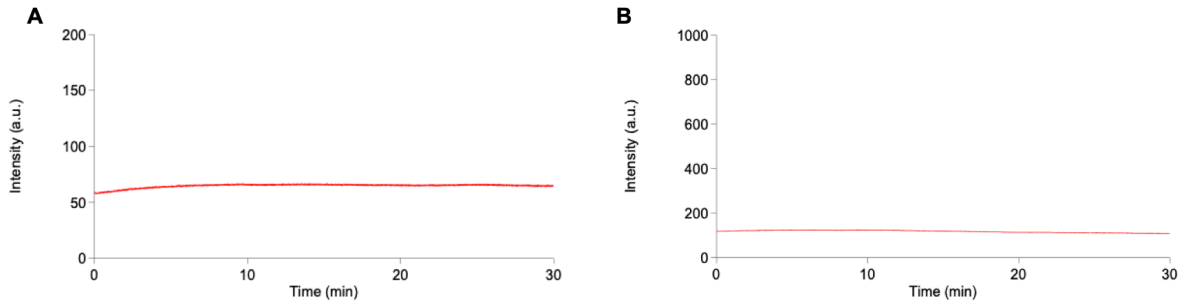


Figure 19. Reaction time at (A) 200 mg/L and (B) 800 mg/L HSA concentration in artificial urine

#### 4.1.3.2 TC-380 to HSA solution ratio

The reaction time measured in an artificial urine environment is known to be 20 minutes. Using the same steps as the previous measurement in DI water, two concentrations of 200 and 800 mg/L were selected for comparison. The results are as follows.

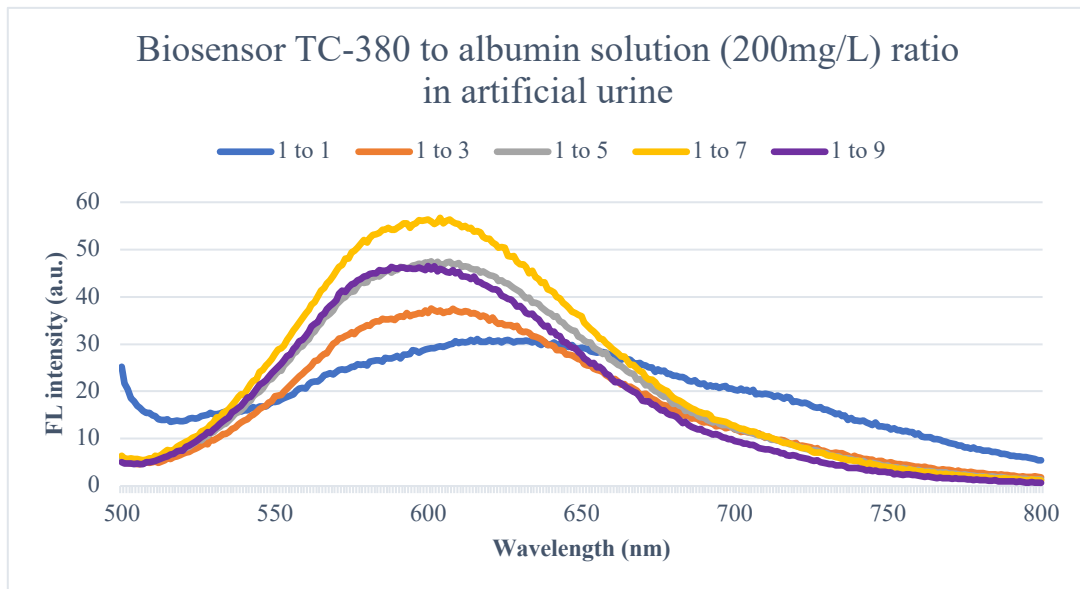


Figure 20. TC-380 to albumin ratio at 200 mg/L HSA concentration in artificial urine

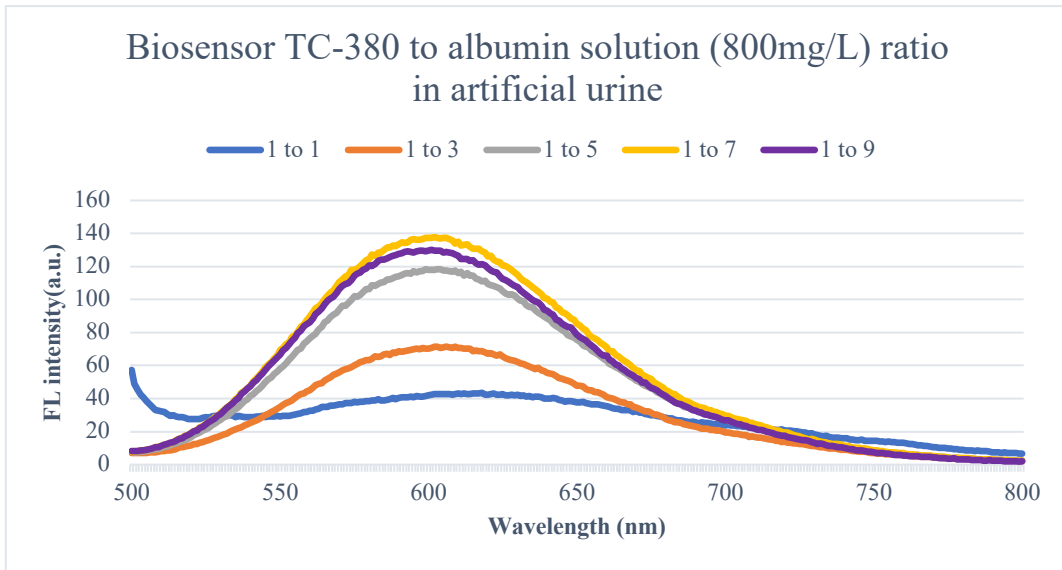


Figure 21. TC-380 to albumin ratio at 800 mg/L HSA concentration in artificial urine

It can be seen from the above two figures that at a concentration of 200 mg/L, 1:7 is the optimal ratio, and all ratios in fluorescence intensity are at low level. At a concentration of 800 mg/L, 1:7 is still the best ratio. But there is a greater increase in FL intensity between 1:5, 1:7, 1:9 and 1:1, 1:3.

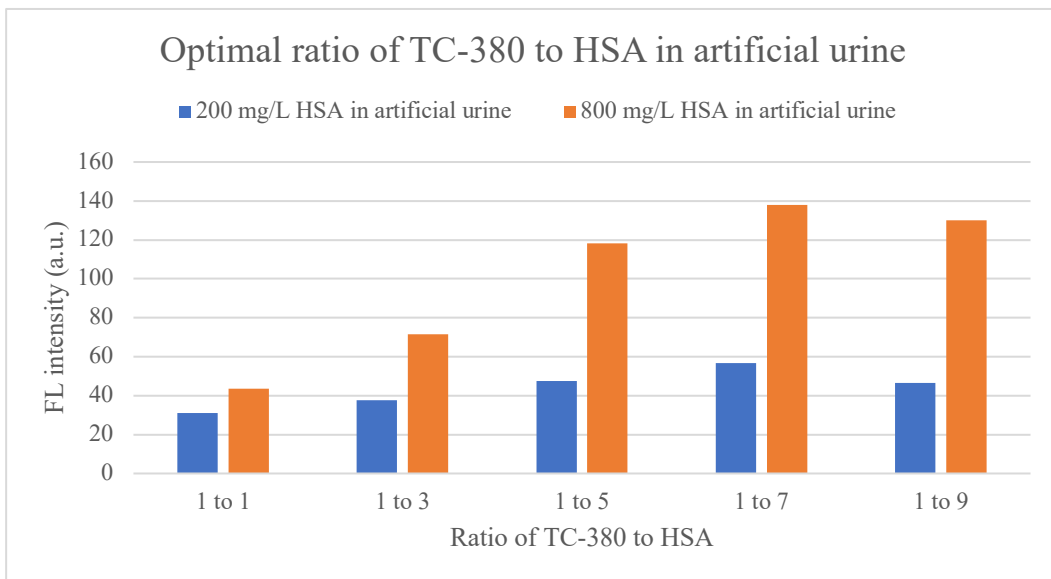


Figure 22. Different ratios of TC-380 to HSA solution at 200 and 800 mg/L HSA concentration in artificial urine

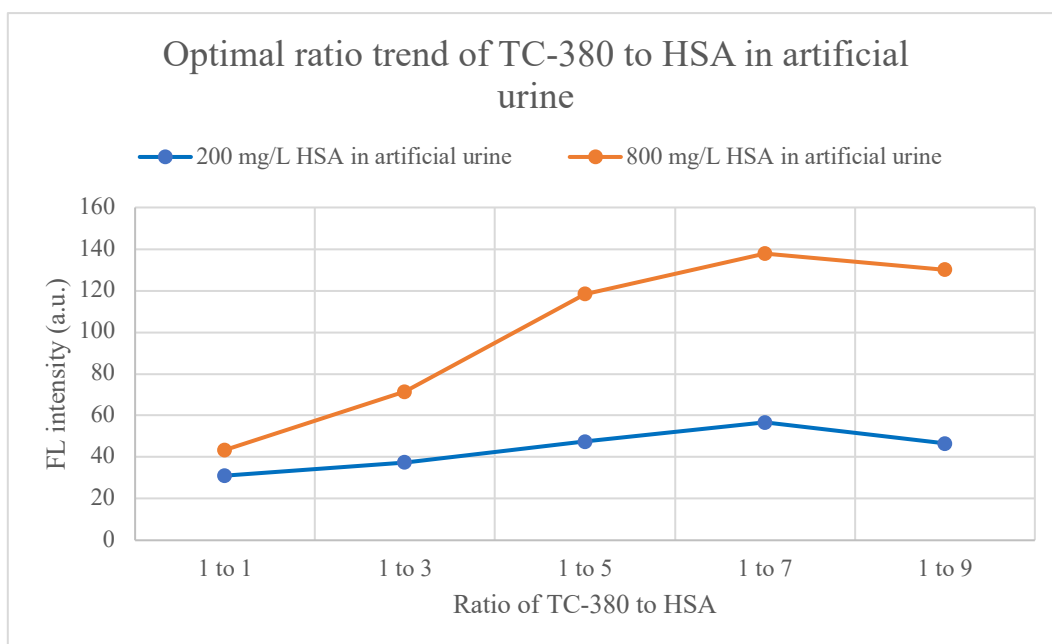


Figure 23. Trends of different ratios of TC-380 to HSA at 200 and 800 mg/L HSA concentration in artificial urine

From the results, there is a significant difference between the high and low concentration albumin solutions, which shows that TC-380 is directly related to the level of the albumin concentration. Furthermore, it can be seen that as the reaction ratio increases, which indicates that more albumin molecules are added, the fluorescence intensity gradually increases and reaches the maximum value at 1:7. After 1:7, the intensity began to weaken. This shows that at the ratio of 1:7, all of TC-380 have been reacted. At this time, if the albumin solution is continued to be added, there will only be the function of dilution, resulting in the reduction of the FL intensity. Hence, 1:7 is the optimal bioprobe to albumin solution ratio for TC-380 in an artificial urine circumstance.

#### 4.1.3.3 Correlation between different HSA concentrations and their fluorescence intensity

The previous two measurements in artificial urine have determined that the reaction time is 20 minutes and the ratio is 1:7. Under this condition, the correlation between different HSA concentration and their fluorescence intensity obtained by TC-380 excitation at 481nm is shown below.

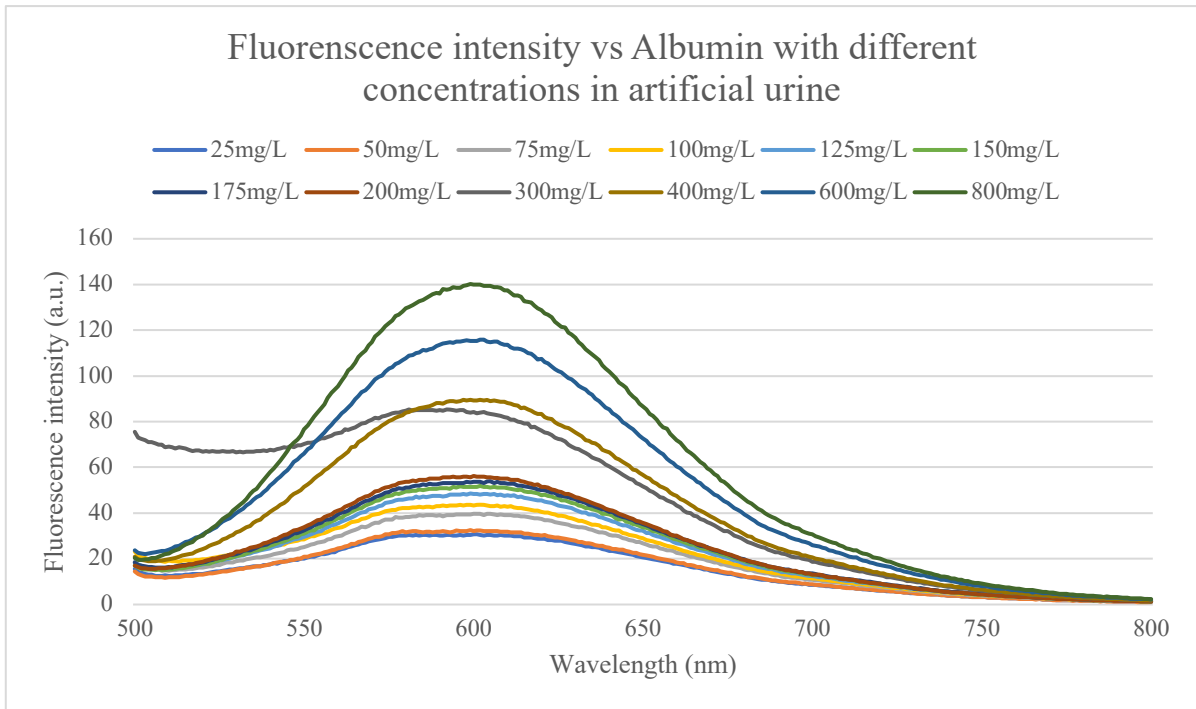


Figure 24. Correlation between different HSA concentration and their fluorescence intensity in artificial urine

The result is similar to the relationship in DI water, the emission peaks are all around 602nm, the fluorescence intensity increases with the increase of HSA concentration, and the positive correlation is obvious from 25 mg/L to 800 mg/L HSA concentration.

#### 4.1.3.4 Master curve

The master curve in artificial urine is shown in the Figure 25 below. The fluorescence intensity presents an obvious positive linear relationship with the increase of the HSA concentration gradient.  $R^2 = 0.9729$  proves that the curve fits well. Due to interference of artificial urine contains a lot of ions ( $\text{Na}^+$ ,  $\text{K}^+$ ,  $\text{Mg}^{2+}$ ,  $\text{SO}_4^{2-}$ ,  $\text{CO}_3^{2-}$  etc.), the fluorescence intensity decreases overall. However, the presence of these ions does not affect the linear relationship between albumin and TC-380, that is, the ions does not affect the detection of TC-380 towards albumin. TC-380 can still detect albumin stably in artificial urine in the microalbumin concentration range of 25-200 mg/L.

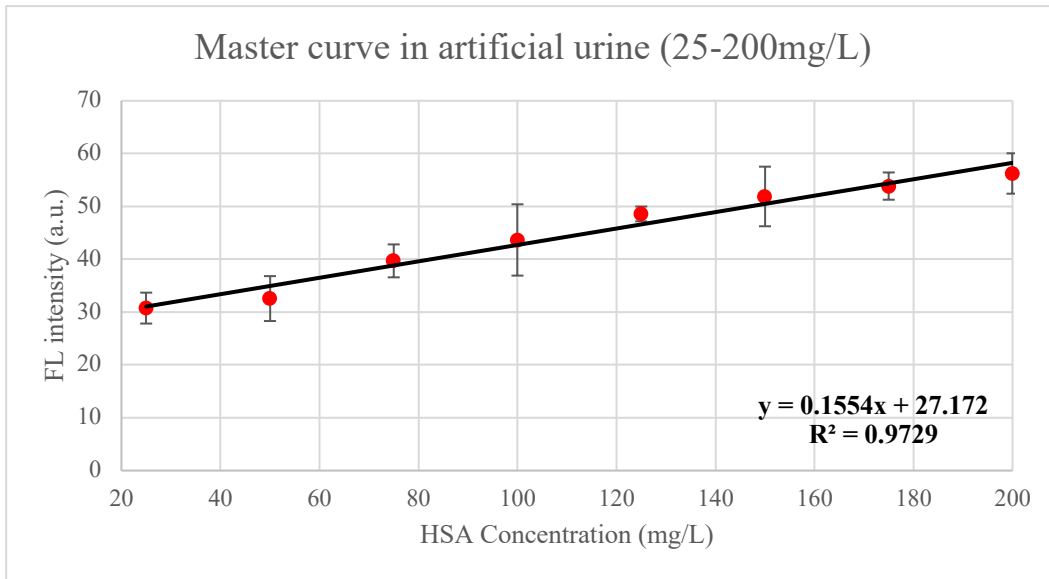


Figure 25. Master curve in artificial urine from 25- 200 mg/L HSA concentration using traditional spectrometer

When the master curve is extended to the range of 25 mg/L to 800 mg/L, the linear relationship is still the same, which proves that TC-380 can detect albumin widely and sensitively in artificial urine environment.

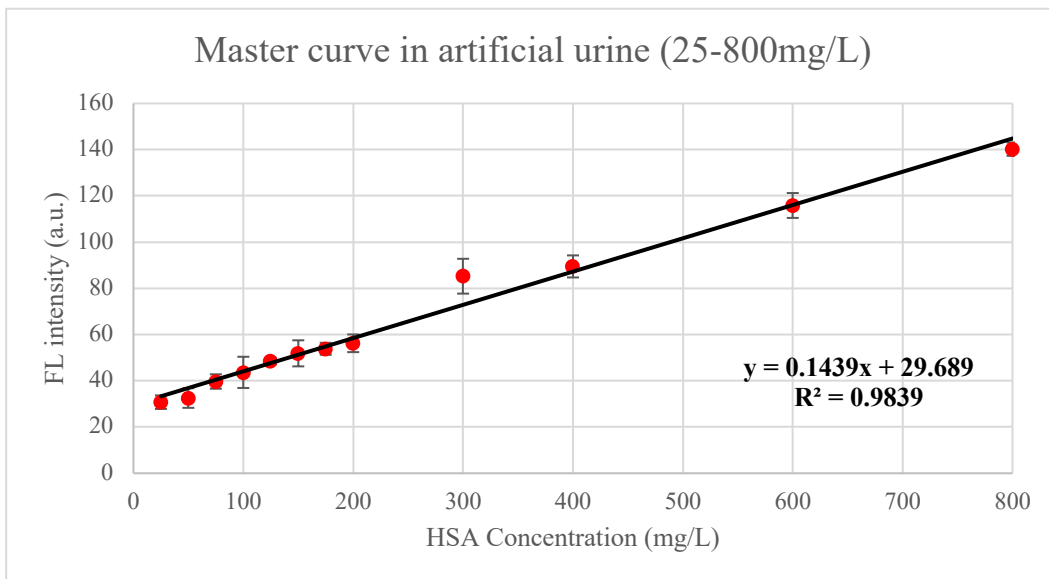


Figure 26. Master curve in artificial urine from 25- 800 mg/L HSA concentration using traditional spectrometer

#### 4.1.3.5 Validation

The fluorescence intensity values of the five samples under the three groups of concentrations (50, 100, 200 mg/L) are relatively stable, and the average value is 34, 42, 55 a.u. respectively. The result is shown as Figure 27 below.

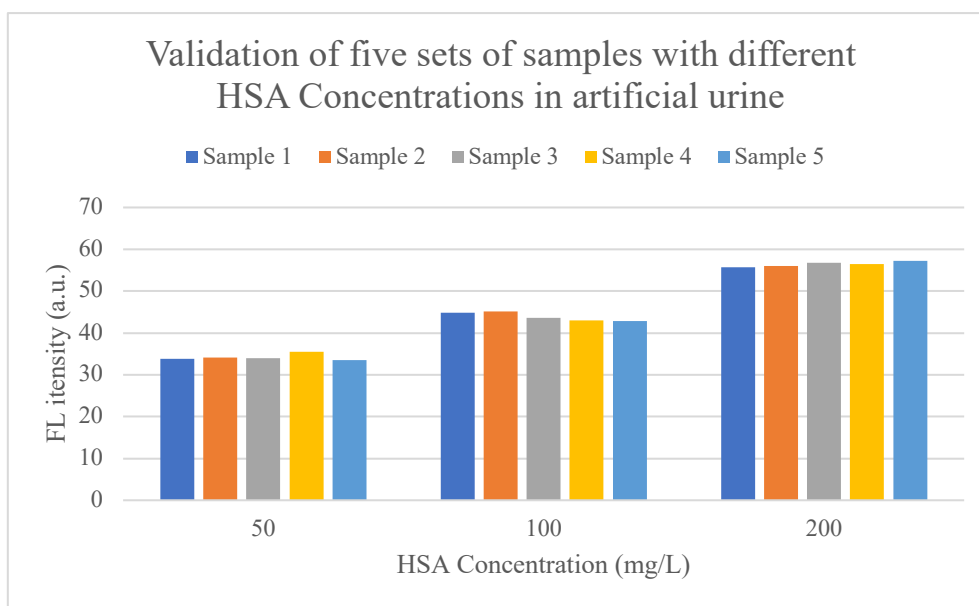


Figure 27. Validation of Master curve in artificial urine using five sets of samples with three different HSA concentrations: 50, 100, 200 mg/L

The average value and standard deviation of each concentration are calculated as  $45.09 \pm 4.79$ ,  $107.56 \pm 6.66$  and  $188.21 \pm 4.04$  respectively. Change rates at 50, 100, 200 mg/L HSA concentration are 9.82%, 7.56% and 5.89%. Above all, the concentrations of HSA detected by TC-380 were all within 10% of the artificially added concentrations.

[HSA] (mg/L)		Change (%)
Added artificially	Detected mean $\pm$ SD	
50.00	$45.09 \pm 4.79$	9.82 %
100.00	$107.56 \pm 6.66$	7.56 %
200.00	$188.21 \pm 4.04$	5.89 %

Table 7. Concentration of HSA detected by the SOP for TC-380 in artificial urine

The validation result proves that the master curve is reasonable. In addition, even if there are a large number of irrelevant ions, there is still a small rate of change between the actual average concentration and the artificially added concentration in artificial urine. This fact shows indirectly that HSA detection has relative high repeatability in artificial urine environment. Therefore, TC-380 has excellent detection performance in artificial urine.

#### 4.1.3.6 Creatinine influence

It can be seen from the figure that there is no influence before and after adding creatinine. The slopes of the two curves are almost the same and the variation range of the two curves is within

the standard error of each other. Furthermore, it proves that adding creatinine will slightly decrease the fluorescence intensity but the linear relationship remains unchanged. Therefore, the detection of TC-380 to HSA is not affected generally, indicating that TC-380 has a high level of specificity for HSA in this microalbumin range.

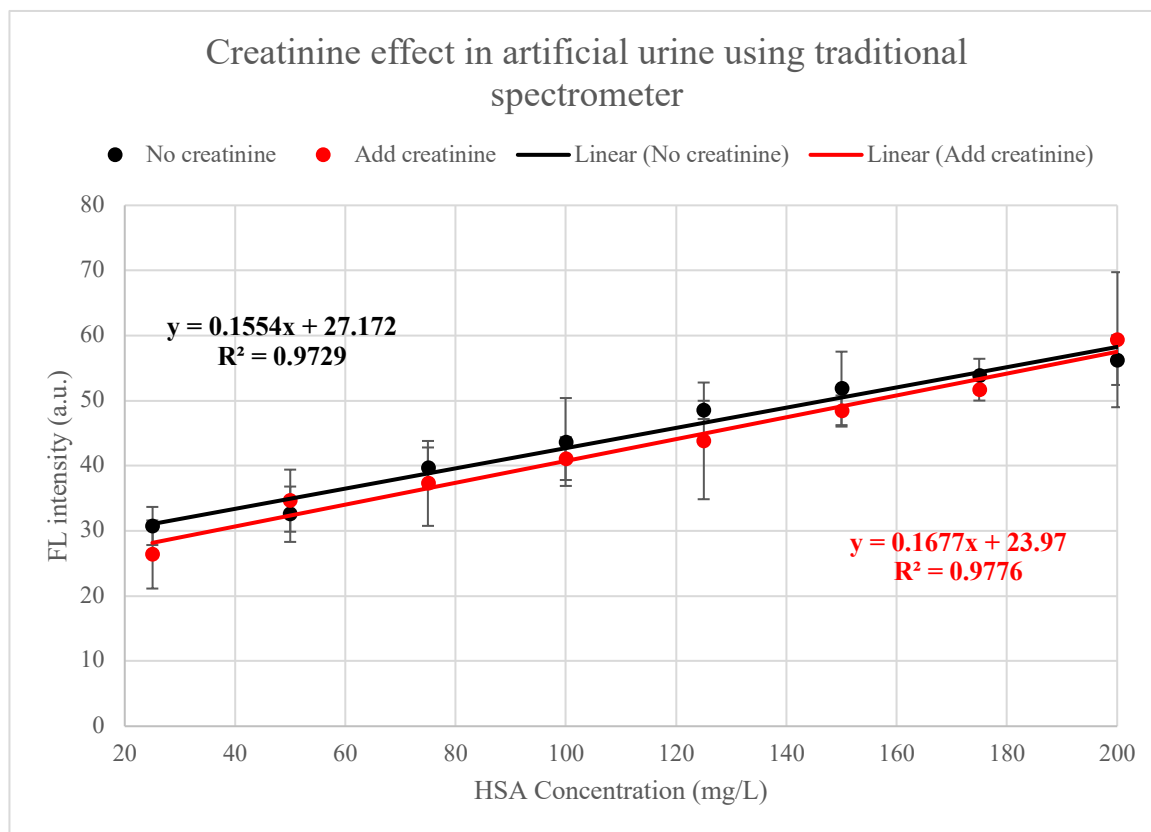


Figure 28. Creatinine influence in artificial urine

#### 4.1.4 Optimal working conditions of TC-380 in human urine

##### 4.1.4.1 Dilution of urine ratio

The results are shown in the Figure 29 and 30 below. From the blank sample, it can be seen that when urine sample is excited at 481nm, autofluorescence will be generated at about 540nm. As the multiple of the dilution ratio gradually increases, the fluorescence intensity will decrease accordingly. Unfortunately, the intensity of autofluorescence is still much greater than the emission peak of the TC-380 specifically binding to albumin. Therefore, the autofluorescence peak gradually broadened after dilution to cover the characteristic peak at 602 nm. In other words, a valid reaction peak in the urine cannot be detected even if it is diluted 9 times and the positions of the two peaks are relatively close, which means they cannot be distinguished.



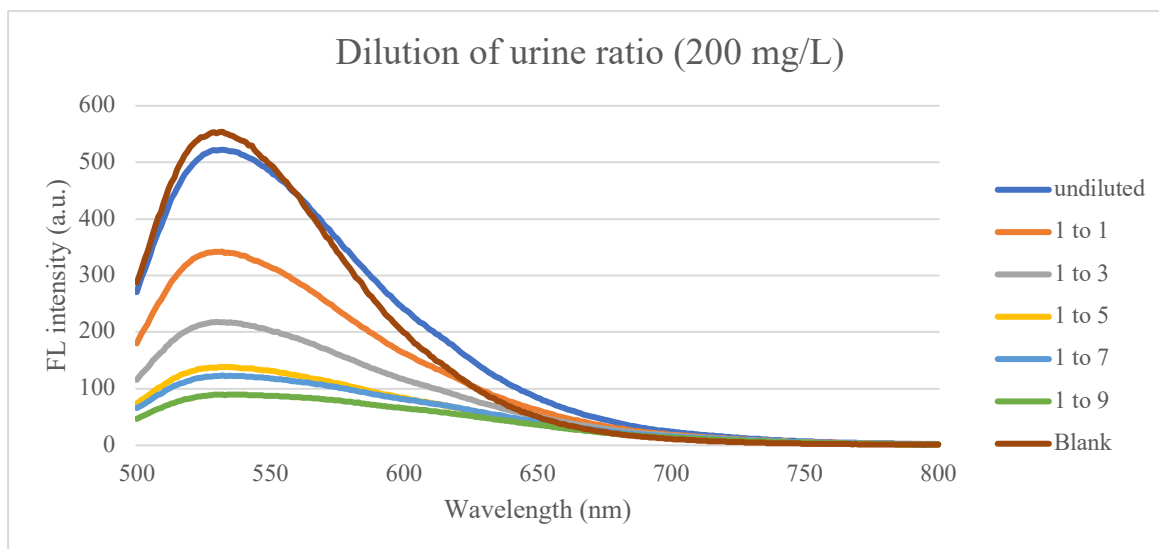


Figure 29. Dilution of urine ratio at 200 mg/L HSA concentration in human urine

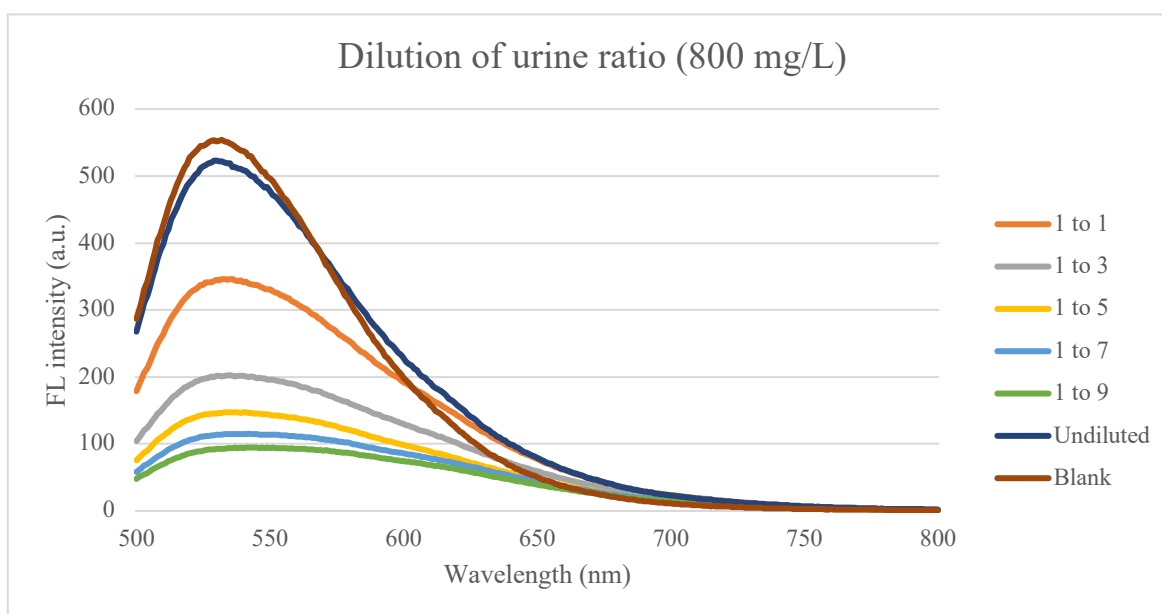


Figure 30. Dilution of urine ratio at 800 mg/L HSA concentration in human urine

#### 4.1.4.2 Obstacles to urine testing in traditional spectrometer and potential improvement

From the results of urine dilution, it is impossible to avoid the problem of autofluorescence in urine in the detection environment of traditional spectrometers. The problem of autofluorescence also caused the subsequent detection steps to fail. Therefore, the emergence of fiber optic systems is an ideal way to improve this problem because fiber optic systems not only can reduce electromagnetic interference but also can maximize the collection of scattered light and ensure the minimum light loss during transmission. The advantages of the optical fiber system allow it to theoretically have higher sensitivity, which also means that the optical fiber system may achieve enhanced sample fluorescence intensity. Therefore, there is an

expectation that the fiber optics system is still able to detect the characteristic peak of the probe to albumin under the interference of autofluorescence and FL intensity of this reaction peak becomes stronger. In this way, the interference of autofluorescence can be minimized, or even to the extent that it does not affect albumin detection at all.

#### **4.1.5 Comparison between DI water and artificial urine using traditional spectrometer**

##### *4.1.5.1 Master curve comparison between DI water and artificial urine*

The master curves in deionized water and artificial urine are shown in the Figure 31 below. Firstly, the linear correlation is proved no matter where TC-380 exists. Afterwards, the curve in DI water has a greater slope than the curve in artificial urine, which indicates that the sensitivity of water detection is higher than that of artificial urine. The reason is that, in fact, the presence of multiple ions in artificial urine affects the detection of albumin by TC-380, thereby reducing the fluorescence intensity. There are almost no interference items in the DI water at the same time. Theoretical analysis is consistent with actual results.

If the detection sensitivity in DI water is higher than that of artificial urine in theory, the master curve of DI water should all be above the master curve of artificial urine in microalbumin range (25-200 mg/L). However, the fact is that the two master curves intersect at an albumin concentration of 100 mg/L. This shows that the use of a general spectrometer for albumin detection below 100 mg/L may not be sensitive enough. In fact, the detected fluorescence value is also at a low level, reflecting the limitation of the detection sensitivity of the ordinary spectrometer itself and its possible insufficient detection limit.

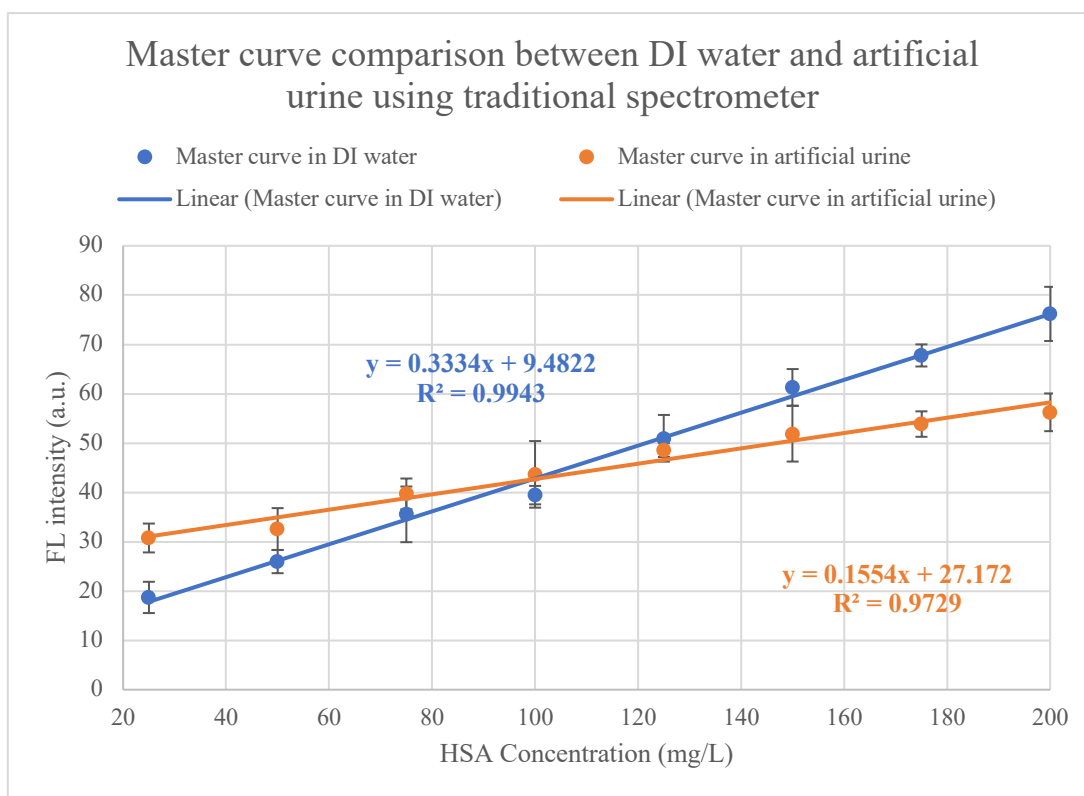


Figure 31. Master curve comparison between DI water and artificial urine using traditional spectrometer

#### 4.1.5.2 Detection limit in spectrometer

From the Figure 32, in DI water, 1 mg/L and 5 mg/L increase the intensity of about 2 a.u. compared with the blank, but the difference is small. When the albumin concentration increased to 25 mg/L, the fluorescence intensity increased nearly three times compared to the blank value. Similarly, the difference between 1, 5 mg/L and the blank is relatively small in artificial urine. However, when the concentration rises to 25 mg/L, the FL intensity increases to more than twice the original. Consequently, in order to ensure that the measured results are easy to distinguish and obvious, the conclusion is that the detection limit in DI water and artificial urine is 25 mg/L.

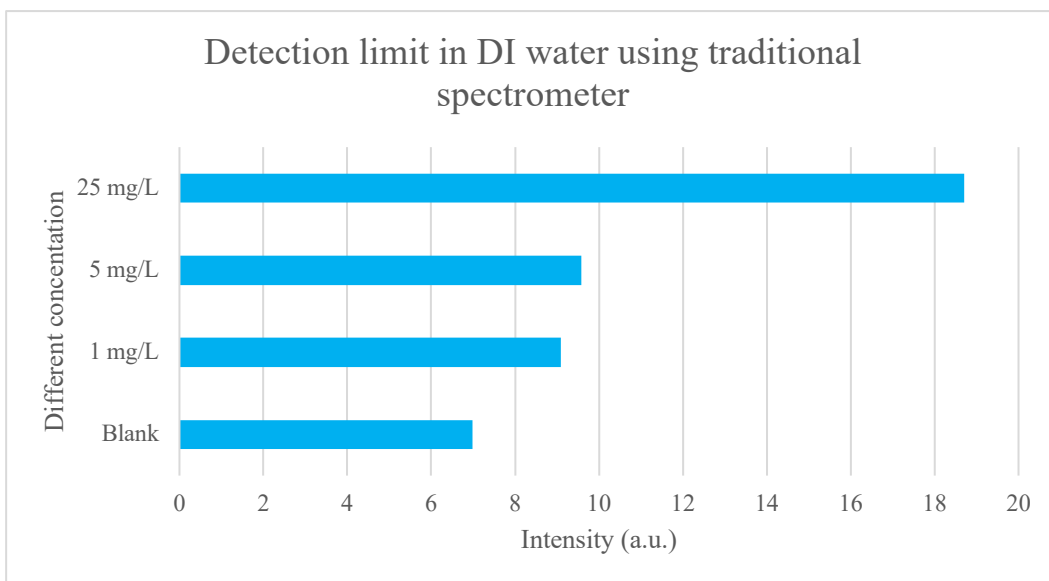


Figure 32. Detection limit in DI water using traditional spectrometer

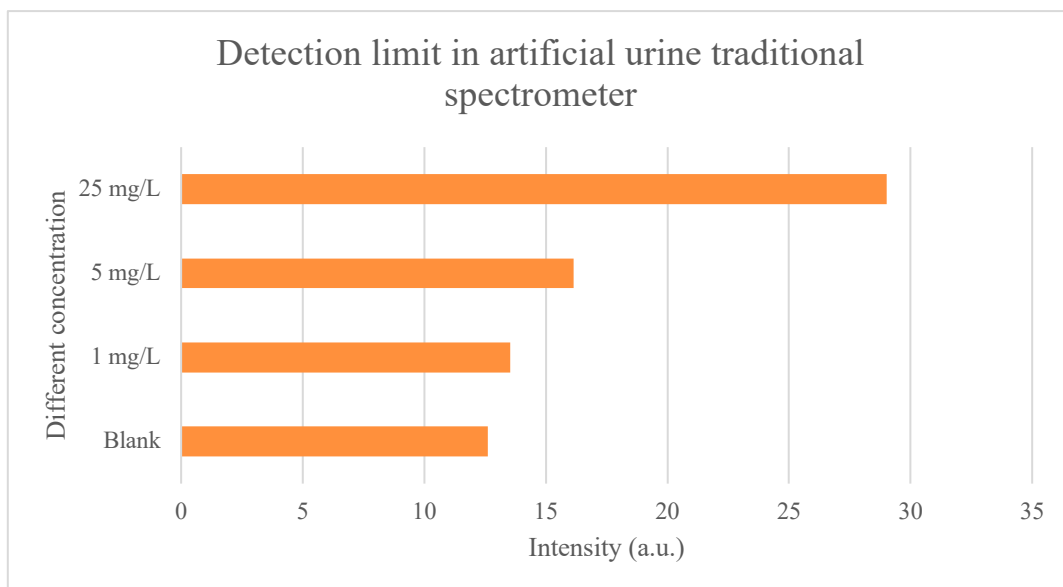


Figure 33. Detection limit in artificial urine using traditional spectrometer

#### 4.1.6 Result of SOP using spectrometer

Based on the above measurements, the result of SOP using spectrometer is summarized as Table 8 below.

Optimal operating conditions	Deionized water	Artificial urine	Human urine
Excitation and Emission Wavelength	481/602 nm		

Bioprobe concentration	10 $\mu$ M		
HSA concentration	0~800 mg/L		
Reaction time	20 minutes		
Bioprobe: albumin solution ratio	1:5	1:7	—
Master curve	Linear		—
Creatinine effect	—	No influence	—
Detection limit	25 mg/L		—

Table 8. Result of Standard operating procedure of TC-380 ('—' represents no results or no measurements)

## 4.2 Optical fiber system

### 4.2.1 Measurement of seven bioprobes

According to the previous spectrometer measurements, the AIE characteristics of the seven probes have been measured but the result is not desirable. Five sets of bioprobes are not detected in their own emission wavelength. Therefore, based on the advantages of the optical fiber system itself and combined with the excitation wavelength measured before. The results of scanning and detection by using the fiber optic system are shown below.

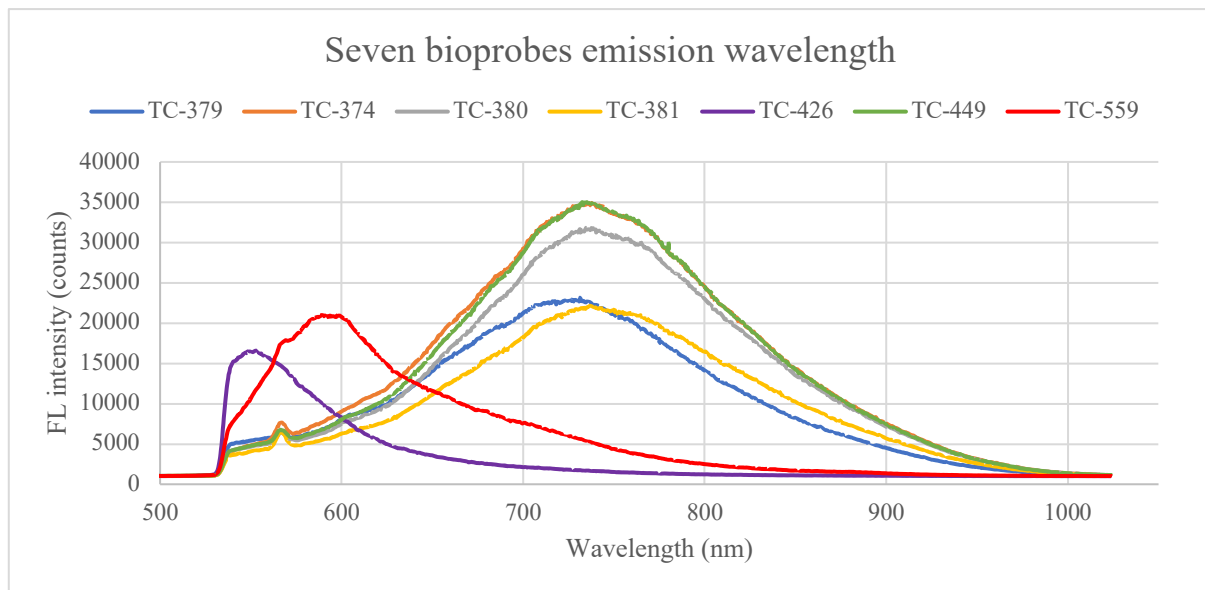


Figure 34. AIE attributes in emission wavelength of 7 bioprobes using fiber optics

From the scanning results above, the excitation and emission wavelengths of the seven probes measured by the optical fiber system are listed as shown in the following table.

Name	Excitation wavelength (nm)	Emission wavelength (nm)
TC-374	466	737
TC-379	458	731
TC-380	481	738
TC-381	468	737
TC-426	518	552
TC-449	466	735
TC-559	511	590

Table 9. Excitation and emission wavelength of 7 bioprobes

Under the fiber optics system, the AIE characteristics of all probes can be directly measured, which is in sharp contrast with the scanning results of ordinary spectrometers. In order to prove that the fiber optic system has better detection sensitivity, TC-380 continues to be used as a research object. Furthermore, keeping the same experimental conditions and steps under the two systems, the pros and cons of the two systems can be evaluated through parallel setups.

#### **4.2.2 Optimal working conditions of TC-380 in deionized water**

##### *4.2.2.1 Reaction time and TC-380 to HSA solution ratio*

According to the previous measurement of DI water in the spectrometer, the optimal reaction time and TC-380 to HSA solution ratio have been obtained. Therefore, these parameters are directly used in fiber optics measurements. Specifically, reaction time is 20 minutes and TC-380 to HSA solution ratio is 1:5.

##### *4.2.2.2 Correlation between different HSA concentrations and their fluorescence intensity*

Under fiber optics sensor, the correlation between different HSA concentration and their fluorescence intensity obtained by TC-380 excitation at 481nm is shown below.

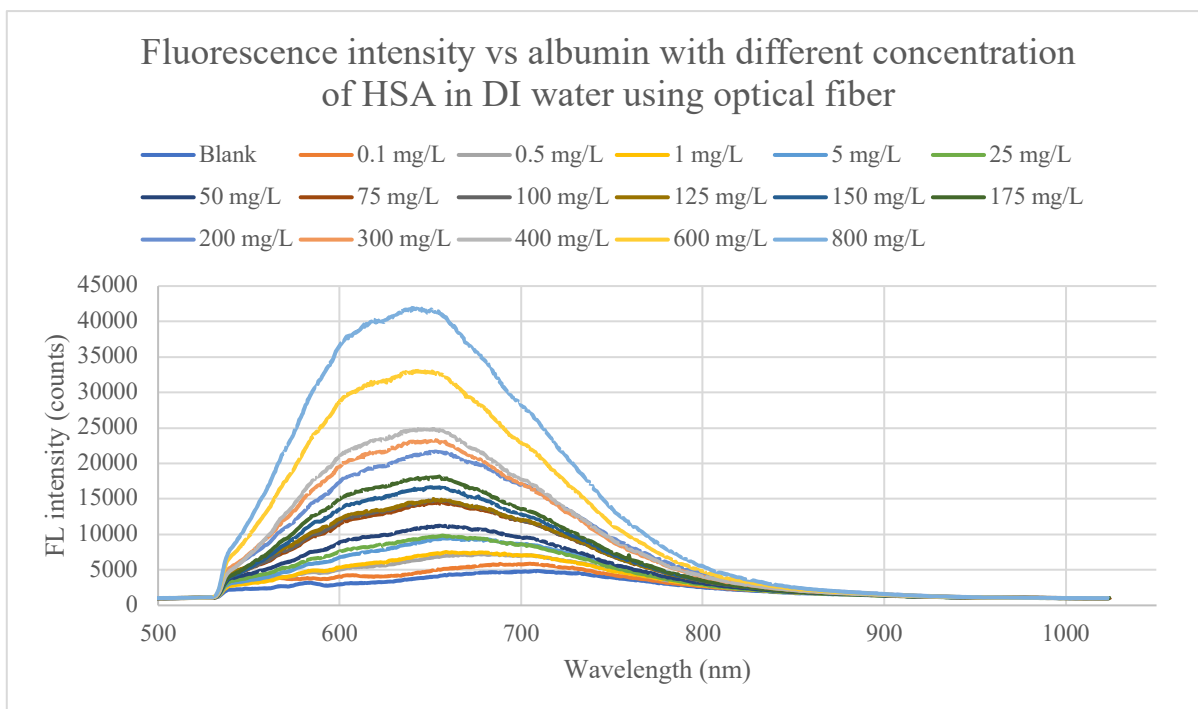


Figure 35. Correlation between different HSA concentration and their fluorescence intensity in DI water using optical fiber

It can be seen from the above figure that the emission peaks of all samples are around 645 nm, which is different from the emission peak of 602 nm in spectrometer testing. As the HSA concentration increases from low to high, the fluorescence intensity also goes up. Obviously, there is a positive correlation from 0 mg/L to 800 mg/L HSA concentration, which also proves that the degree of response of TC-380 to albumin is HSA concentration dependent. The result of correlation in DI water obtained by the optical fiber is consistent with the result obtained by the normal spectrometer except that the location of emission peak is slightly different.

#### 4.2.2.3 Master curve

The result is shown as Figure 36 below. The master curve shows a positive linear relationship that fluorescence intensity increases with the HSA concentration increases.  $R^2 = 0.9306$  proves that the curve fits relatively well. Therefore, TC-380 can stably detect albumin in the microalbumin concentration range of 25-200 mg/L using fiber optics sensor.

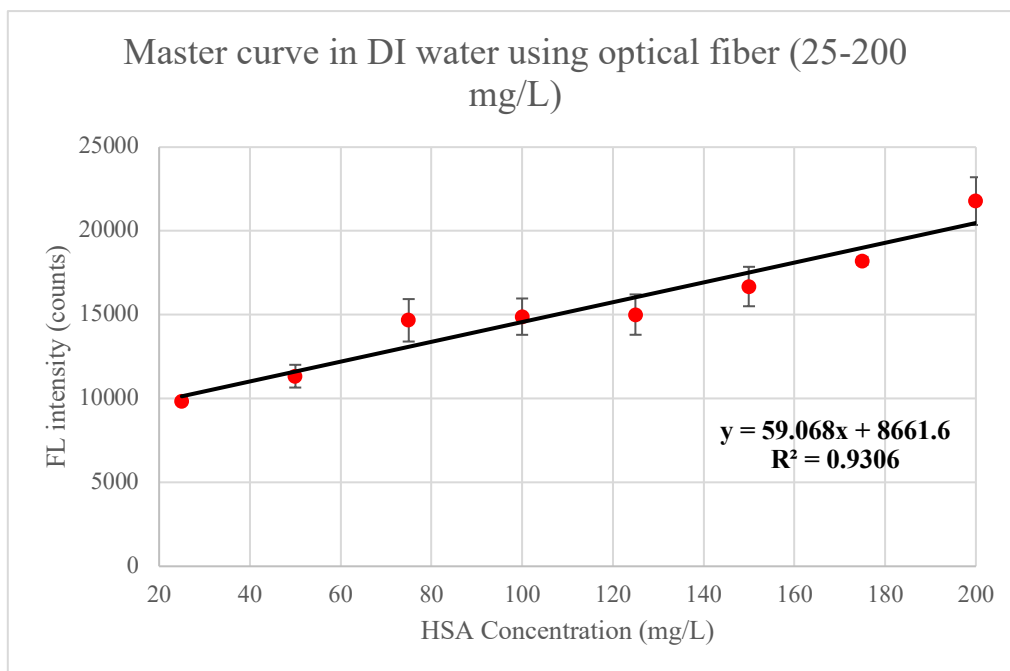


Figure 36. Master curve in DI water from 25- 200 mg/L HSA concentration using fiber optics

When the master curve is extended to the range of 0 mg/L to 800 mg/L, the linear relationship is still significant. It indicates that TC-380 can sensitively detect albumin in a wide range in the environment of deionized water using fiber optics.

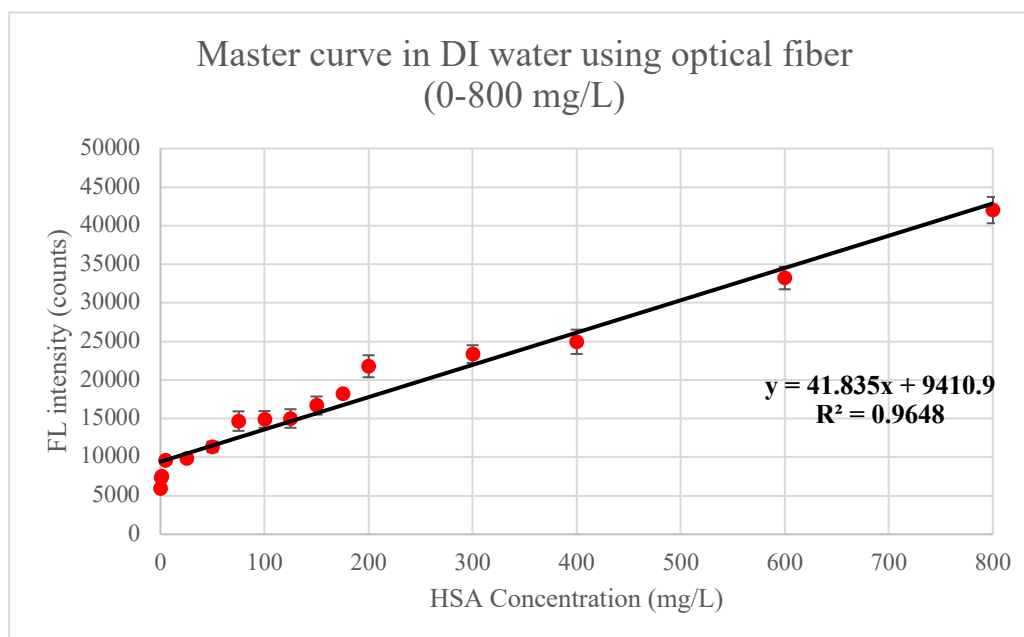


Figure 37. Master curve in DI water from 0 - 800 mg/L HSA concentration using fiber optics

#### 4.2.2.4 Validation

From the result of validation, as the selected concentration increases, the fluorescence intensity increases accordingly. At each concentration, the fluorescence intensity of the five groups of



samples fluctuates slightly, but generally remains near a stable value, which are around 11000, 15000, and 21000 counts respectively.

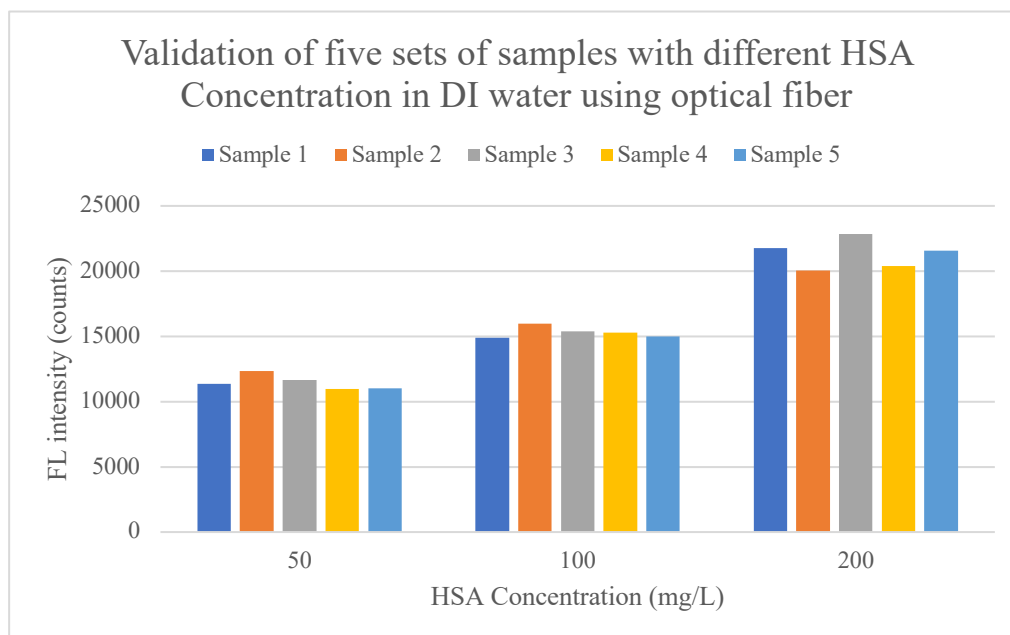


Figure 38. Validation of Master curve in DI water using five sets of samples with three different HSA concentrations: 50, 100, 200 mg/L under fiber optics system

The average value and standard deviation of each concentration are calculated as  $47.43 \pm 9.68$ ,  $112.38 \pm 7.06$  and  $214.32 \pm 19.25$  respectively. Change rates at 50, 100, 200 mg/L HSA concentration are 5.14%, 12.38% and 7.16%. The concentrations of HSA detected by TC-380 at 50 mg/L and 200 mg/L were within 10% of the artificially added concentrations. At 100 mg/L artificially added concentrations, the rate of change is 12.38%.

[HSA] (mg/L)		Change (%)
Added artificially	Detected mean $\pm$ SD	
50.00	$47.43 \pm 9.68$	5.14 %
100.00	$112.38 \pm 7.06$	12.38 %
200.00	$214.32 \pm 19.25$	7.16 %

Table 10. Concentration of HSA detected by the SOP for TC-380 in DI water using fiber optics

Under the fiber optic system, the validation result still proves the rationality of the master curve. Comparing the two systems, the fitting degree and validation results of the master curve under the optical fiber in the aqueous solution are not as good as those in the spectrometer. The potential reason is that the measurement of the optical fiber system must be performed in a

dark environment. In fact, we cannot guarantee to completely eliminate all the ambient light in the environment, and a small part of the ambient light will still cause some interference to the detection result. Nevertheless, the relatively small change rates and close values between the actual average concentration and the artificially added concentration all indicate that the curve is feasible. Therefore, it can be concluded that TC-380 works well in aqueous solutions of microalbumin (25-200 mg/L) using fiber optics system.

### 4.2.3 Optimal working conditions of TC-380 in artificial urine

#### 4.2.3.1 Reaction time and TC-380 to HSA solution ratio

According to the previous measurement of artificial urine in the spectrometer, the optimal reaction time and TC-380 to HSA solution ratio have been obtained. Therefore, these parameters are directly used in fiber optics measurements. Specifically, reaction time is 20 minutes and TC-380 to HSA solution ratio is 1:7.

#### 4.2.3.2 Correlation between different HSA concentrations and their fluorescence intensity

Under fiber optics sensor, the correlation in artificial urine between different HSA concentration and their fluorescence intensity obtained by TC-380 excitation at 481nm is shown below.

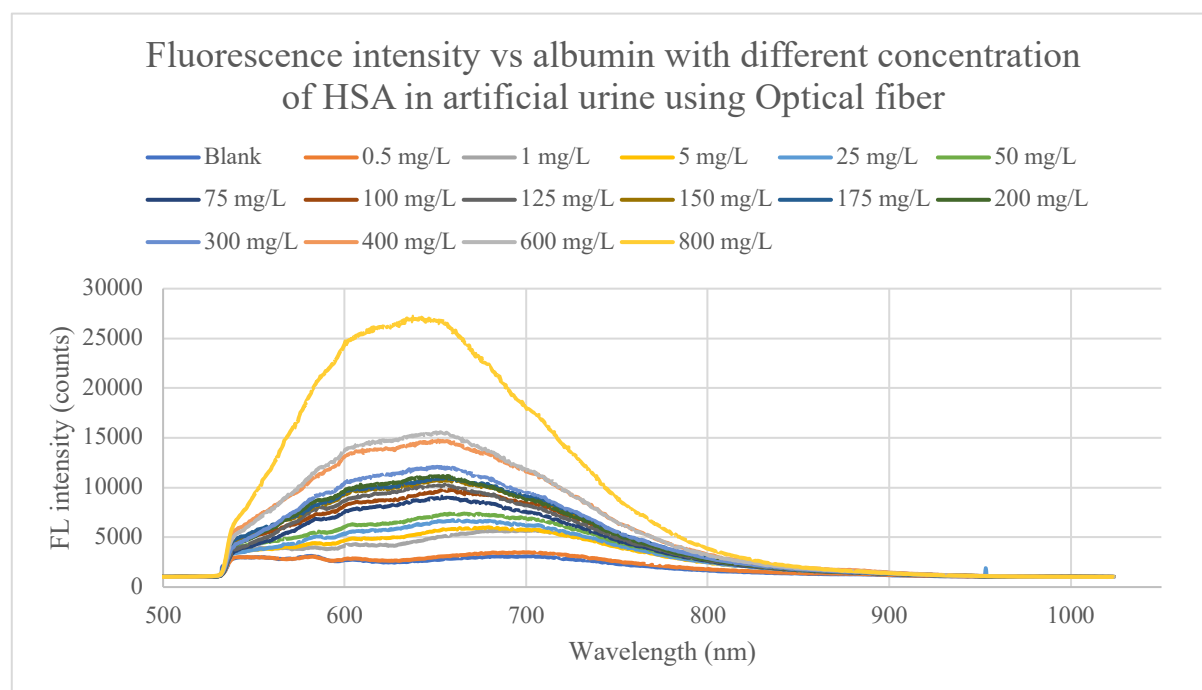


Figure 39. Correlation between different HSA concentration and their fluorescence intensity in artificial urine using optical fiber

From the results, similar to the results measured in DI water using optical fibers, the emission peak of all samples is around 645 nm, which is different from the emission peak of 602 nm in the spectrometer test. As the HSA concentration increases from low to high, the fluorescence

intensity also increases. Moreover, the presence of interfering ions in artificial urine leads to a certain decline in overall fluorescence intensity compared to the result in DI water. However, the positive correlation between albumin concentration and corresponding fluorescence intensity from 0 mg/L to 800 mg/L did not change. The result of correlation in artificial urine obtained by optical fiber are consistent with those obtained by conventional spectrometer, except that the location of the emission peak is slightly different.

#### 4.2.3.3 Master curve

The result is shown as Figure 40 below. Compared to the result in DI water using optical fiber system, the overall fluorescence intensity has decreased due to the presence of various ions in artificial urine. The master curve shows a positive linear relationship that fluorescence intensity increases with the HSA concentration increases.  $R^2 = 0.9028$  proves that the curve fits relatively well. Therefore, TC-380 can stably detect albumin in the microalbumin concentration range of 25-200 mg/L using fiber optics sensor.

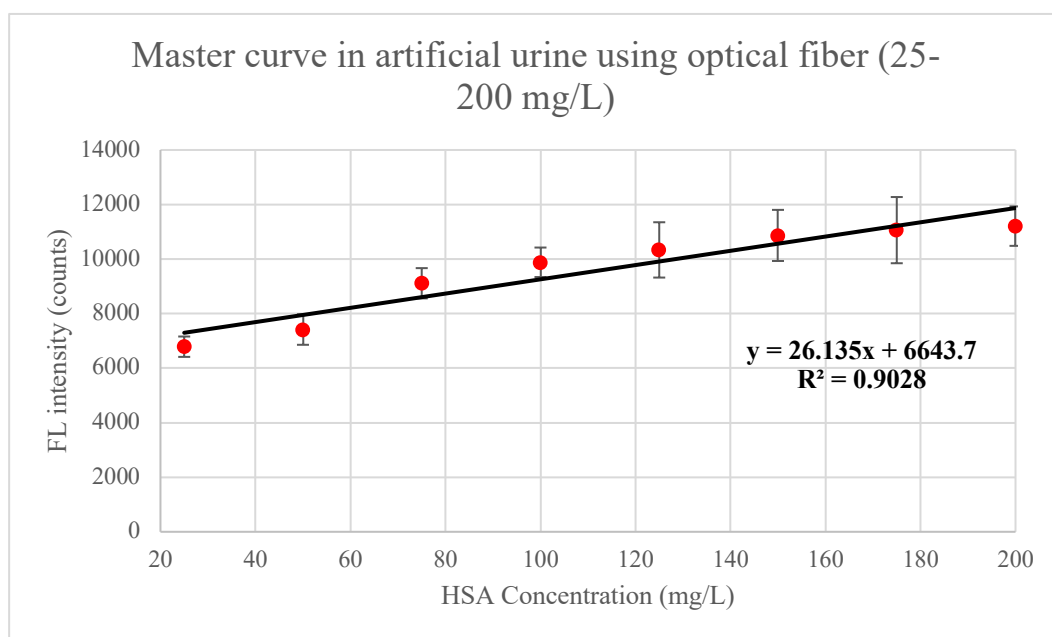


Figure 40. Master curve in artificial urine from 25- 200 mg/L HSA concentration using fiber optics

When the master curve is extended to the range of 0 mg/L to 800 mg/L, the linear relationship is still significant. It indicates that TC-380 can sensitively detect albumin in a wide range in the environment of artificial urine using fiber optics.

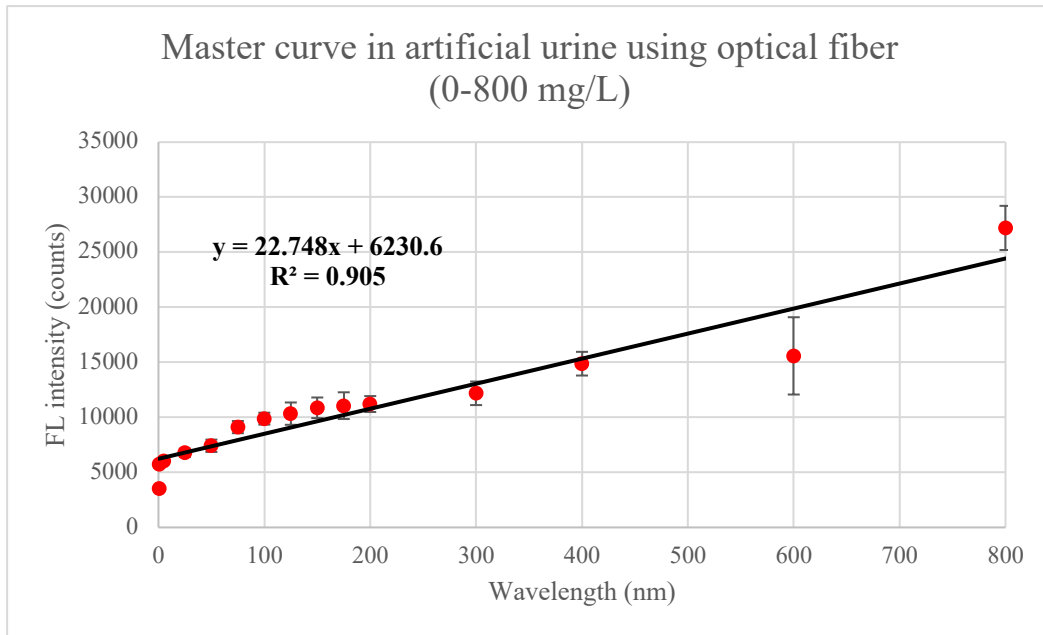


Figure 41. Master curve in artificial urine from 0- 800 mg/L HSA concentration using fiber optics

#### 4.2.3.4 Validation

From the result of validation, as the selected concentration increases, the fluorescence intensity increases accordingly. At each concentration, the fluorescence intensity of the five groups of samples fluctuates slightly, but generally remains near a stable value, which are around 7500, 9000, and 12000 counts respectively.

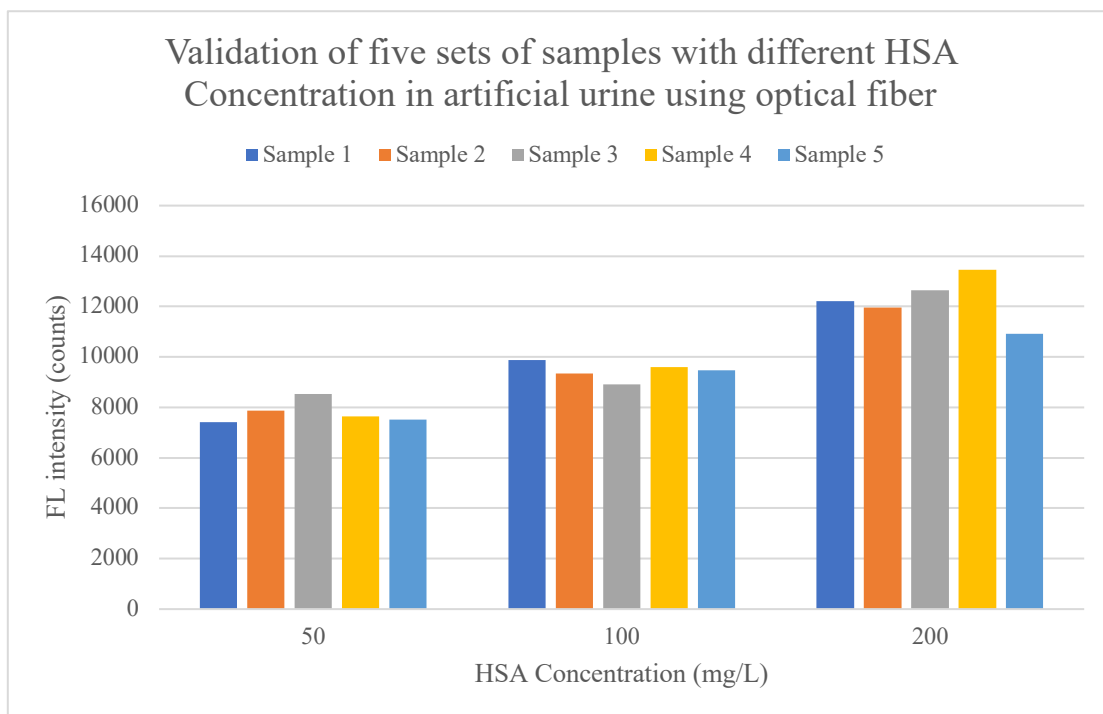


Figure 42. Validation of Master curve in artificial urine using five sets of samples with three different HSA concentrations: 50, 100, 200 mg/L under fiber optics system

The average value and standard deviation of each concentration are calculated as  $44.11 \pm 17.09$ ,  $106.86 \pm 13.56$  and  $214.14 \pm 35.72$  respectively. Change rates at 50, 100, 200 mg/L HSA concentration are 11.78%, 12.38% and 7.07%. The concentrations of HSA detected by TC-380 at 200 mg/L were within 10% of the artificially added concentrations. At 50 and 100 mg/L artificially added concentrations, the rate of change is 11.78% and 12.38%.

[HSA] (mg/L)		Change (%)
Added artificially	Detected mean $\pm$ SD	
50.00	$44.11 \pm 17.09$	11.78 %
100.00	$106.86 \pm 13.56$	12.38 %
200.00	$214.14 \pm 35.72$	7.07 %

Table 11. Concentration of HSA detected by the SOP for TC-380 in artificial urine using fiber optics

Under the fiber optics system, the validation results still prove the rationality of the master curve. Comparing these two systems, the degree of fit and validation of the master curve under the fiber optics in the artificial urine is not as stable as in the spectrometer because of the potential influence of a small part of ambient light in the environment. However, the relatively small rate of change and the close value between the actual average concentration and the artificially added concentration all indicate that the curve is feasible. Therefore, it can be concluded that using the fiber optic system, TC-380 works well in the microalbumin artificial urine solution (25-200 mg/L).

#### 4.2.3.5 Creatinine influence

Primarily, the result of creatinine effects obtained by using a general spectrometer is consistent with the result of optical fibers. It can be seen from the figure that there is no influence before and after adding creatinine. The slopes of the two curves are relatively close and the variation range of the two curves is within the standard error of each other. Furthermore, it proves that adding creatinine will slightly decrease the fluorescence intensity but the linear relationship remains unchanged. Therefore, the detection of TC-380 to HSA is not affected generally, indicating that TC-380 has a high level of specificity for HSA in this microalbumin range.

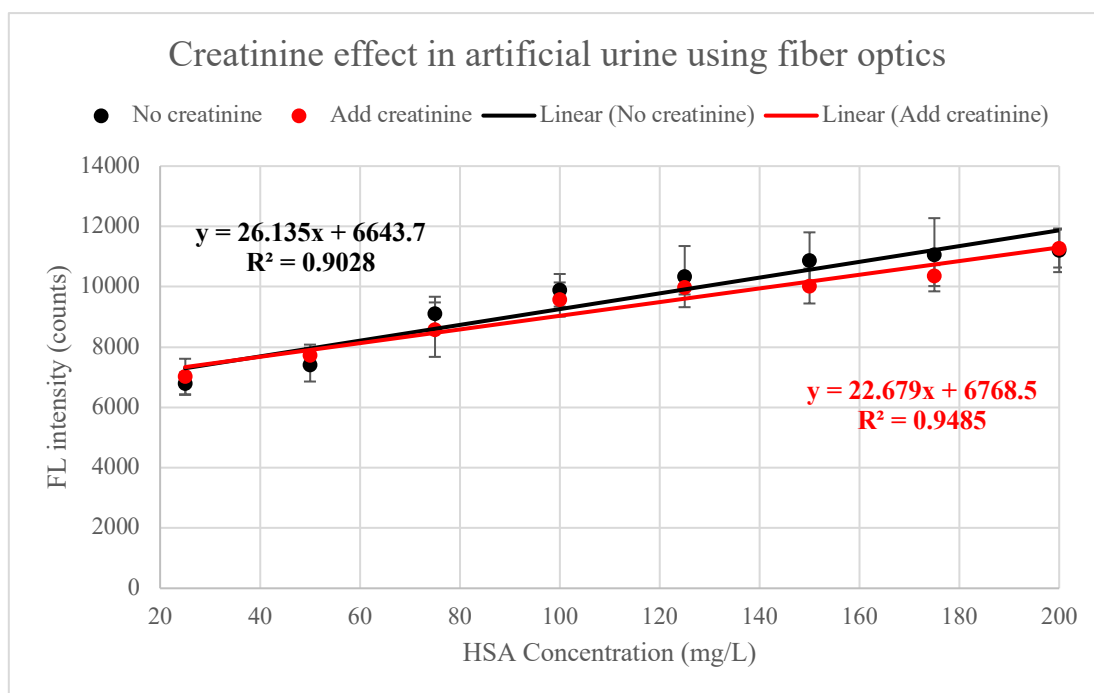


Figure 43. Creatinine influence in artificial urine using fiber optics

#### 4.2.4 Optimal working conditions of TC-380 in human urine

##### 4.2.4.1 Dilution of urine ratio

From the results. In the fiber optics system, the autofluorescence is produced at about 550 nm when the blank sample is excited at 481 nm. By comparing the two albumin concentrations 200 mg/L and 800 mg/L, with the gradual increase of the dilution factor, the autofluorescence intensity will decrease accordingly. Different from the results of ordinary spectrometers, although the peak shape gradually widens with the increase of dilution, when the dilution ratio starts from 1:5, it can be seen that there is an increase in fluorescence intensity near 650 nm and reaches the maximum value at 1:9.

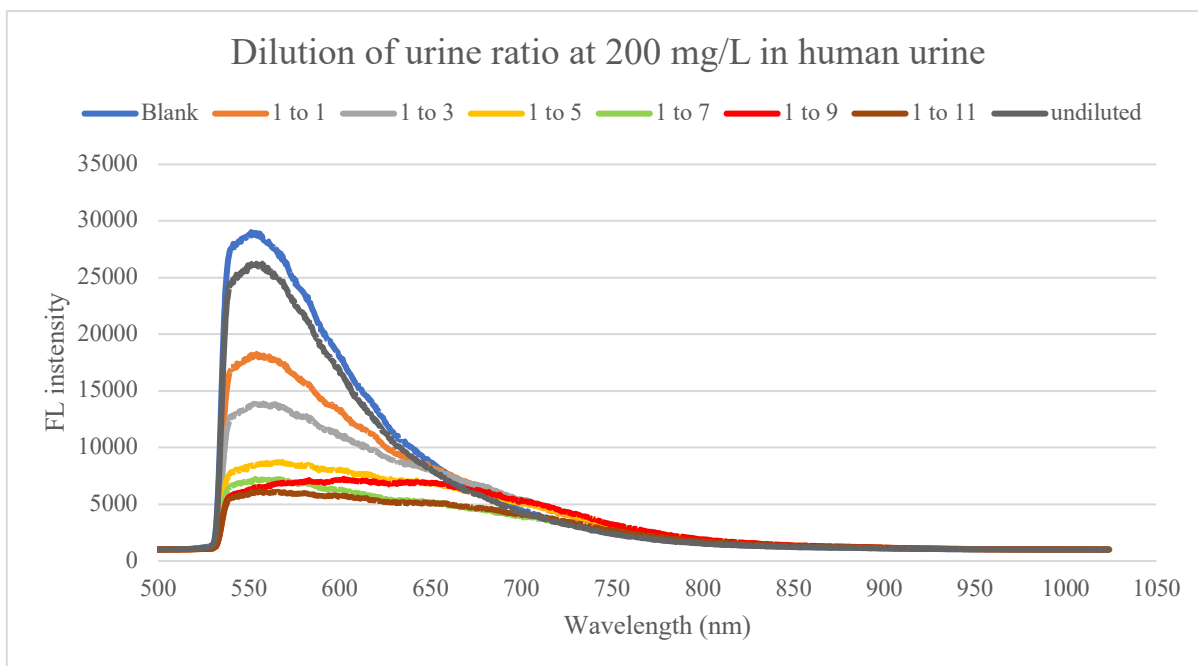


Figure 44. Dilution of urine ratio at 200 mg/L in human urine

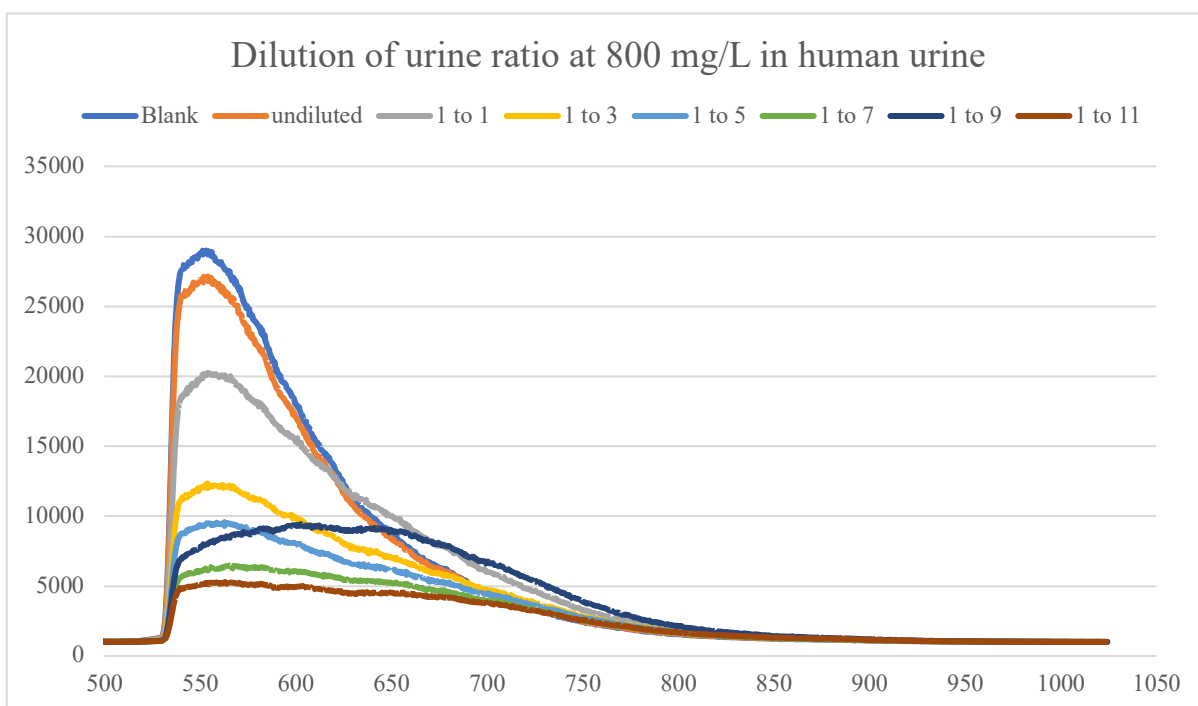


Figure 45. Dilution of urine ratio at 800 mg/L in human urine

In order to compare the results of dilution more intuitively, the emission peak value 645nm is selected as the reference point, and the normalized dilution curves at 200 mg/L and 800 mg/L concentrations are drawn. The results are shown in the following two Figures 46 and 47.

After normalization, it is clear that as the urine dilution ratio increases, the reaction peak at around 650 nm will gradually emerge and reach the maximum value at 1:9 at 200 mg/L and

800 mg/L albumin concentration. Under the same measurement conditions, the autofluorescence still exists, but the reaction peak can be captured under the fiber optic system compared with ordinary spectrometers. This shows that the optical fiber system can detect the signal of the measured sample in the environment of human urine. Therefore, based on the maximum FL intensity of the reaction peak in the dilution results, the optimal dilution ratio in human urine is set to 1:9.

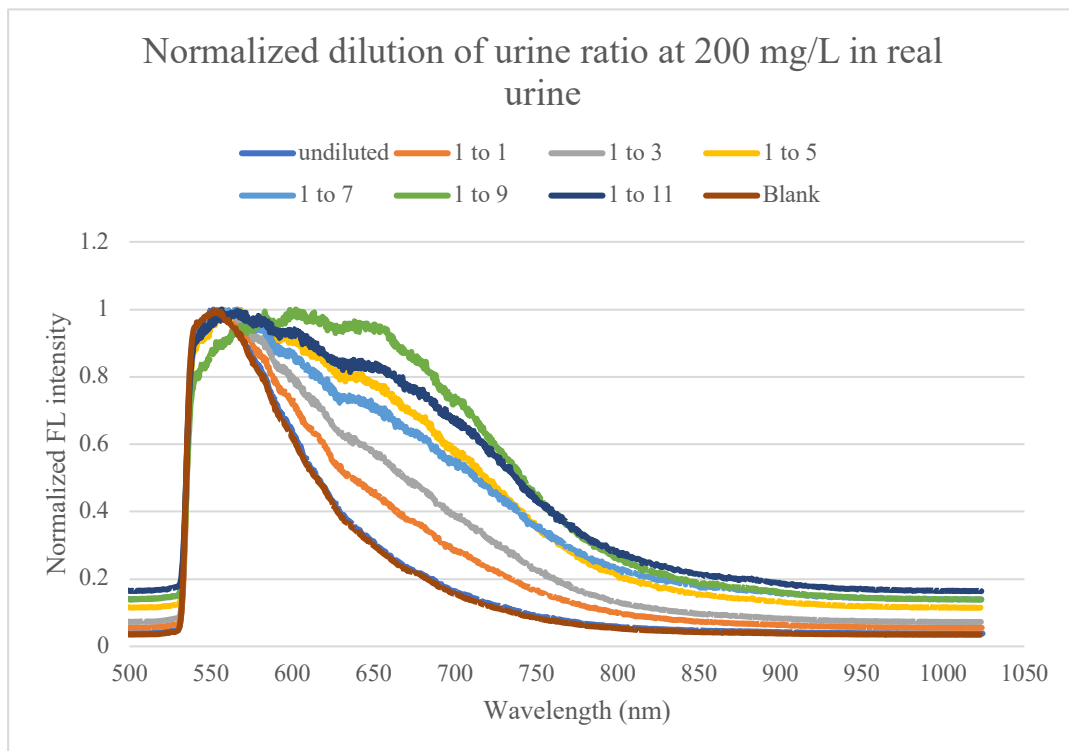


Figure 46. Normalized dilution of urine ratio at 200 mg/L in human urine



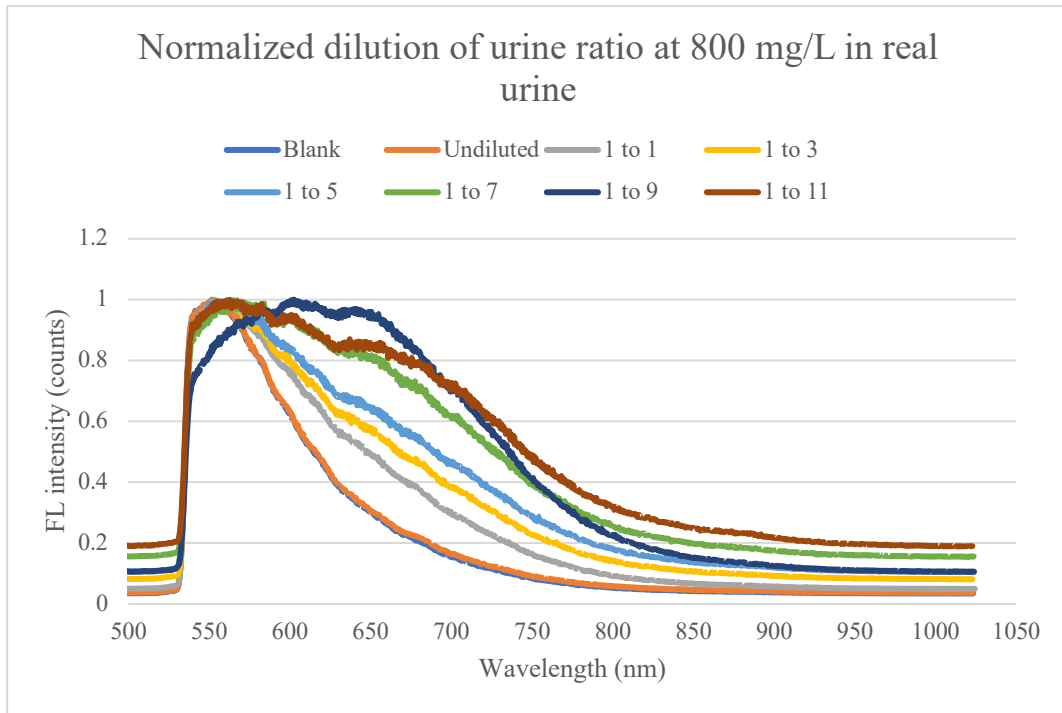


Figure 47. Normalized dilution of urine ratio at 800 mg/L in human urine

#### 4.2.4.2 Reaction time

According to the previous measurement of artificial urine in the spectrometer, the best reaction time has been 20 minutes, and this result provides a reference for human urine testing. Therefore, this parameter is directly used in optical fiber measurement, that is, the reaction time of urine measurement is consistent with artificial urine. Specifically, the measurement was started after 20 minutes of reaction in a human urine environment.

#### 4.2.4.3 TC-380 to HSA solution ratio

In this case, the previously measured parameters are fixed, which means that the excitation wavelength of TC-380 is 481nm, the dilution of urine ratio is 1:9 and the reaction time is 20 minutes. The results of different ratios at 200 and 800 mg/L HSA concentrations are shown below.

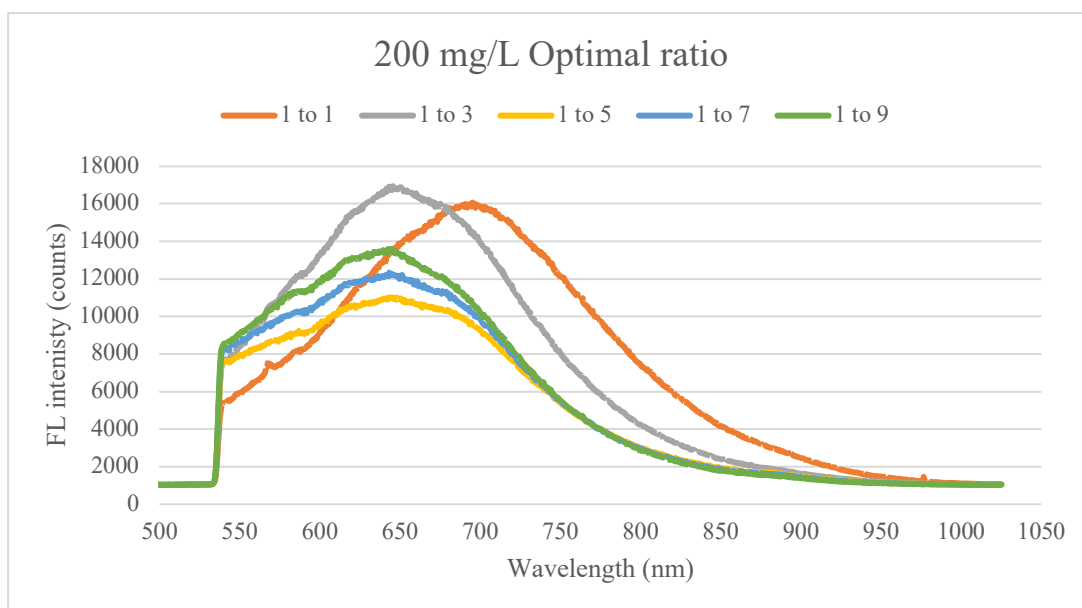


Figure 48. TC-380 to albumin ratio at 200 mg/L HSA concentration in human urine

From the results, at a concentration of 200 mg/L, the reaction peak is at 700 nm at 1:1 and the reaction peak shifts to about 650 nm at 1:3. Afterwards, as the reaction ratio increased, the reaction peak stabilized at 645 nm after 1:5. Furthermore, with the addition of albumin solution, the fluorescence intensity is at a high level from 1:1 to 1:3. From 1:3 to 1:5, there is a significant decrease in FL intensity. After the reaction peak stabilized, the FL intensity gradually increased on this basis of 1:5 and reached the maximum at 1:9.

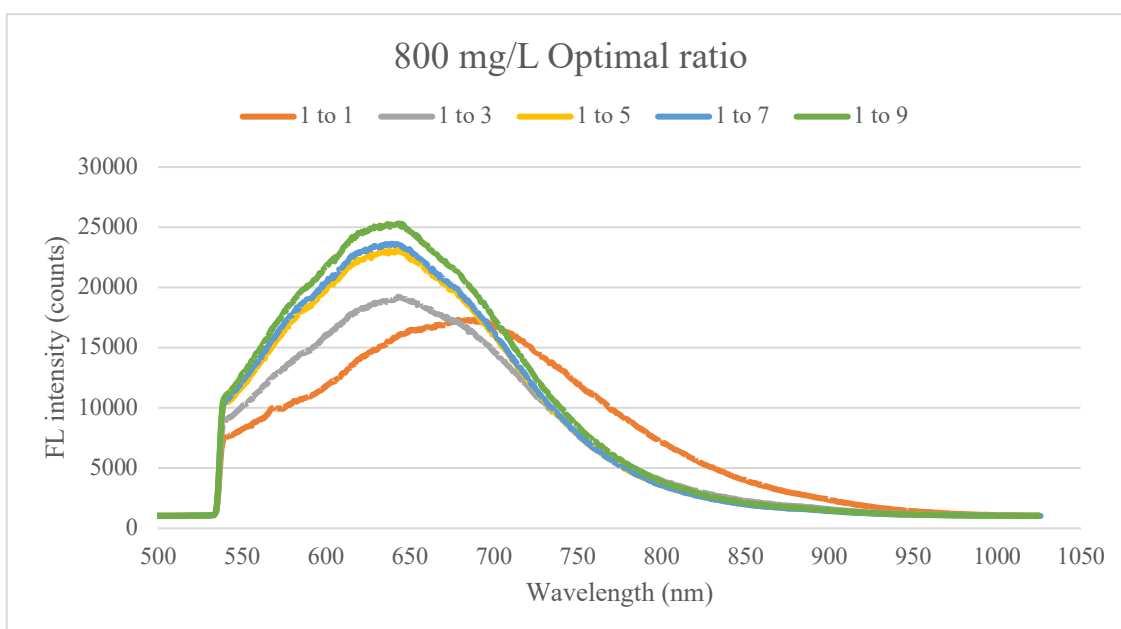


Figure 49. TC-380 to albumin ratio at 800 mg/L HSA concentration in human urine

At albumin concentration of 800 mg/L, the difference from 200 mg/L is that the reaction peak moves from 700nm at 1:1 to 645nm at 1:3 and remains stable thereafter. Besides, from 1:1 to 1:9, the fluorescence intensity gradually increases, and finally reaches the maximum at 1:9. By selecting the points on each emission peak at different ratios, the ratio versus fluorescence intensity histogram are shown in the Figure 50 below.

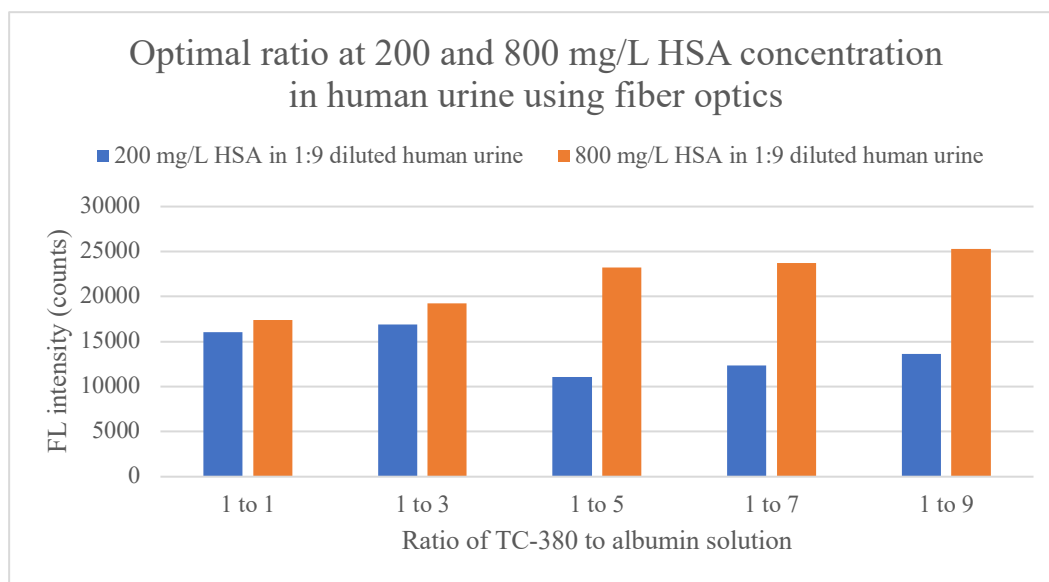


Figure 50. Different ratios of TC-380 to HSA solution at 200 and 800 mg/L HSA concentration in human urine

First of all, it is known that the emission peak of TC-380 is 740 nm in a fiber optical system. Additionally, when TC-380 has completely reacted with albumin, the peak has blue shifts to near 645 nm. At a concentration of 200 mg/L, the probe only reacted with a part of the albumin in the initial stage of the reaction, and the peak only stayed at 700nm. However, with the continuous addition of albumin solution, the emission peak gradually moved closer to 645nm. At 1:5, it can be considered that the reaction has basically stabilized. Moreover, with the increase of the reaction ratio, that is, the continuous addition of albumin, the entire reaction reached the optimal condition at 1:9. At a concentration of 800 mg/L, the albumin concentration is already at a higher level, therefore the reaction process is accelerated. It has stabilized at 1:3 and the fluorescence intensity reaches the maximum at 1:9, which also shows that the reaction is in the best state.

Hence, considering the results of the above two different concentrations 200 mg/L and 800 mg/L, the optimal TC-380 to albumin solution ratio should be selected from the values after the reaction peak stabilizes at 645 nm. Combined with the level of fluorescence intensity, 1 to 9 is considered to be the optimal reaction ratio under these conditions at 200 mg/L and 800 mg/L albumin concentration.

#### 4.2.4.4 Correlation between different HSA concentrations and their fluorescence intensity

Under fiber optics sensor, the correlation in human urine between different HSA concentration and their fluorescence intensity obtained by TC-380 excitation at 481nm is shown below.

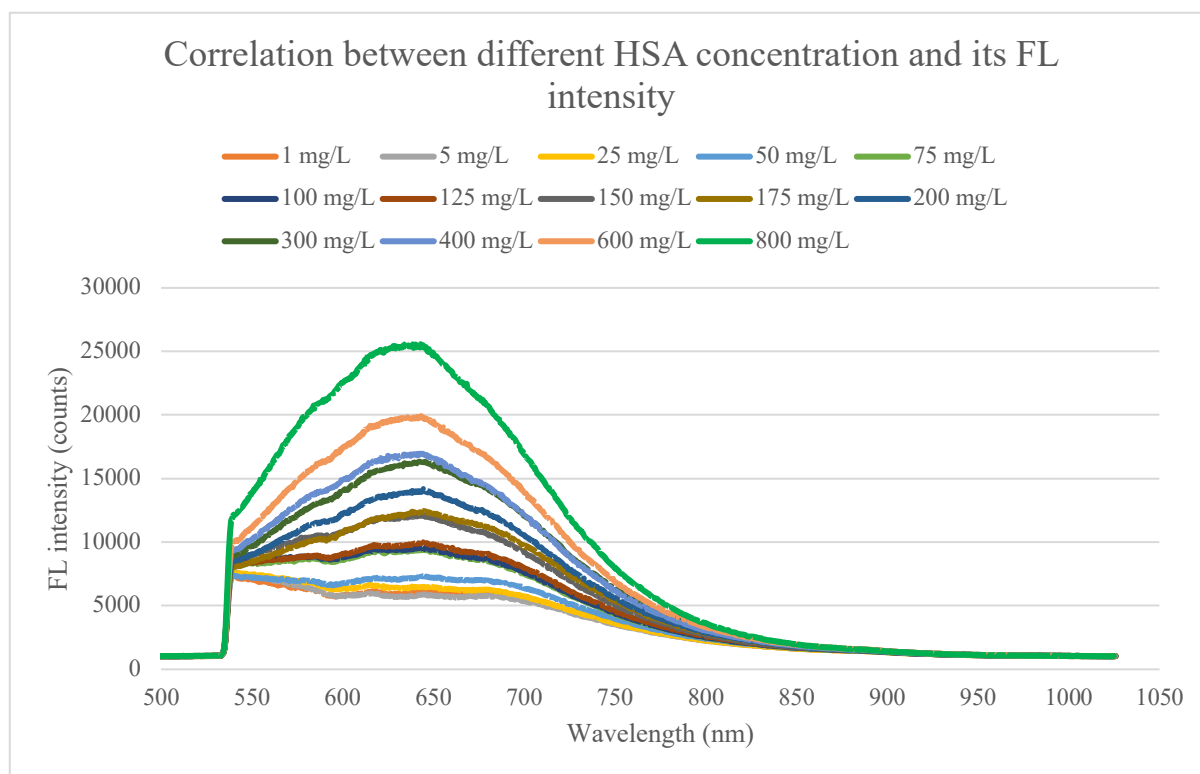


Figure 51. Correlation between different HSA concentration and their fluorescence intensity in human urine using optical fiber

From the results, similar to the results measured in DI water and artificial urine using optical fibers, the emission peak of all samples is around 645 nm. As the HSA concentration increases from low to high, the fluorescence intensity also increases. In addition, compared with the results in deionized water and artificial urine, the presence of interfering ions and unknown proteins in human urine further led to a decrease in overall fluorescence intensity. However, the positive correlation between albumin concentration and corresponding fluorescence intensity (from 0 mg/L to 800 mg/L) remains unchanged. In the three different environments, the consistency of the peak shape and the positive correlation of the measurement results indicate the significant and feasible detection ability of TC-380.

#### 4.2.4.5 Master curve

The result is shown as Figure 52 below. Compared to the result in artificial urine using optical fiber system, the overall fluorescence intensity has decreased due to the presence of various ions and some proteins in human urine. The master curve shows a positive linear relationship that fluorescence intensity increases with the HSA concentration increases.  $R^2 = 0.9452$  proves

that the curve fits relatively well. Therefore, TC-380 can stably detect albumin in the microalbumin concentration range of 25-200 mg/L using fiber optics sensor.

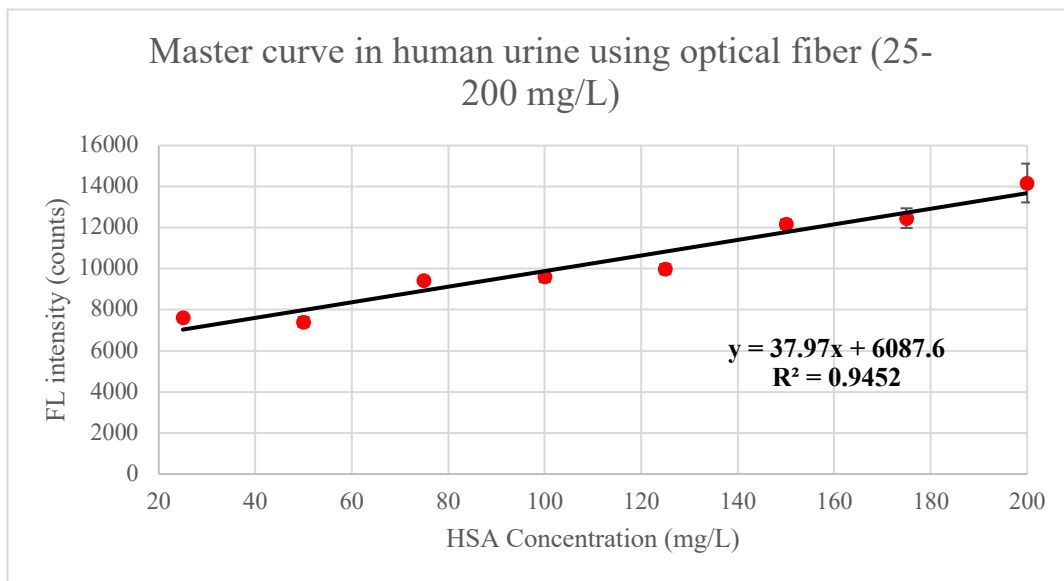


Figure 52. Master curve in human urine from 25- 200 mg/L HSA concentration using fiber optics

When the master curve is extended to the range of 0 mg/L to 800 mg/L, the linear relationship is still significant. It indicates that TC-380 can sensitively detect albumin in a wide range in the environment of human urine using fiber optics.

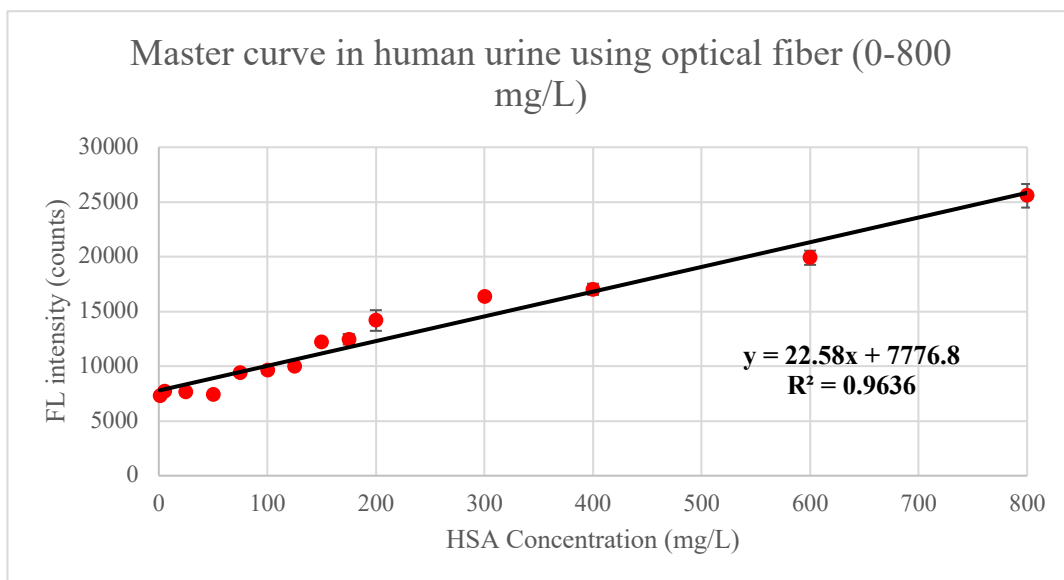


Figure 53. Master curve in human urine from 0- 800 mg/L HSA concentration using fiber optics

#### 4.2.4.6 Validation

From the verified results, as the selected concentration increases, the fluorescence intensity also increases. At each concentration, the fluorescence intensity of the five groups of samples

has certain fluctuations especially at the 200 mg/L albumin concentration. Nonetheless, it still maintains a relatively stable level overall, about 8000, 10,000, and 13,000 counts respectively.

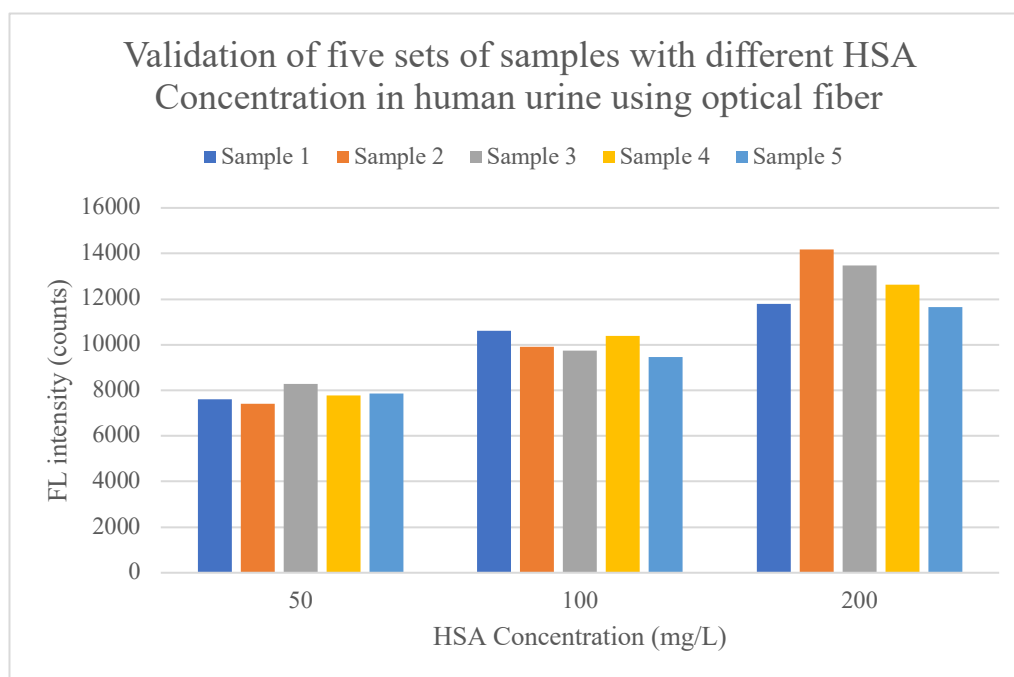


Figure 54. Validation of Master curve in human urine using five sets of samples with three different HSA concentrations: 50, 100, 200 mg/L under fiber optics system

The average value and standard deviation of each concentration are calculated as  $44.61 \pm 8.47$ ,  $103.73 \pm 12.40$  and  $175.46 \pm 28.49$  respectively. Change rates at 50, 100, 200 mg/L HSA concentration are 10.78%, 3.73% and 12.27%. The concentrations of HSA detected by TC-380 at 100 mg/L were within 10% of the artificially added concentrations. At 50 and 200 mg/L artificially added concentrations, the rate of change is 10.78% and 12.27%.

[HSA] (mg/L)		Change (%)
Added artificially	Detected mean $\pm$ SD	
50.00	$44.61 \pm 8.47$	10.78 %
100.00	$103.73 \pm 12.40$	3.73 %
200.00	$175.46 \pm 28.49$	12.27 %

Table 12. Concentration of HSA detected by the SOP for TC-380 in human urine using fiber optics

Under the optical fiber system, similar to the results in deionized water and artificial urine, the validation results in human urine still prove the rationality of the master curve. Due to the interference factors in human urine and the sensitivity of the fiber optic system to external light, it will inevitably interfere with the experimental results, and the relatively small change rate

(within 20%) and the close value between the actual average concentration and the artificially added concentration all indicate that the curve is feasible. Therefore, it can be concluded that using the fiber optic system, TC-380 works well in microalbumin range of human urine (25-200 mg/L).

#### 4.2.4.7 Creatinine influence

It can be seen from the figure that the addition of creatinine has a significant impact on the detection of albumin, but the linear relationship remains unchanged. From the trend point of view, the fluorescence intensity after adding creatinine at the same concentration is lower than that without adding creatinine. In other words, due to the decrease in slope of master curve, the addition of creatinine reduces the sensitivity of TC-380 for albumin detection. Therefore, the detection of HSA by TC-380 will be affected by creatinine in the human urine environment. The potential reason is that the further expansion of interference prevents the probe from being able to specifically bind to albumin.

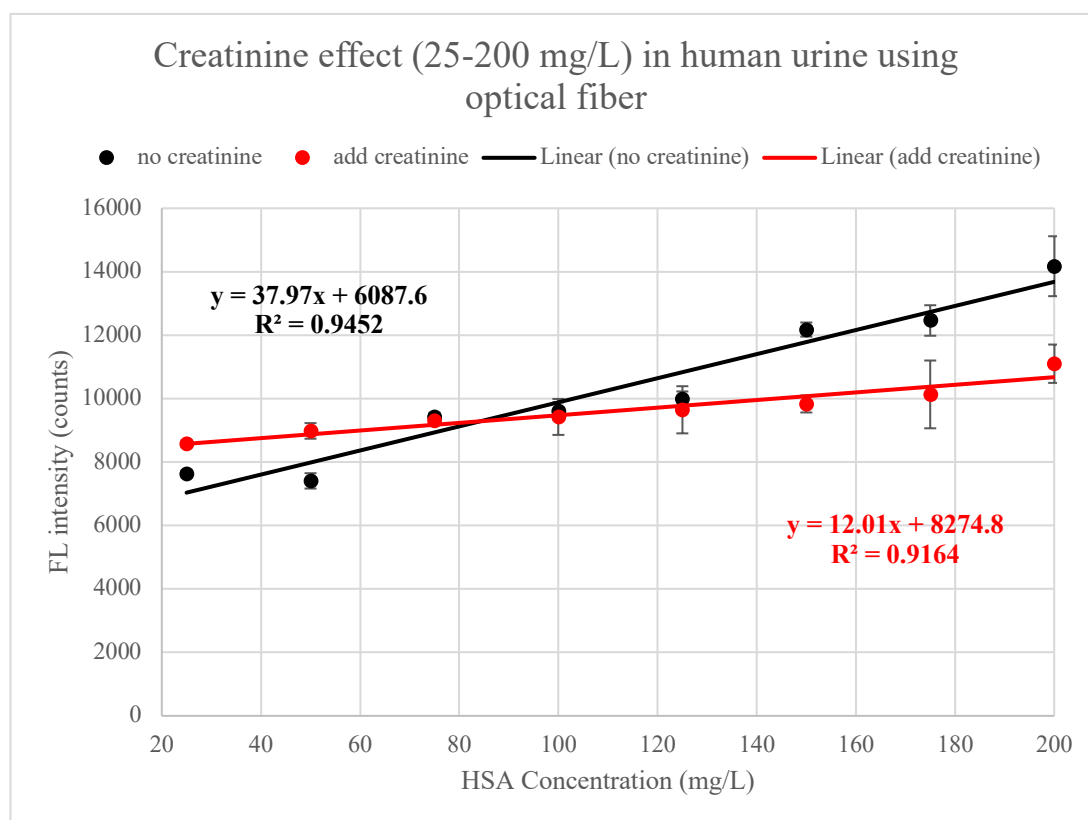


Figure 55. Creatinine influence in human urine using optical fiber

### 4.2.5 Comparison among DI water, artificial and human urine using fiber optics system

#### 4.2.5.1 Master curve comparison among DI water, artificial urine and human urine

The Figure 56 below shows the master curves in deionized water, artificial urine and human urine. First of all, the master curves in three different environments under the fiber optic system

all show a good linear relationship in microalbumin (25-200 mg/L). Secondly, the slope relationship of the three is DI water > human urine > artificial urine, which indicates that the sensitivity of albumin detection is DI water > human urine > artificial urine.

The reason why the sensitivity in human urine is greater than that in artificial urine is that the sample in urine has actually been diluted nine times, which greatly reduces internal interference. And compared with artificial urine, the concentration of each ion in urine will be lower than artificial urine due to dilution, thereby reducing the interference of ions on albumin binding.

Unlike the case where the two main curves intersect under an ordinary spectrometer, the three master curves are generally hierarchical under the optical fiber system. In other words, according to the relationship that the detection sensitivity of DI water > human urine > artificial urine, the curve represented by one environment is above the other curve in the microalbumin range. Moreover, the two curves do not intersect, or the intersection point is infinitely close to the lower concentration. In fact, the result is more in line with theoretical expectations. This also shows that the detection sensitivity or detection limit of the instrument itself is relatively sufficient compared to ordinary spectrometers.

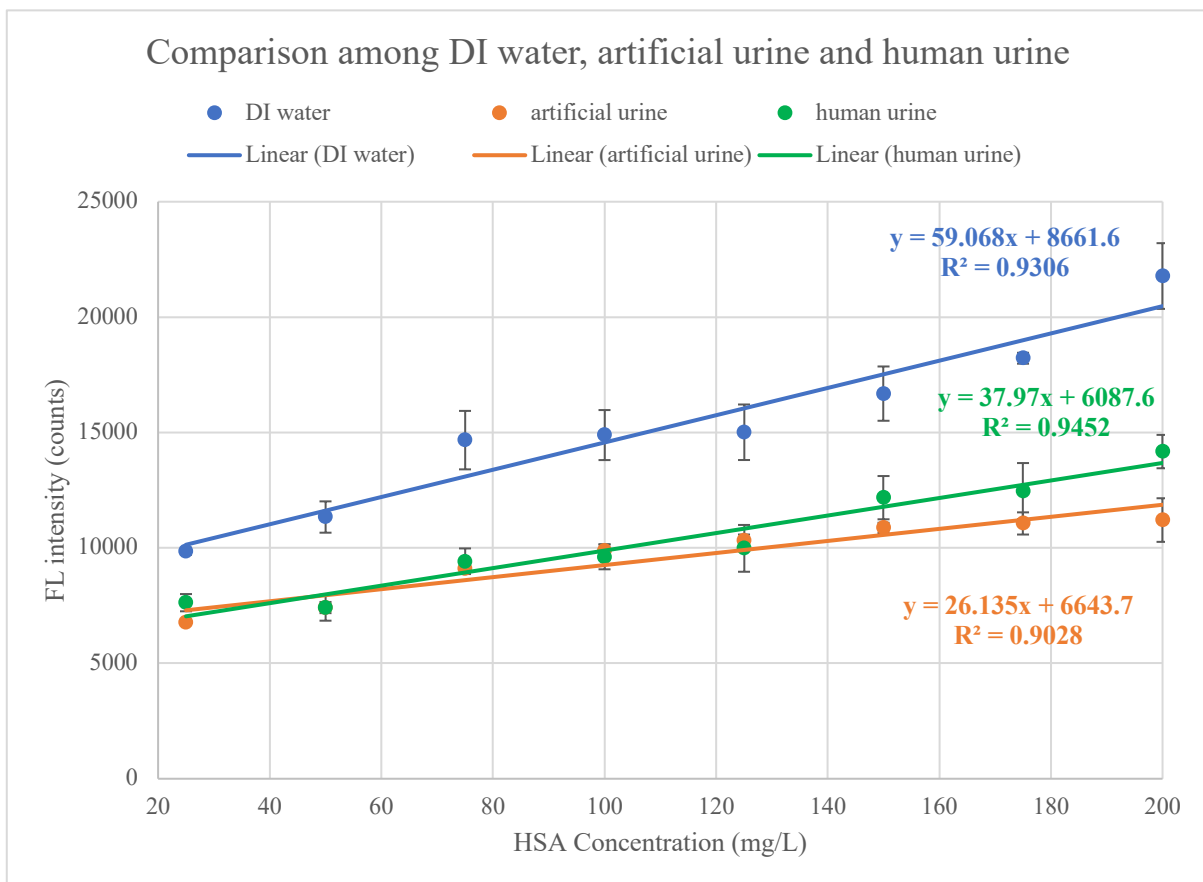


Figure 56. Master curve comparison among DI water, artificial urine and human urine using fiber optics system



#### 4.2.5.2 Detection limit in fiber optics system

As shown in the figures, in DI water, the fluorescence intensity of the blank solution is 3537 counts. the FL intensity of 5927 counts at a concentration of 0.1mg/L increased by 67.57%, and there is a significant difference. Similarly, it only increased by 11.65% at a concentration of 0.5 mg/L in an artificial urine environment and the difference is not significant. When the albumin concentration increased to 1 mg/L, the increase reached 90.72%. In human urine, the increase in fluorescence intensity is only 6.92% maximum when the concentration is below 50 mg/L. Only when the concentration is 75 mg/L, the fluorescence intensity increases by 33.05%. After validation, the data conforms to the master curves, hence it can be preliminarily considered that the detection limit in DI water, artificial urine and human urine is 0.1 mg/L, 1 mg/L and 75 mg/L respectively.

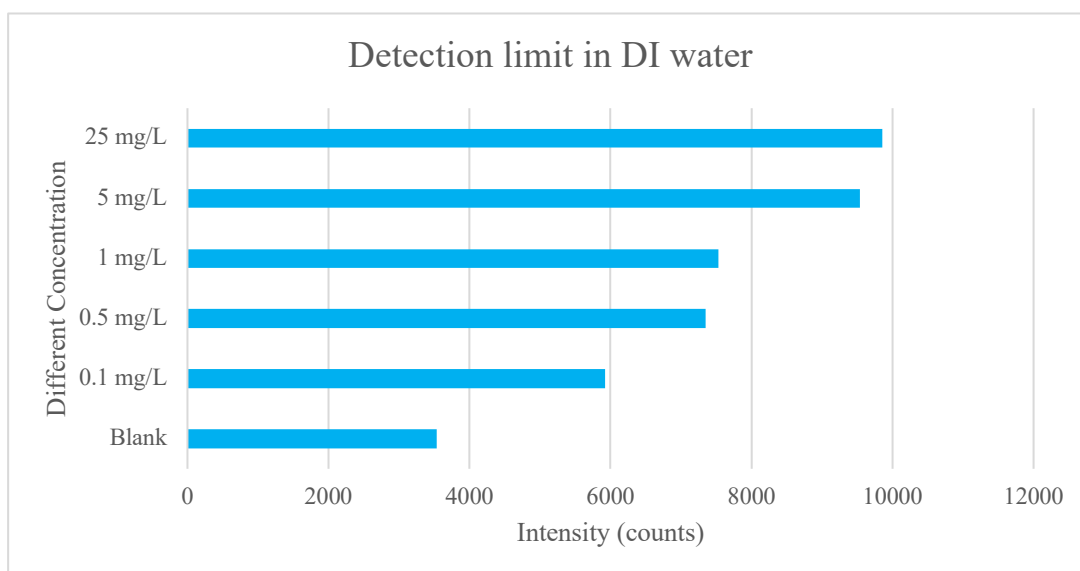


Figure 57. Detection limit in DI water using fiber optics

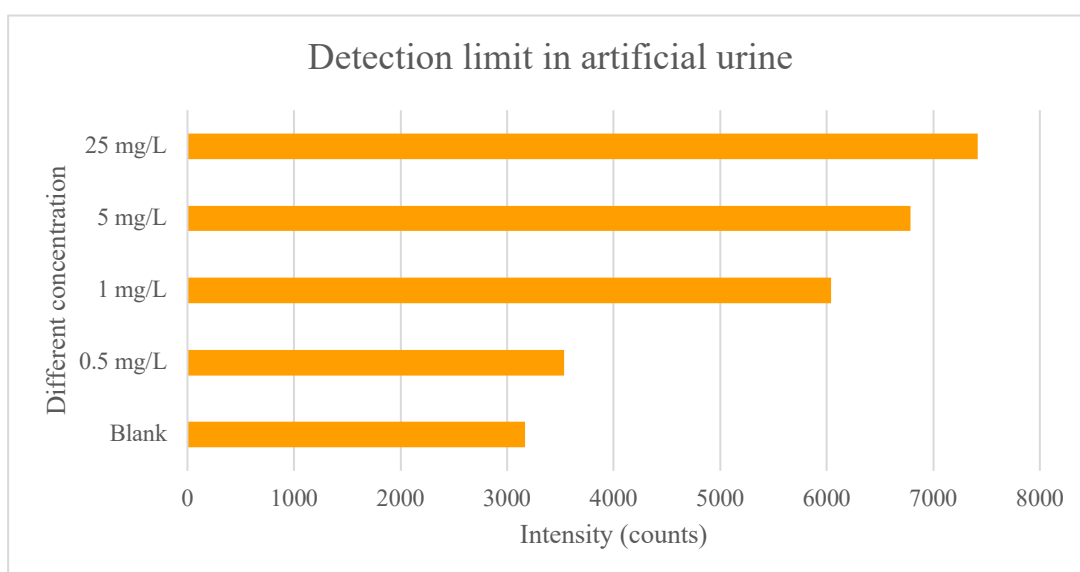


Figure 58. Detection limit in artificial urine using fiber optics

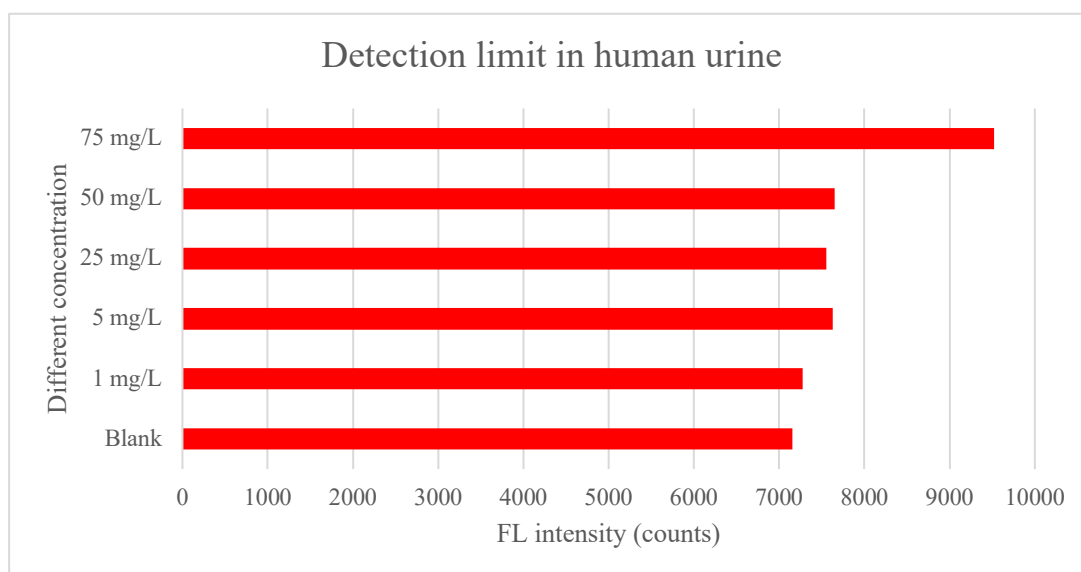


Figure 59. Detection limit in human urine using fiber optics

#### 4.2.6 Result of SOP using fiber optics

Based on the above measurements, the result of SOP using fiber optics system is summarized as Table 13 below.

Optimal operating conditions	Deionized water	Artificial urine	Human urine
Excitation and Emission Wavelength	480/645 nm		
Bioprobe concentration	10 $\mu$ M		
HSA concentration	0~800 mg/L		
Dilution of urine ratio	—		1:9
Reaction time	20 minutes		
Bioprobe: albumin solution ratio	1:5	1:7	1:9
Master curve	Linear		

Creatinine effect	—	No influence	FL intensity decreases
Detection limit	0.1 mg/L	1 mg/L	75 mg/L

Table 13. Result of SOP for TC-380 in optical fiber system ('—' represents no results or no measurements)

## **5 Discussion**

### **5.1 The difference of reaction peak between ordinary spectrometer and optical fiber**

According to the experimental results, under the premise of using the same excitation wavelength, the emission wavelength of the probe reacting with albumin measured by a common spectrometer is 602nm and the result under the optical fiber system is 645nm. The difference in emission wavelength mainly depends on the factors of the instrument. First of all, the spectrometer in this experiment uses an ultraviolet light source emitted by xenon flash lamp. The fiber optic system uses a laser light source. Secondly, the optical fiber system has controllable light source power instead of fixed power in ordinary spectrometer. Thirdly, the light collection mode is different. The optical fiber uses the backscattering mode and the spectrometer is in the right-angle mode. Finally, there are differences in the impact of ambient light. The optical fiber is very susceptible to the influence of background light, the entire experiment is carried out in a dark environment, but the influence of slight ambient light cannot be accurately quantified. The spectrometer instrument itself provides a fixed environment inside the instrument. In general, they are currently potential factors resulting in the different emission wavelengths.

### **5.2 Master curves comparison between two systems in DI water and artificial urine**

Since the fluorescence intensity units of the two systems are different, the master curves cannot be directly compared. In order to understand the detection performance of the two systems more intuitively, the normalized curve is the most reliable. Therefore, the maximum emission wavelength in the master curves measurement is selected as the standard point, and the corresponding normalized master curves are drawn as Figures 60 and 61 below.

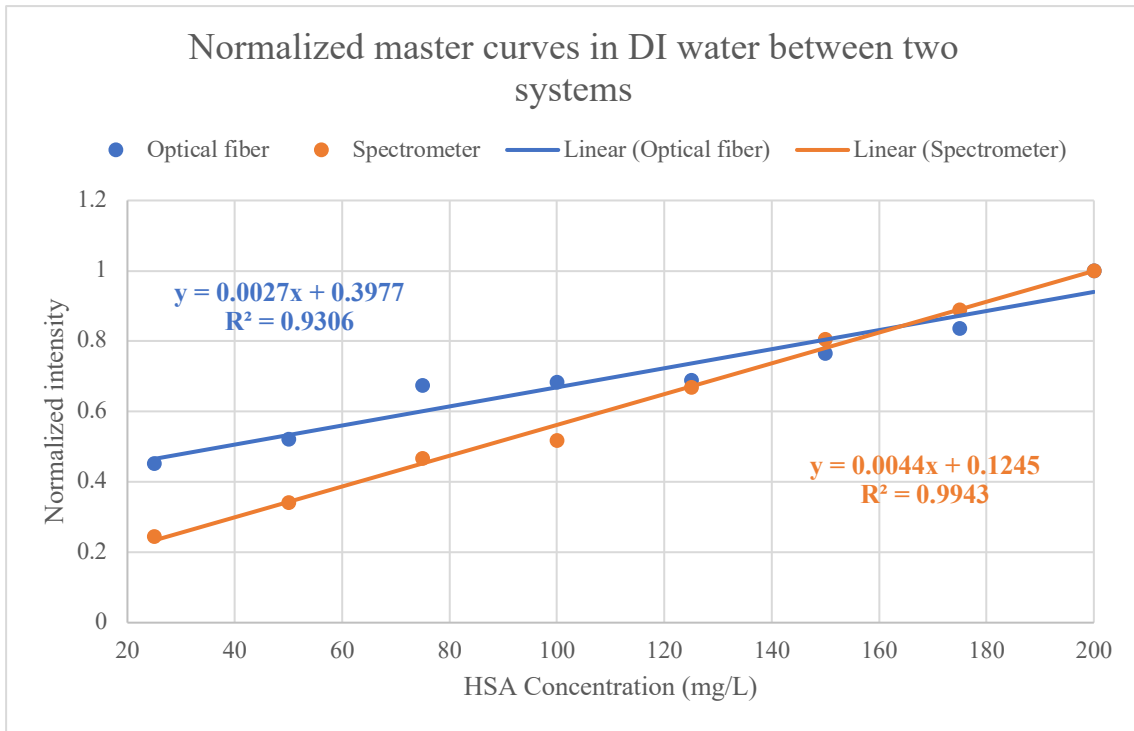


Figure 60. Normalized master curves in DI water between two systems

In the environment of DI water, the result of the spectrometer is slightly higher than that of the fiber optic system, but the difference in the slope of the two curves is very small. Moreover, most of the main curve under the fiber optic system is above the curve of the spectrometer, indicating that low level of albumin concentrations has a higher detection threshold. In summary, it shows that under the situation of keeping the same experimental conditions, the non-interference environment of deionized water generally shows the coherence of TC-380 detection performance.

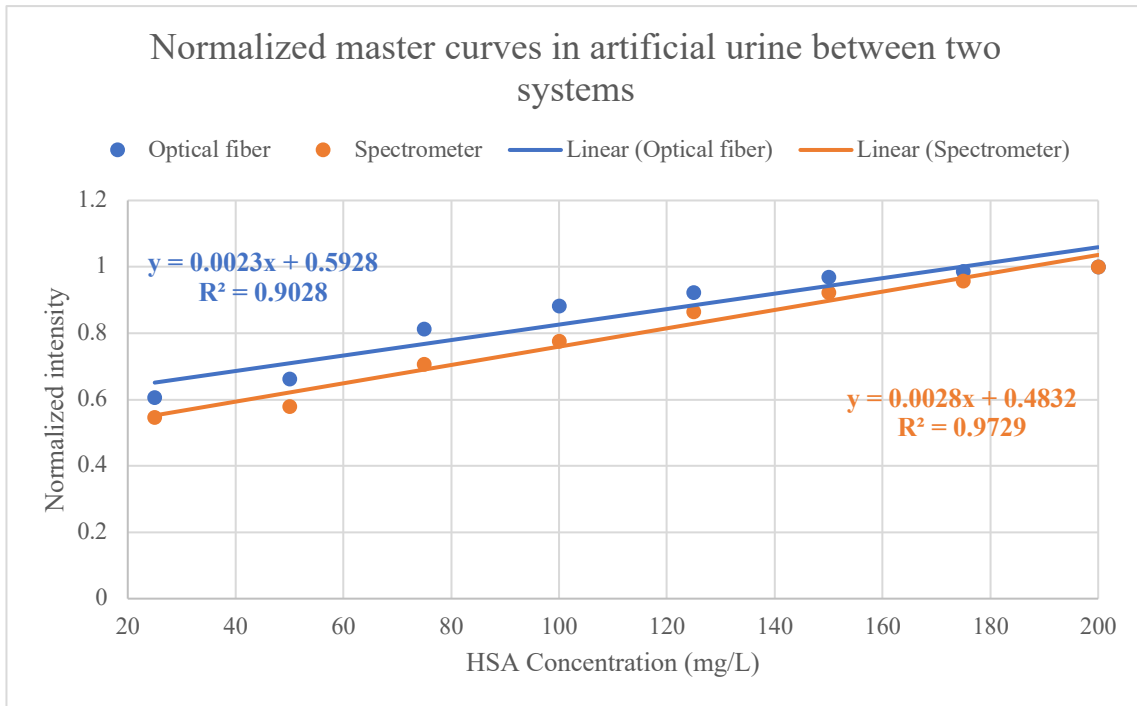


Figure 61. Normalized master curves in artificial urine between two systems

Similarly, there is almost no difference between the master curves of the two systems in the artificial urine environment. This time, in the microalbumin range, the master curve under the optical fiber system is all above the master curve under the spectrometer.

Finally, by comparing the normalized master curves of different instruments in the two environments, master curves are generally the same, verifying that the optical fiber system can still maintain the same degree of matching when the optical fiber system performs the same measurements as the ordinary spectrometer.

## 6 Conclusion

The SOP for the detection and quantitation of HSA by TC-380 in three different environments is developed and evaluated. Firstly, the optimal operating conditions are determined through evaluation and performance of master curves. Afterwards, the addition of creatinine has no significant effect on the high specific response and high sensitivity between TC-380 and HSA except for the urine environment. Secondly, the detection limit of an ordinary spectrometer is 25 mg/L and no effective signal can be detected in the urine environment. Different from it, the fiber optic system can be as low as 0.1 mg/L in DI water, 1 mg/L in artificial urine and 75 mg/L in human urine. Thirdly, the fiber optic system can reliably enhance the reaction peak under the interference of autofluorescence in human urine testing.

In summary, the SOP of TC-380 has achieved excellent results in common spectrometer and fiber optic system. In DI water and artificial urine, the fiber optic system provides the lower detection limits. In human urine, it can enhance the detection signal. It is a fact that TC-380 has achieved encouraging experimental results in detecting albumin in human urine, and the higher sensitivity of the fiber optic system in this process can enhance the ability of albumin detection. Besides, the optical fiber system has the potential for further development in the future for urine detection by AIE bioprobes. Through deeper understanding and research, it is expected to become an effective application for quantitative detection of HSA in human urine.

## **7 Acknowledgment**

I am very grateful for Professor Youhong Tang and Research Assistant Xinyi Zhang from Flinders University. The ideas and support you provided during the experiment helped me a lot. Moreover, I really appreciate Professor Colin Raston and Researcher Xuan Luo from Flinders University, and Doctor Yinlan Ruan and Research Assistant Hong Ji from the University of Adelaide for giving me the support of the experimental equipment. Besides, I am also grateful for Doctor Yuning Hong and Research Assistant Bicheng Yao because you provided all the bioprobes related to this thesis.



## 8 Reference

- Baig, A., 2011. Biochemical composition of normal urine. *Nature Precedings*, 1-1.
- Birková, A. et al., 2020. Human fluorescent profile of urine as a simple tool of mining in data from autofluorescence spectroscopy. *Biomedical signal processing and control*, 56, pp.Biomedical signal processing and control, February 2020, Vol.56.
- Chen, T. et al., 2017. Quantitative urinalysis using aggregation-induced emission bioprobes for monitoring chronic kidney disease. *Faraday Discussions*, 196, 351–362.
- Chutipongtanate, S. & Thongboonkerd, V., 2010. Systematic comparisons of artificial urine formulas for in vitro cellular study. *Analytical biochemistry*, 402(1), 110–112.
- Gaitonde D. Y., Cook D. L., Rivera I. M., 2017, Chronic kidney disease: Detection and evaluation, *American Family Physician* 96 (12), 776-783.
- Grillet, A. et al., 2008. Optical fiber sensors embedded into medical textiles for healthcare monitoring. *IEEE Sensors Journal*, 8(7), 1215–1222.
- Hong, Y., Lam, J. W., & Tang, B. Z., 2011. Aggregation-induced emission. *Chemical Society Reviews*, 40(11), 5361-5388.
- James, M. T, Hemmelgarn, B. R., Tonelli, M., 2010. Early recognition and prevention of chronic kidney disease. *The Lancet (British Edition)* 375.9722: 1296-309.
- Kasik, I. et al., 2006. Optical fibers for optical sensing. In *Optical Chemical Sensors. NATO Science Series II: Mathematics, Physics and Chemistry*. Dordrecht: Springer Netherlands, 59–76.
- Lee P., Wu X., 2015, Modifications of human serum albumin and their binding effect. *Current pharmaceutical design*, 21(14): 1862-1865.

- Levey A. S., et al., 2005. Definition and classification of chronic kidney disease: A position statement from kidney disease: Improving global outcomes (KDIGO). *Kidney International*, 67(6), 2089-2100.
- Levitt, D., Levitt, M., 2016. Human serum albumin homeostasis: a new look at the roles of synthesis, catabolism, renal and gastrointestinal excretion, and the clinical value of serum albumin measurements. *International Journal of General Medicine*, 9, 229–255.
- Liu, G., Ma, Z., 2018. Study on a novel portable urine analyzer based on optical fiber bundles. *Measurement: Journal of the International Measurement Confederation*, 130, 412–421.
- Magalhães J. M. C. S., Machado A. A. S. C., 2002. Array of potentiometric sensors for the analysis of creatinine in urine samples. *The Analyst*, 127(8), 1069-1075.
- Martin, H., 2011. Laboratory measurement of urine albumin and urine total protein in screening for proteinuria in chronic kidney disease. *The Clinical biochemist. Reviews*, 32(2), 97–102.
- Nahas, M. E., 2005. The global challenge of chronic kidney disease, *Kidney International* 68.6 (2005): 2918-2929.
- Narva, A. S., 2008. The national kidney disease education program and other related efforts in the United States. *Scandinavian Journal of Clinical and Laboratory Investigation*, 68(sup241), 12-15.
- Nicholson, J.P., Wolmarans, M.R., Park, G.R., 2000. The role of albumin in critical illness. *British Journal of Anaesthesia*, 85(4), 599–610.
- Peterson, J. I., Vurek, G. G., 1984. Fiber-optic sensors for biomedical applications. *Science*, 224(4645), 123-127.

- Prakash, S., 2017. Role of human serum albumin and oxidative stress in diabetes. *Journal of Applied Biotechnology and Bioengineering*, 3(1), 00057.
- Rosenberg, M. et al., 2018. A fluorescence intensity ratiometric fiber optics-based chemical sensor for monitoring pH. *Advanced Materials Technologies*, 3(12), p.n/a.
- Ruan, S., Ebendorff-Heidepriem, H., Ruan, Y., 2018. Optical fibre turn-on sensor for the detection of mercury based on immobilized fluorophore. *Measurement : Journal of the International Measurement Confederation*, 121, 122–126.
- Ruan, S., et al., 2016. Online remote monitoring of explosives by optical fibres. *RSC Advances*, 6(105), 103324–103327.
- Ruan, Y. et al., 2007. Detection of quantum-dot labelled proteins using soft glass microstructured optical fibers. *Optics express*, 15(26), 17819–17826.
- Seitz, W.R.R., 1984. Chemical sensors based on fiber optics. *Analytical Chemistry*, 56(1), 16–34.
- Senior, J. & Kazovsky, 1987. *Optical fiber communications: Principles and practice*. *Physics Today*, 40(10), 128.
- Tu, Y. et al., 2019. Specific and quantitative detection of albumin in biological fluids by tetrazolate-functionalized water-soluble AIEgens. *ACS Applied Materials & Interfaces*, 11(33), 29619–29629.
- Wang, C., 2020. Evaluation of microalbuminuria using a novel biosensor, Flinders University.
- White, S. L., Polkinghorne, K. R., Atkins, R. C., Chadban, S. J., 2010. Comparison of the prevalence and mortality risk of CKD in Australia using the CKD epidemiology collaboration (CKD-EPI) and modification of diet in renal disease (MDRD) study GFR

estimating equations: The AusDiab (Australian Diabetes, Obesity and Lifestyle) Study. *American Journal of Kidney Diseases* 55.4: 660-70.

- Couser, W. G., Remuzzi, G., Mendis, S., Tonelli, M., 2011. The contribution of chronic kidney disease to the global burden of major noncommunicable diseases. *Kidney International* 80.12: 1258-1270.
- Yu, C.Y.Y. et al., 2016. A photostable AIEgen for nucleolus and mitochondria imaging with organelle-specific emission. *Journal of Materials Chemistry B*, 4(15), 2614–2619.
- Zhang, Z. et al., 2019. Product design: Enzymatic biosensors for body fluid analysis. *Industrial and Engineering Chemistry Research*, 58(31), 14284–14294.
- Zhou, Y., et al., 2019. AIEgens in cell-based multiplex fluorescence imaging. *Science China Chemistry*, 62(10), 1312–1332.